

國立交通大學

工學院精密與自動化工程學程

碩士論文

鏡頭光機公差分析之研究

A Study of Opto-mechanical Tolerance Analysis
on Lens System

研究生：鄭陳嶽
指導教授：陳仁浩 教授
 林聰穎 助理教授
 曾錦煥 教授

中華民國九十六年一月

鏡頭光機公差分析之研究

A Study of Opto-mechanical Tolerance Analysis on Lens System

研究生：鄭陳嶽

Student : Chen-Chin Cheng

指導教授：陳仁浩

Advisor : Ren-Haw Chen

林聰穎

Tsung-Yin Lin

曾錦煥

Ching-Huan Tseng

國立交通大學

工學院精密與自動化工程學程



A Thesis

Submitted to Degree Program of Automation and Precision Engineering

College of Engineering

National Chiao Tung University

in Partial Fulfillment of the Requirements

for the Degree of

Master of Science

in

Automation and Precision Engineering

January 2007

Hsinchu, Taiwan, Republic of China

中華民國 九十六年 一月

鏡頭光機公差分析之研究

研究生：鄭陳嶽

指導教授：陳仁浩 博士

林聰穎 博士

曾錦煥 博士

國立交通大學工學院專班—精密與自動化工程學程

摘 要

傳統光學系統的公差分析對於實際的製程能力考慮不盡周全，而且由機械誤差產生的組裝變異也未考慮；如欲達到“為製造設計(Design for Manufacturing)”的目的，機械工程師有必要提供系統組裝合成公差的資訊，作為光學工程師公差分析的輸入值，讓真實的製程能力反應在光學性能之上，本研究的目的是建構一個鏡頭系統的光機公差分析模型，以計算鏡片在鏡筒內的累積偏心角度公差與偏心距離公差；具曲面特性的球面鏡片與非球面鏡片的光機公差模型與組裝方法在本研究中發展完成，該模型由點幾何構成，以VSA-3D[®]軟體編輯，並以蒙地卡羅(Monte Carlo)方法模擬，模擬結果以敘述統計呈現；最後以兩個“投入式(drop-in)”組立設計的鏡群組為案例，計算鏡片在鏡筒內的累積偏心角度公差、偏心距離公差及鏡片光學軸的累計偏移量，其結果顯示該模型可模擬一個鏡頭系統的關鍵品質參數；所以，鏡頭系統的性能在大量生產之前可藉本光機公差模擬模型預測其品質與良率。

A Study of Opto-mechanical Tolerance Analysis on Lens System

Student: Chen-Chin Cheng

Advisors: Dr. Ren-Haw Chen

Dr. Tsung-Yin Lin

Dr. Ching-Huan Tseng

Degree Program of Automation and Precision Engineering

National Chiao Tung University

ABSTRACT

The traditional tolerance analysis of optical systems does not consider the capability of the real manufacturing process, and the variation occurs in the assembly process caused by the tolerances of optical and mechanical components. In order to have a “Design for Manufacturing” optical system, the mechanical engineer has to provide the resultant system assembly variation as an input to the optical design and analysis to anticipate the performance of the optical system. The purpose of this study is to develop an opto-mechanical tolerance model to calculate the element tilt, decenter and despace stack-up within a cell. A surface based opto-mechanical tolerance models of sphere lens, aspheric lens, and assembly algorithm have been developed in this study. The model is represented as point geometry, implemented by VSA-3D[®] software, and simulated by Monte Carlo method. The simulation results are conducted by descriptive statistics. Two “drop-in” assembly design lens groups were studied to calculate the stack-up element tilt and decenter within a cell and the resultant deviations of the optical axes away from the mechanical datum axis. The results indicate that the opto-mechanical tolerance model can analyze the critical to quality parameters of a lens system. As a result, the performance of the lens system can be anticipated by the opto-mechanical tolerance model before mass production.

誌 謝

完成這篇論文才深深體會到陳之藩在「謝天」中這段話「無論什麼事，得之於人者太多，出之於己者太少，因為要感謝的人太多了，就感謝天吧。」所傳達的深刻意涵，有太多的師長、長官及朋友的鼓勵與協助我才得以完成這段學業。

重拾書本回到教室中聽課已是大學畢業二十年之後的事了，雖然知道自己應該彌補這一段學業，但也一直沒有積極行動。三年前趙偉忠博士問我是否申請在職進修之後才積極面對考試，這段時間 ITRI 蔡榮源組長、趙偉忠博士、張奇偉博士等給了我很多的協助，老長官機械所所長吳東權博士（當時是副所長）熱心地幫我寫推薦信，碰面時總是關心地問我何時畢業。

來到交大榮幸地加入曾錦煥教授的最佳設計實驗室，曾老師總是配合我的上班時間，單獨給我指導時間，引導我收集、過濾、研讀文獻資料，同時分享其「創意人生」之哲學；很不幸敬愛的曾老師於九十四年九月意外辭世，洪景華老師與蔡忠杓老師適時引導大家未來的方向，感謝陳仁浩老師接下指導教授的工作，大師兄林聰穎博士則擔任共同指導教授，在兩位老師共同督促指導下逐步完成這篇論文。另外實驗室的學弟們也給我很大的協助，跑程式、交作業、作報告及一些雜務，他們總是毫不遲疑地主動幫忙。

這篇論文的主題是從事鏡頭光機設計者都會面臨的問題，單純機械組件的累積公差較容易計算，但是透鏡的曲面使得問題變得複雜化，多年前游李興博士從事鏡頭開發時曾問我這個問題，當時雖然已經開始思考這個議題但尚無解決方案，去年配合論文研究下定決心務必找出解法；這期間除了定期與指導老師討論外，同事張銓仲在透鏡偏心定義上給予我很多幫忙，美國 Kodak 公司的 John Griffith 則提醒我建構一個 surface based 公差模擬模型的必要性。

最後要感謝我的家人這段時間對我的支持、鼓勵與容忍，尤其是我內人，她幾乎擔下所有的家務與小孩課業指導的工作，這段時間由於她的辛勞付出我才得以專心於課業上。

TABLE OF CONTENTS

摘 要	i
ABSTRACT	ii
誌 謝	iii
TABLE OF CONTENTS	iv
LIST OF TABLES	vi
LIST OF FIGURES	vii
NOTATIONS.....	ix
Chapter 1. Introduction	1
1.1. Opto-mechanical design of lens system	1
1.2. Literature Review	1
1.3. Objective and study method	4
1.4. Thesis Outlines.....	6
Chapter 2. Tolerance analysis.....	7
2.1. Statistics and Data Analysis for Tolerancing.....	8
2.1.1. Descriptive Statistics.....	9
2.1.2. Distributions.....	12
2.1.3. Manufacturing Process Capability Metrics	14
2.2. Tolerance Analysis Process	16
2.3. Worst Case Tolerance Analysis.....	22
2.4. Statistical Tolerance Analysis.....	23
2.4.1. The Root Sum of the Squares (RSS) model.....	23
2.4.2. The Modified Root Sum of the Squares (MRSS) model	27
2.5. Contribution Analysis	28
2.6. Computer Aided Tolerancing	29
Chapter 3. Lens System.....	34
3.1. Centered Optics	34
3.2. Lens Mounting Principles	35
3.3. Lens Assemblies Design.....	38
3.4. Variations in Lens Element.....	41
3.5. Variations in Lens Assembly	45
Chapter 4. Opto-mechanical tolerance model.....	47
4.1. Tolerance modeling.....	47
4.2. Opto-mechanical tolerance model on optical components	49
4.2.1. Spherical lens	49
4.2.2. Aspheric lens	55
4.3. Assembly variations in lens assembly	58

4.3.1.	Rolling center in assembly	58
4.3.2.	Rolling limit in assembly	63
4.4.	Tolerance model of mechanical components	64
4.5.	Assembly model	66
Chapter 5.	Case Study	69
5.1.	Portion of a zoom lens design	69
5.2.	Programming flow chart.....	74
5.3.	The statistical distribution of the tolerances	80
5.4.	The simulation results	82
5.5.	Discussion	99
Chapter 6.	Conclusions and future works	103
REFERENCES	104



LIST OF TABLES

Table 2-1	Converting dimensions to equal bilateral tolerance	20
Table 2-2	The tolerance contribution analysis of Figure 2-8.....	29
Table 4-1	GD&T symbols represented as the perpendicular tolerance zone.....	48
Table 4-2	GD&T symbols represented as the circular tolerance zone	49
Table 5-1	The fabrication data and tolerance of optical elements.....	71
Table 5-2	The assembly tolerance requirements	74
Table 5-3	Statistical distributions of tolerance	81
Table 5-4	The simulation results	102



LIST OF FIGURES

Figure 1-1	Representing optical components by local coordinate systems.....	4
Figure 2-1	Comparison of tolerance analysis and tolerance allocation.....	8
Figure 2-2	Skewed distribution	11
Figure 2-3	Normal distribution.....	13
Figure 2-4	The standard normal distribution.....	14
Figure 2-5	Process capability	15
Figure 2-6	Process capability with shifted mean.....	16
Figure 2-7	Tolerance analysis process.....	17
Figure 2-8	One dimensional assembly	18
Figure 2-9	Horizontal loop diagram	18
Figure 2-10	The gap in Figure 2-8 analyzed by CAT without process drift.....	32
Figure 2-11	The gap in Figure 2-8 analyzed by CAT with process drift.....	33
Figure 3-1	Perfect centered optical lens	35
Figure 3-2	Centering principle	36
Figure 3-3	A perfectly centered lens and spacer.....	36
Figure 3-4	A special case which self-centering will not occur.....	37
Figure 3-5	A perfectly centered and edged lens mounted in a perfect cell	37
Figure 3-6	Self-centering condition.....	38
Figure 3-7	A optical subsystem assembled by “drop-in” technique.....	39
Figure 3-8	Subcell assembly lens barrel design	40
Figure 3-9	Center thickness variation causes surfaces despace	42
Figure 3-10	Lens OD variation causes element tilt and decenter.....	43
Figure 3-11	Centering tolerances.....	44
Figure 3-12	Lens mounted in barrel	46
Figure 4-1	Misalignment of lens during centering and edging	50
Figure 4-2	Opto-mechanical tolerance model of biconvex sphere lens	53
Figure 4-3	Opto-mechanical tolerance model of meniscus convex lens, biconcave lens and meniscus concave lens.....	54
Figure 4-4	Opto-mechanical tolerance model of plano-convex lens, and plano-concave.....	55
Figure 4-5	Center of curvature of aspheric surface at radial distance y_1	56
Figure 4-6	Opto-mechanical tolerance model of biconvex aspheric lens	58
Figure 4-7	Rolling center of convex surface on cell shoulder.....	59
Figure 4-8	Rolling center of concave surface on cell shoulder	60
Figure 4-9	Manufacturing variation and rolling center	61
Figure 4-10	Rolling center of spacer on convex surface	62

Figure 4-11	Rolling center of spacer on concave surface.....	62
Figure 4-12	Components rolling limit within cell.....	63
Figure 4-13	Tolerance model of cell.....	64
Figure 4-14	Tolerance model of spacers.....	65
Figure 4-15	Frame transformation.....	67
Figure 4-16	Degrees of freedom of a rigid body.....	67
Figure 5-1	Portion of a zoom lens design.....	70
Figure 5-2	Drawing of opto-mechanical interface of Group II.....	72
Figure 5-3	Drawing of opto-mechanical interface of Group III.....	73
Figure 5-4	Flow chart of sphere lens tolerance model.....	75
Figure 5-5	Flow chart of aspherical lens tolerance model.....	76
Figure 5-6	Flow chart of spacer tolerance model.....	77
Figure 5-7	Flow chart of cell tolerance model.....	78
Figure 5-8	Assembly flow diagram.....	79
Figure 5-9	The element tilt of L5.....	82
Figure 5-10	The element tilt of L6.....	83
Figure 5-11	The element tilt of L7.....	84
Figure 5-12	The element tilt of L8.....	85
Figure 5-13	The element tilt of L9.....	86
Figure 5-14	The element tilt of L10.....	87
Figure 5-15	The element tilt of L11.....	88
Figure 5-16	The element decenter of L5.....	89
Figure 5-17	The element decenter of L6.....	90
Figure 5-18	The element decenter of L7.....	91
Figure 5-19	The element decenter of L9.....	92
Figure 5-20	The element decenter of L10.....	93
Figure 5-21	The element decenter of L11.....	94
Figure 5-22	Despace of L6.....	95
Figure 5-23	Despace of L7.....	96
Figure 5-24	Despace of L9.....	97
Figure 5-25	Despace of L6.....	98
Figure 5-26	The variation of optical axis and mechanical axis.....	101

NOTATIONS

a_i	: sensitivity factor
$C1, C2$: center of curvature
C_f	: correction factor of the MRSS tolerance
C_p	: process capability index
C_{pk}	: capability index relative to process centering
ε_m	: element decenter of a lens
ε_o	: resultant optical decenter tilt of a lens
ε_s	: surface decenter of a lens
ID	: Inside diameter
LSL	: lower specification limit
μ_i	: i^{th} moment about the mean
N	: maximum permissible number of fringe spacings
\bar{o}	: optical axis vector
OD	: Outside diameter
P_i	: percent contribution of the tolerance of i^{th} component
θ	: contact angle
\bar{r}	: point vector
$R1, R2$: radius of curvature
$r1, r2$: tolerance of radius of curvature
S	: sample standard deviation
S^2	: sample variance
σ^2	: population variance
T	: nominal central thickness
t	: tolerance of the central thickness
t_{mrss}	: MRSS expected equal bilateral tolerance
t_{rss}	: RSS expected equal bilateral tolerance
t_{wc}	: Worst Case expected equal bilateral tolerance
τ_m	: element tilt of a lens
τ_o	: resultant optical axis tilt of a lens
τ_s	: surface tilt of a lens
USL	: upper specification limit



$V1, V2$: vertex of curvature
 y : arithmetic mean of data observations
 Z : Z transform
 z : sag of a surface



Chapter 1. Introduction

1.1. Opto-mechanical design of lens system

The lens is a typical optical system. In general, the optical design of a lens is often less than half of the total design work. The other major half of the design work is the opto-mechanical design. Optical design controls the light while the light is controlled by the surface where refraction or reflection occurs. Opto-mechanics is defined as the science or engineering of maintaining the proper shapes and positions of the functional elements in an optical system. Therefore, the system performance requirements can be satisfied. Opto-mechanical design plays one of the major roles in any optical system development, particularly where the optics and mechanics interface [1]. Deflection and manufacturing tolerance affect the shape and position of the surface in a lens system. Even very small shape or position variations will cause extra aberrations which degrade the optical performance of a lens system dramatically. As a result, tolerance is a critical design issue in the opto-mechanical design of a lens system [1, 2].

1.2. Literature Review

Variation is a physical result of manufacturing process. Parts and assemblies always differ from each other and from what we want them to be. Tolerance refers to the amount of variation that designers can tolerate in a part or assembly. Variation affects the quality, cost and timing of a product tremendously. Tolerance analysis plays an important role in reducing variation in the manufacturing process so as to improve the quality, cost, and the deliver time. For an optical system, the variation will lead to certain image quality degradation that will be a serious problem. Hilbert [3] stated that the objective of the optical tolerancing is to

determine the combination of dimensional ranges for optical elements, and their relative position in assemblies. It will minimize manufacturing costs when satisfying performance requirements.

Drake [4] had developed software to automate the design process of the optical system. The traditional approach to the opto-mechanical tolerance design is a top-down process. The optical designers set system performance requirements and to the mechanical engineers. They typically designate these requirements, tolerances of tilts, decenters and locations of optical elements with respect to an optical axis. A significant drawback of this top-down process is that the tolerances determined by optical designers do not consider the real manufacturing and assembly process. As a result, some tolerances are too tight for the optical fabrication, and the yield rate of the mass production is difficult to improve. Texas Instruments had developed a new bottom-up approach. Its software program with Monte Carlo analysis integrates design parameters, constraints, mechanical dimensions, process capabilities, and manufacturing requirements to predict the performance of opto-mechanical design.

As mentioned above tolerance analysis is very important in opto-mechanical system design. Nikon had developed a statistical tolerancing system that enables the quantitative analysis of the optical performance, productivity, and sensitivity analysis prior to manufacturing. Based on Monte Carlo method, the system was realized as computer software. It makes the designer be able to determine an optimum set of tolerance for a given optical product by taking into account of manufacturing and assembling variations occurring in mass production [5].

Twelve primary parameters were chosen by Magrill [6] to simulate the variations of lens mounting assembly caused by manufacturing errors. A primary parameter is defined as any parameter that does not depend on other parameters and can be specified and checked

independently. Therefore, only mechanical parameters can be used as primary parameters. The sensitivity of the opto-mechanical system depends not only on optical design but also on the mechanical layout.

Lee [7] had studied the factors which affect surface tilt and decentration during the mounting cell. Some useful formulas which provide the tilt and decenter of optical components in mounting cell was summarized.

Thompson [8] had developed a theory to represent fabricated optical components by a set of simple local coordinate systems linked by physically relevant stationary pivot points. The properties of optical elements, mechanical spacers, and the techniques for their characterization are developed. The basic units of a fabricated optical element was separated in four distinct optical units: a first spherical refracting cap, a tilted plane parallel block, an oriented wedge, and a second spherical refracting cap, as shown in Figure 1-1(a). Local coordinate system associated with each optical surface is defined to represent the spherical refracting cap by three variables: r , δx , and ρ as shown in Figure 1-1(b). An optical element contains two local coordinate systems, LSYA and LSXA. Two local coordinate systems are linked by three parameters to represent a fabricated optical component as shown in Figure 1-1(c). Finally a set of three vectors and three associated scalars is used to specify the compound angular in tilt and wedge as shown in Figure 1-1(d). The vector set provides an excellent method for modeling the mechanical properties associated with an optical element. The origins of the local coordinate systems are stationary pivot points. Through stationary pivot points, the errors in radii, thickness, and wedge are easily identified and applied. The spacer that separates two optical elements is treated as an optical element with an index of refraction of one.

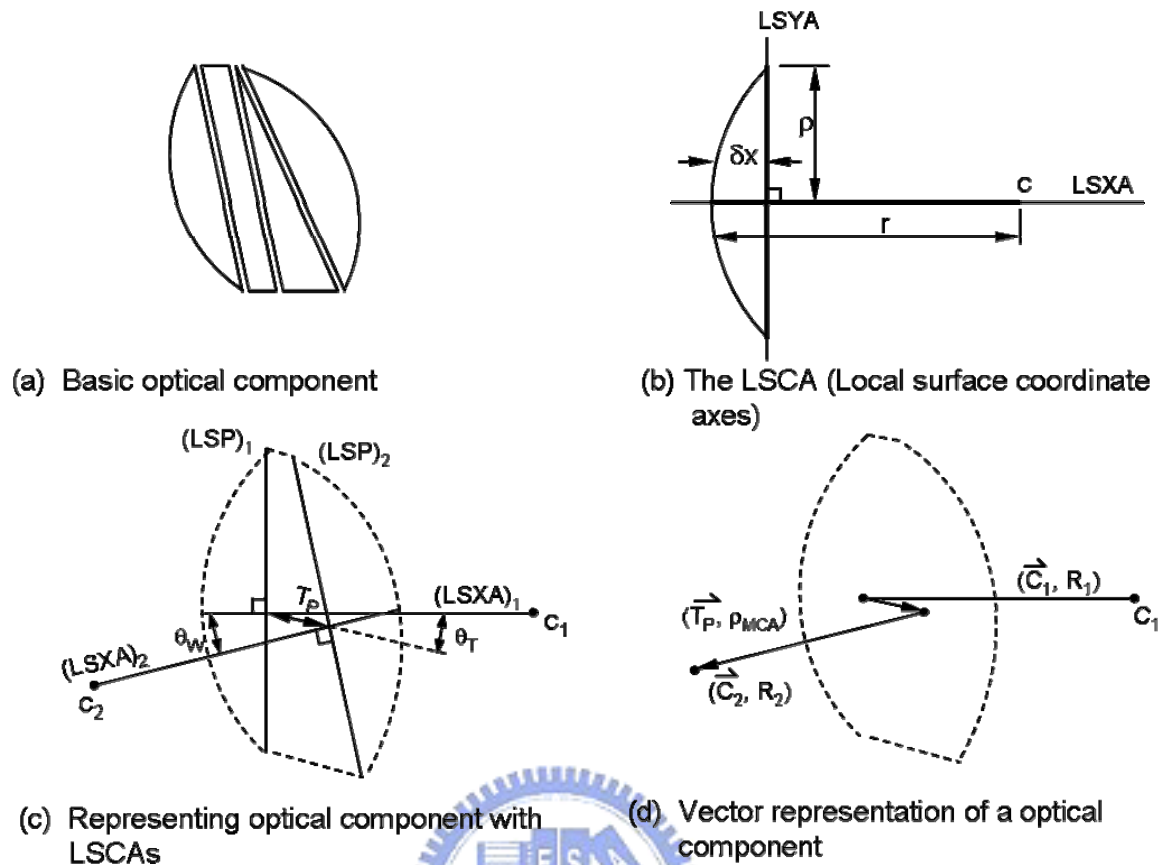


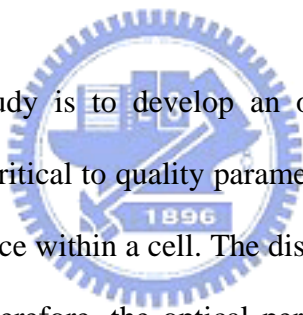
Figure 1-1 Representing optical components by local coordinate systems

De Witt IV [9] had presented a means of characterizing the rigid body motions of optical element from their nominal positions as caused by manufacturing tolerances and thermal effects. Several cases of element tilt or decenter effect caused by mechanical mounting components were discussed. However, the model considered the worst case only, and was complicated if it is applied to the stack-up situation.

1.3. Objective and study method

Several studies [4-6] have tried to improve the drawbacks of the top-down design process. The performance of a lens system is greatly influenced by the tolerances of the optical and mechanical components. Currently the tolerance requirement of a lens system is determined by optical designer. The real manufacturing process capability and the variation

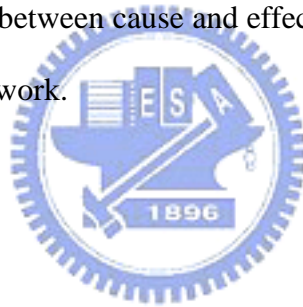
occur in assembly process are not considered. That makes some of the lens development project is found difficult to improve the yield rate before or during mass production. In the real world, the resultant position variation of the optical component is determined by the tolerance stack-up of the optical component itself and the mechanical components used to mount the optical element. The dimensional and geometric variations of the optical and mechanical component are determined by the capability of the manufacturing processes. If the optical performance is analyzed by the resultant tolerances that are derived from the actual opto-mechanical stack-up, it is reasonable for engineers to predict the mass production yield rate of a lens system. Then, the design can be modified or improved to meet the requirements for mass production. The cost and delivery of a development project can be minimized, and the quality will fit for use. This is the “Design for Manufacturing” (DFM) concept.



The objective of this study is to develop an opto-mechanical tolerance model that calculates the variation of the critical to quality parameters for a lens system, such as the lens element tilt, decenter and despace within a cell. The distribution of these parameters can be an input to the optical design. Therefore, the optical performance will be predictable than the top-down approach, and the manufacturability of the optical system will be improved. The opto-mechanical tolerance model is implemented by VSA-3D[®] software [10]. First, all the optical and mechanical components is represented as the point geometry that is derived from the engineering specifications of the component, and from some geometric calculation and vector operation. Second, the tolerances are assigned to the corresponding location points of each component. Third, the system is assembled by defining the stationary points and the rolling limit conditions. Fourth, parameters which are critical to the quality such as the stack-up element tilt, decenter and despace within a cell are defined as the output. Finally, Monte Carlo simulation is carried out by VSA-3D[®] software to calculate the output measurements of the opto-mechanical parameters in statistical description.

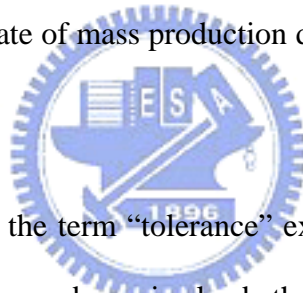
1.4. Thesis Outlines

In this study, Chapter 1 makes a brief introduction to the opto-mechanical design of lens design. The literature is reviewed on the tolerance issue in opto-mechanical design. Then the objective and study method is introduced. Chapter 2 introduces the elementary statistics used for data analysis, the tolerance analysis process, traditional tolerance analysis method, and sensitivity analysis. Lens mounting and assembly design are introduced in Chapter 3. The sources of variation of components and assembly are also explained. Chapter 4 develops the surface based opto-mechanical tolerance model of sphere lens, aspheric lens, and the assembly algorithm. Two “drop-in” assembly design lens groups are studied in Chapter 5 to verify the opto-mechanical tolerance model. The simulation results are discussed about the rationality and the relationship between cause and effect. Chapter 6 makes conclusions on this study and points out the future work.



Chapter 2. Tolerance analysis

Tolerancing techniques have been evolved over years. Seeking for the interchangeability of mechanical parts is the early historical context of tolerances. Design for the mass production sets the modern context of tolerances. By giving the design parameters, tolerance analysis will indicate the probable assembly variation of a product in advance. According to the manufacturing process capability, engineers can improve the product quality and cut down the cost before mass production. In order to satisfy customers' requirement and the quest for efficiency in producing product, remarkable advances have been made in tolerancing techniques. Nowadays the product design processes and manufacturing processes are quite different from decade before. Tolerance analysis and tolerance allocation techniques have let engineers predict the yielding rate of mass production during product development and design stage.



Creveling [11] noted that the term “tolerance” exists because we live in a probabilistic universe. The second law of thermodynamics leads that all natural processes are irreversible, the entropy of a system plus its environment always increases. Boltzmann had made a connection between entropy and probability [12]. Every manufacturing process can be treated as an energy-transformation process that always involves random events. Therefore, tolerances must exist in the world because things always contain variations. For instance, temperature, humidity, atmosphere pressure, friction, tool wear, and material defects are the most common factors which cause variations. Tolerances play a key role in defining the constraints required to promote consistent transformation of energy.

Tolerances are defined as limits or boundary. In the mechanical engineering field, ASME Y14.5M-1994 Standard [13] defines tolerance as follows:

“The total amount a specific dimension is permitted to vary. The tolerance is the difference

between maximum and minimum limits.”

Tolerance design is an important part in the mechanical design. The tolerance selection strongly influences the functional performance and manufacturing cost of a mechanical product. The balance between the performance and cost through tolerance analysis and tolerance allocation is an essential concern in modern engineering design.

Tolerance analysis and tolerance allocation are the central issues of tolerance design. The difference between these two problems is illustrated in Figure 2-1 [14]. In tolerance analysis, the component tolerances are all known or specified and the resulting assembly tolerance is calculated. In tolerance allocation, on the other hand, the assembly tolerance is known from design requirements, while the component tolerances are unknown [15].

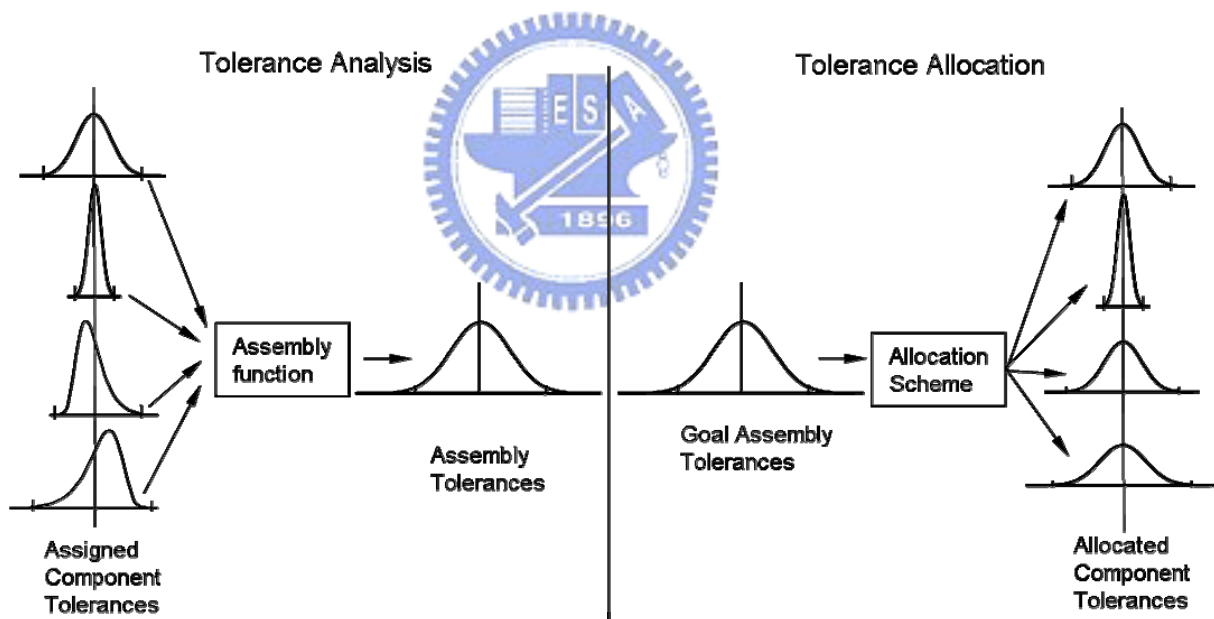


Figure 2-1 Comparison of tolerance analysis and tolerance allocation

2.1. Statistics and Data Analysis for Tolerancing

Measurement and data collection is necessary for applying tolerance analysis to calculate the variation (or distribution) of the target dimension. In general, it is difficult to modify the design to improve a product’s performance by looking at the raw data collected

from manufacturing process. The data must be organized into a useful form for building knowledge and for drawing conclusions that carry out the product or process performance improvement.

Statistics is the fundamental knowledge for engineer to properly gather and process sample data in tolerance analysis. These data will come directly from the manufacturing process, from an experiment on a product, or from the random number generator. Data that are a sample from a population can be mathematically processed into descriptive values called “sample statistics”. Data that comprise an entire population can be mathematically processed into descriptive values called “population statistics”. Some population statistics can never be quantified because they are large amount and uncountable, or they are in process, so that it is not possible to gather the entire data set. For example, if the manufacturing process data come out from a production line, it is only possible to manage sample data from populations.



2.1.1. Descriptive Statistics

It is required to take four “Moments” to quantify the key effects that are critical to tolerance analysis. Moment is a measurement related to the mean raised to a specific power [11].

The First Moment of the Data about the Mean: the Arithmetic Average

The first characteristic is the mean value from the dispersed data. It is a measure of central tendency. The first moment about the mean can be calculated from the following equation:

$$\mu_1 = \frac{1}{n} \sum_{i=1}^n (y_i - \bar{y})^1 \quad (2-1)$$

where

$$\bar{y} = \frac{1}{n} \sum_{i=1}^n y_i \quad (2-2)$$

y_i is the data observations.

n is the total number of data points.

\bar{y} is the arithmetic mean of data observations.

It is found that the value of this summation is zero. The central tendency of the sample data is given by the sample mean, \bar{y} , shown in Equation (2.2).

The Second Moment about the Mean: the Variance

The second moment about the mean is formally called the variance. Sample variance listed in Equation (2-3) gives a measure of the dispersion of the data. It is based on the average of the squared deviations of the individual data points from the sample mean as shown in Equation (2-4). The value $n-1$ is the degrees of freedom. It has been proved to provide an estimation of more accurate value of the sample variance.

$$\mu_2 = S^2 \quad (2-3)$$

$$S^2 = \frac{1}{n-1} \sum_{i=1}^n (y_i - \bar{y})^2 \quad (2-4)$$

The population variance is shown in Equation (2-5).

$$\sigma^2 = \frac{1}{N} \sum_{i=1}^N (y_i - \bar{y})^2 \quad (2-5)$$

where N is total number of population.

The square root of the sample variance is the sample standard deviation, shown in Equation (2-6), and denoted as S . It is another commonly used measure of variability in the data.

$$S = \sqrt{S^2} = \sqrt{\frac{1}{n-1} \sum_{i=1}^n (y_i - \bar{y})^2} \quad (2-6)$$

The Third Moment about the Mean: the Skew

The skew is the measure of the symmetry of a data distribution about the mean. Take the third moment about the mean to obtain a value indicative of the skew:

$$\mu_3 = \frac{1}{n} \sum_{i=1}^n (y_i - \bar{y})^3 \quad (2-7)$$

Skew is then represented by the equation:

$$Skew = \frac{\mu_3}{S^3} = \frac{1}{n} \sum_{i=1}^n \left(\frac{y_i - \bar{y}}{S} \right)^3 \quad (2-8)$$

When the distribution of the sample data is symmetrical about the mean, then the skew is zero. The skew will assume to be a positive value when the data is biased to the right, and a negative value when the data is biased to the left, as shown in Figure 2-2.

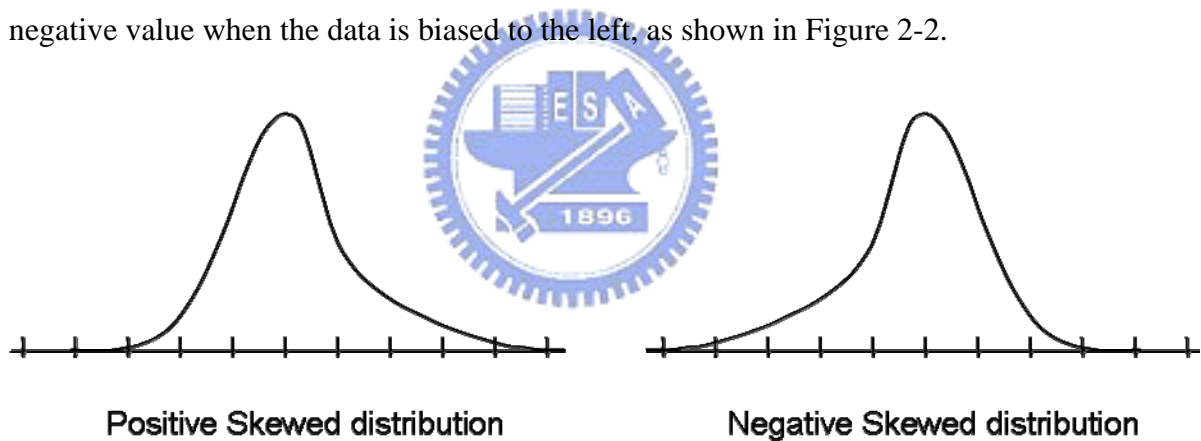


Figure 2-2 Skewed distribution

The Fourth Moment about the Mean: The Kurtosis

The fourth moment will provide a numerical value associated with the peakedness or flatness of the data as it is distributed about the mean. It is also known as kurtosis.

$$\mu_4 = \frac{1}{n} \sum_{i=1}^n (y_i - \bar{y})^4 \quad (2-9)$$

Kurtosis is represented by the equation:

$$Kurtosis = \frac{\mu_4}{S^4} = \frac{1}{n} \sum_{i=1}^n \left(\frac{y_i - \bar{y}}{S} \right)^4 \quad (2-10)$$

There are three general distribution types used to define the nature of kurtosis. The first one is mesokurtic distribution which is normally distributed about the mean, and the kurtosis will equal to 3.0. The second one is the platykurtic distribution in which the data is dispersed in a manner that is flat in nature, and the kurtosis will be less than 3.0. The third one is the leptokurtic distribution in which the data is dispersed in a manner that is very peaked in nature. Then the kurtosis will be greater than 3.0 in this case.

A zero-based kurtosis commonly used in statistical analysis computer programs is obtained by substrate 3 from the kurtosis value.

$$zero\text{-based kurtosis} = \frac{1}{n} \sum_{i=1}^n \left(\frac{y_i - \bar{y}}{S} \right)^4 - 3 \quad (2-11)$$



2.1.2. Distributions

The dimensional variation of the manufacturing process usually has a definite pattern. The specific pattern of the data sample leads to how the data can be analyzed. Most products are assembled by components with the inherent variation of dimension. Their distribution approximates to be a normal (or Gaussian) distribution. If y is a normal random variable, the probability distribution of y is

$$f(y) = \frac{1}{\sigma\sqrt{2\pi}} \exp\left[-\frac{1}{2} \left(\frac{y - \mu}{\sigma} \right)^2 \right], \quad -\infty < y < \infty \quad (2-12)$$

where $-\infty < \mu < \infty$ is the mean of the distribution and $\sigma^2 > 0$ is the variance. The normal distribution is shown in Figure 2-3. This pattern represents how the manufacturing process affects the certain dimensions of a part. Moreover, it reflects the variation of a product's

system performance.

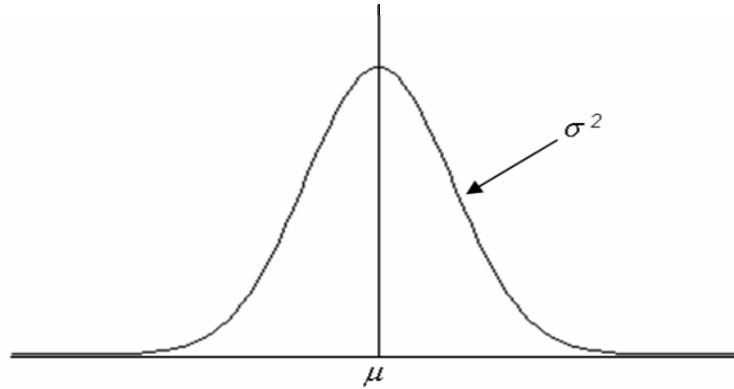


Figure 2-3 Normal distribution

The characteristic of a distribution is important in computer aided statistically tolerance analysis. The results of the Monte Carlo simulation is depend on the distribution characteristics of the input variables. Mean and variation are the two basic sample statistics used to describe the distribution's center location and the width of the variability. If the distribution is normal or approximately normal, statistical tolerance analysis method is the most commonly used technique. If the distributions are not normal, special methods are required to properly analyze the data.

An important special case of the normal distribution is the standard normal distribution; that is, $\mu = 0$ and $\sigma^2 = 1$. Random variable

$$Z = \frac{y - \mu}{\sigma} \quad (2-13)$$

will transform Equation (2-12) into standard normal distribution in variable Z . Then the probability density function is:

$$f(Z) = \frac{1}{\sqrt{2\pi}} \exp\left[-\frac{Z^2}{2}\right] \quad (2-14)$$

The standard normal distribution is shown in Figure 2-4. By integrating the area under the curve of the standard normal distribution, the percent of samples that will be beyond the specification limit can be calculated. A Z table that lists the integrating area under of the standard normal distribution will be found in statistics books. For example, if $Z = 2.5$ the area under the curve between $Z = -\infty$ and $Z = 2.5$ is 0.9938. As a result, the probability of Z beyond 2.5 will be 0.62%.

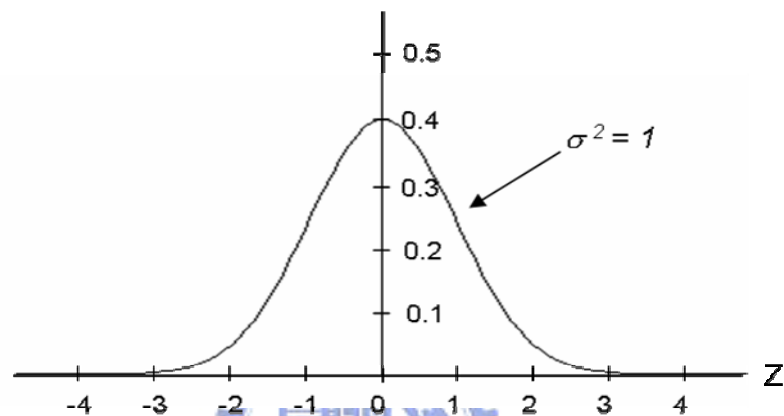


Figure 2-4 The standard normal distribution

2.1.3. Manufacturing Process Capability Metrics

Tolerances are always related to manufacturing processes and to materials used in the manufacturing of a product. Furthermore, tolerances must be designed in conjunction with the application of a specific manufacturing process. If a tolerance band is chosen without considering a specific manufacturing process, it is risky for all the required tolerance to match the capacity of a given process. The manufacturing process capability index, typically expressed as C_p or C_{pk} , is the ratio of design tolerance boundaries to the measured variability of the manufacturing process output response [11].

Process Capability Index

Historically, process capability has been defined by industry as $\pm 3\sigma$, shown in Figure 2-5. For any one feature or process output, the area contained between plus and minus three standard deviations is equal to 99.73 percent of the total area under the normal distribution curve. Process Capability Index (Cp) is defined arithmetically as below.

$$Cp = \frac{USL - LSL}{6S} \quad (2-15)$$

where

USL is the upper specification limit.

LSL is the lower specification limit.

S is the standard deviation.

The Cp index can be thought of as a short-term metric of process capability because it displays capability from recent statistically samples of data. In Six Sigma metrics the design target is $\pm 6\sigma$, then the Cp = 2.

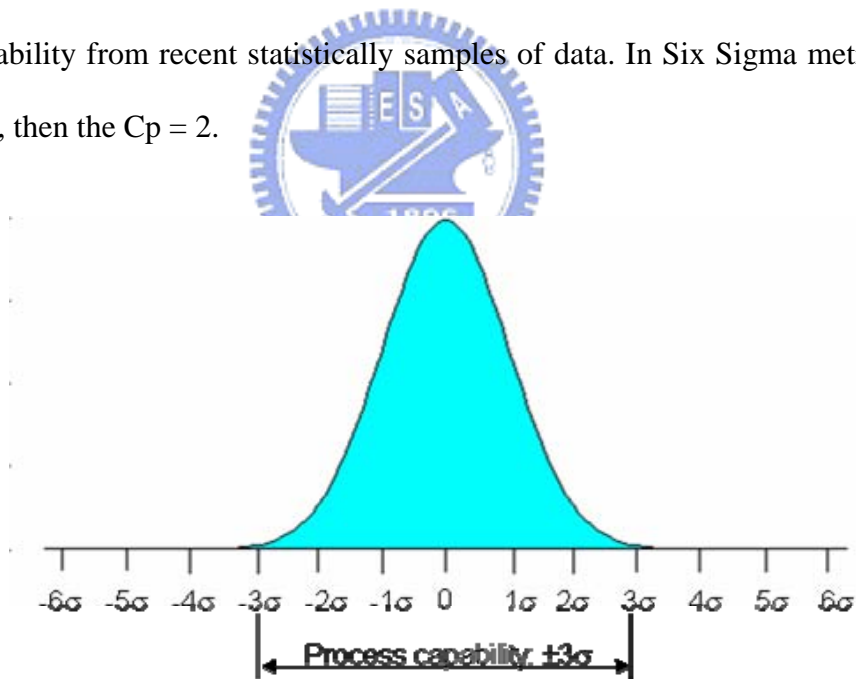


Figure 2-5 Process capability

Process Capability Index Relative to Process Centering (Cpk)

The Cp index has a disadvantage. It does not account for shifts and drifts that occur

during the long-term course of manufacturing. The metric Cpk is design to account for this off-target performance of the average output of the manufacturing as shown in Figure 2-6. It is defined as follows:

$$Cpk = Cp(1 - k) \quad (2-16)$$

$$k = \frac{|\bar{y} - T|}{\frac{(USL - LSL)}{2}} \quad (2-17)$$

where

T is the target specification.

k is the number of standard deviations with the process mean departs from target T .

The Cpk index will be thought of a long-term process capability. It can be used to account for the time-based variability of manufacturing. In Six Sigma philosophy the process mean can shift 1.5 standard deviations even when the process is monitored by modern statistical process control over an extended period of time. In that case, $Cpk = 1.5$.

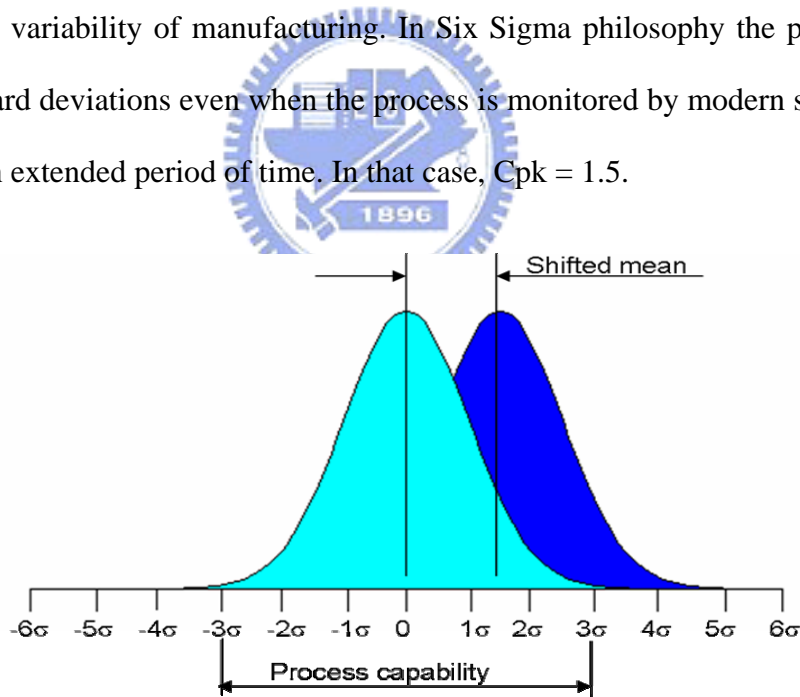


Figure 2-6 Process capability with shifted mean

2.2. Tolerance Analysis Process

The tolerance analysis process can be summarized and illustrated in Figure 2-7 [16].

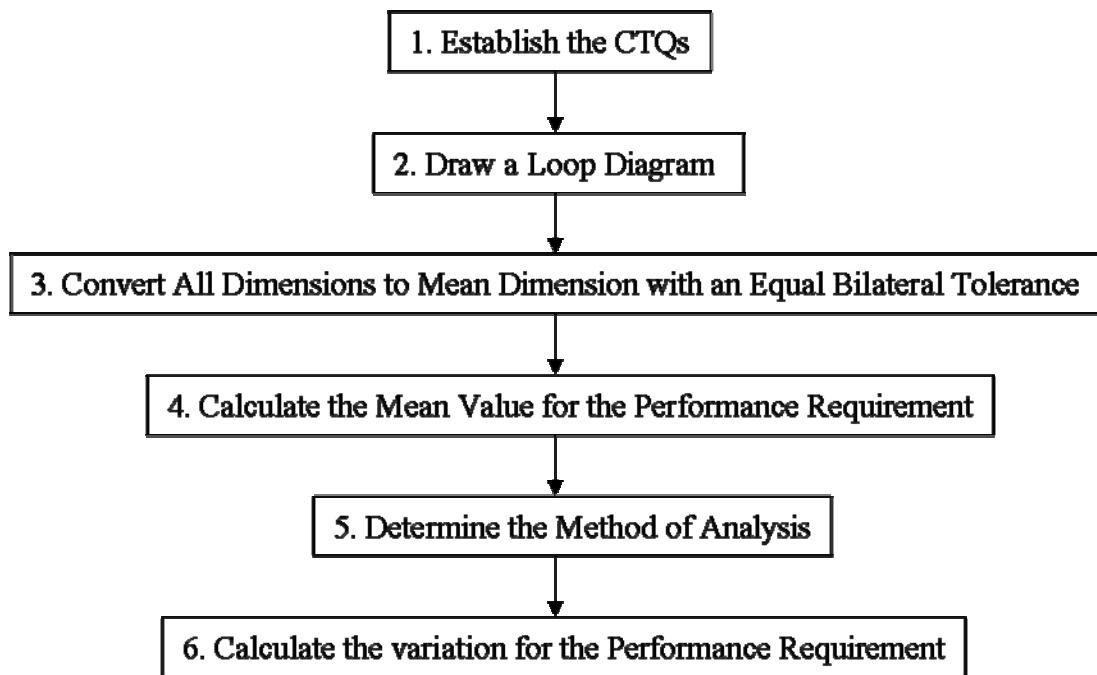


Figure 2-7 Tolerance analysis process

Establishing the CTQs



The first step in the process is to identify the critical to quality (CTQ) characteristics. The CTQs are the requirements that determine the performance of the system or the key dimensions of an assembly. The variation of the key dimensions of an assembly will make great impact on the quality of the system. These CTQs will deploy the requirements of mechanical subassemblies and detail part. The CTQs also determine the factors needed to be analyzed. Figure 2-8 illustrates an one dimensional assembly with five components. In this example the CTQ is that the “gap” must always be great than zero.

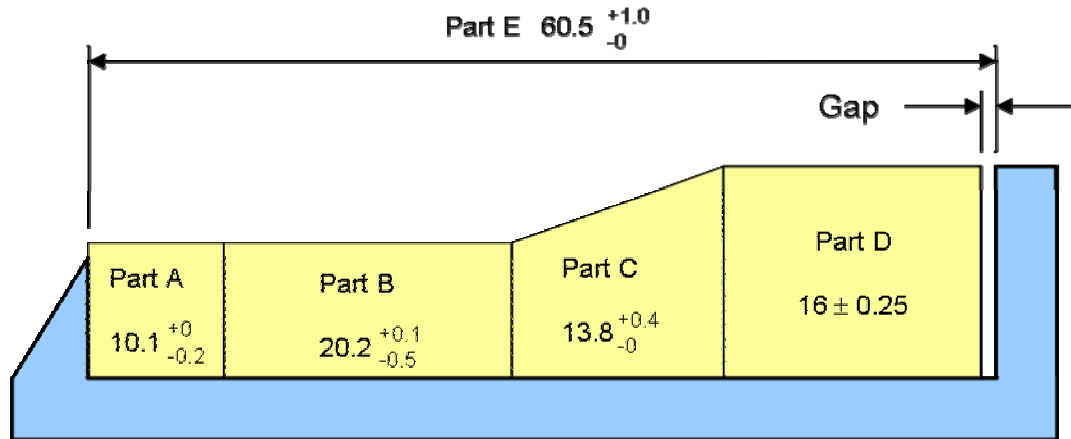


Figure 2-8 One dimensional assembly

Draw a Loop Diagram

The second step in the process is to draw a loop diagram. The loop diagram is a graphical representation of each CTQ characteristics. It is also a mathematical model of each CTQ analysis. Each CTQ requires a separate loop diagram. Simple loop diagrams are usually horizontal or vertical. For one-dimensional analyses, horizontal loop diagrams will graphically represent the dimensional contributors for horizontal “gap” or target dimension. The method of drawing a horizontal loop diagram is described below. Vertical loop diagrams will be drawn by the same way. Figure 2-9 illustrates the horizontal loop diagram of the example shown in Figure 2-8.

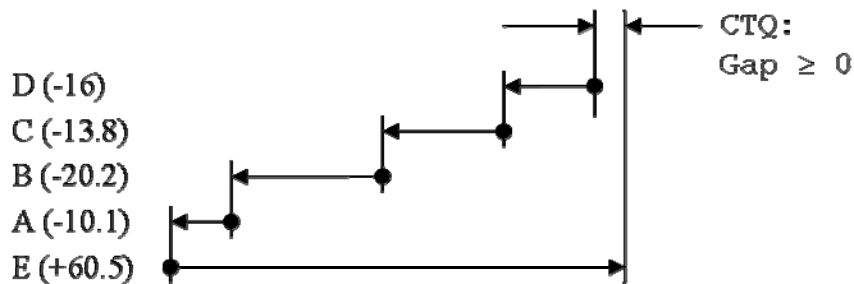


Figure 2-9 Horizontal loop diagram

The steps for drawing the loop diagram are described below.

1. Start from the surface on the left of the gap then followed by a series of features that contribute the dimensional variation of the gap. Stop at the surface on the right of the target dimension.
2. Represent the loop diagram by vector chains. Typically, the displacements of the loop diagram to the left are negative and the displacements of the loop diagram to the right are positive. The displacements are vectors which denote the contributing feature dimensions. A series of displacements is called a vector chain. When all vectors in the chain are summed, a net positive value indicates clearance, and a net negative value indicates interference.
3. Assign a variable name to each dimension in the loop.
4. Record sensitivities for each dimension. The magnitude of the sensitivity is the value that the target dimension changes when the contributing dimension changes 1 unit. The sign of the sensitivity has been incorporated with the displacement vector. For the one dimensional loop diagram, all of the sensitivities are usually equal to ± 1 . In the case that a radius is the contributing factor for a diameter, the sensitivity equals to ± 0.5 .
5. Classify the dimensions as “fixed” or “designed.” A fixed dimension is the one in which we can not control the tolerance, such as a vendor part dimension. A designed dimension is the one in which we can modify the tolerance to change or to tune-up the result of tolerance stack. The designed dimensions are what we are going to design for the tolerance during tolerance allocation.

Converting Dimensions to Equal Bilateral Tolerance

The third step in the process is converting dimensions to equal bilateral tolerance.

Because most of the manufacturing processes are normally distributed, manufacturers will obtain maximum yield of each dimension if the manufacturer aims for nominal dimension. This helps them to maximize the number of good parts and to minimize the manufacturing cost. The steps for converting to an equal bilateral tolerance are described below:

1. Convert the dimension with tolerances to an upper limit and a lower limit.
2. Subtract the lower limit from the upper limit to obtain the tolerance band.
3. Divide the tolerance band by two to get an equal bilateral tolerance.
4. Add the equal bilateral tolerance to the lower limit or subtract the equal bilateral tolerance from the upper limit to get the mean dimension.

For example, Table 2-1 converts the dimensions and tolerances in Figure 2-8 to the mean dimensions with equal bilateral tolerances.

Table 2-1 Converting dimensions to equal bilateral tolerance

Part name	Original Dimension /Tolerances	Mean Dimension with Equal Bilateral Tolerances
A	10.1 +0 / -0.2	10 ± 0.1
B	20.2 +0.1 / -0.5	20 ± 0.3
C	13.8 +0.4 / -0	14 ± 0.2
D	16.0 ± 0.25	16 ± 0.25
E	60.5 +1.0 / -0	61 ± 0.5

Calculating the Mean Value for the Requirement

The third step in the process is calculating the mean value for the requirement. This is also the first step in calculating the variation at the gap. Using the mean value, we can check the validity of the mathematical model of the loop diagram easily. The mean value at the gap

is:

$$d_g = \sum_{i=1}^n a_i d_i \quad (2-18)$$

where

d_g is the mean value at the gap.

n is the number of independent dimensions in the stack-up.

a_i is the sensitivity factor.

d_i is the mean value of the i^{th} dimension in the loop diagram.

If d_g is positive, the mean “gap” has a clearance, and if d_g is negative, the mean “gap” has an interference. The sensitivity factor defines the direction and magnitude for the i^{th} dimension. In the one-dimensional stack-up, this value is usually +1 or -1. For the example the mean value of gap in Figure 2-8, except for part E with positive sensitivity of 1 all the other components have negative sensitivity of -1. The mean gap is:

$$\text{Gap} = (-1)16 + (-1)14 + (-1)20 + (-1)10 + (1)61 = 1$$

Determine the Method of Analysis

The fourth step in the process is determining the method of analysis. Different method will result in different variation of the gap or target dimension. The two most commonly used traditional tolerance analysis methods are the “Worst Case” model and the “Statistical” model. The Worst Case model calculates the arithmetic sum of individual tolerance, and it will be described in Section 2.3. There are two traditional statistical methods; the Root Sum of the Squares (RSS) model, and the Modified Root Sum of the Square (MRSS) model. Statistical models will be described in detail in Section 2.4.

Calculating the Variation for CTQs

The last step in the process is calculating the variation for the requirement. During the design process, the design engineer has to make tradeoffs using one of the three traditional models. If the worst case tolerance meets the required CTQs, the tolerance design will stop there. On the other hand, if this model does not meet the requirements, the designer would try to use RSS or MRSS models. It has the risk of certain percentage of products beyond performance requirements.

2.3. Worst Case Tolerance Analysis

The Worst Case model [11, 16, 17] is the simplest and the most conservative tolerance analysis approach. It adds or subtracts all the individual maximum or minimum tolerances, and makes no assumptions of how the dimensions are distributed within the tolerance zone. The Worst Case model asks all components within the tolerance limits. The application occasion is when there are very few parts in the assembly or when 100% yield rate of CTQs is desired. The expected variation at the gap can be calculated as below:

$$t_{wc} = \sum_{i=1}^n |a_i t_i| \quad (2-19)$$

where

t_{wc} is the maximum expected equal bilateral tolerance using Worst Case model.

t_i is the equal bilateral tolerance of the i^{th} component in the stack-up.

The minimum gap is equal to the mean value minus the Worst Case variation at the gap. The maximum gap is equal to the mean value plus the Worst Case variation at the gap. For example, the Worst Case tolerance of the gap in Figure 2-8 is:

$$t_{wc} = |(-1)0.25| + |(-1)0.2| + |(-1)0.3| + |(-1)0.1| + |(1)0.5| = 1.35$$

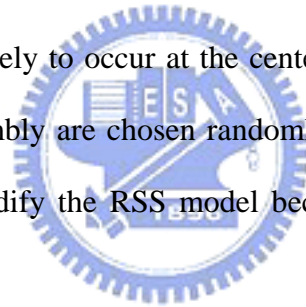
$$\text{Minimum gap} = d_g - t_{wc} = 1 - 1.35 = -0.35$$

$$\text{Maximum gap} = d_g + t_{wc} = 1 + 1.35 = 2.35$$

Above negative minimum gap value means there is interference in the gap. While the CTQ is that the “gap” must be great than zero, we must increase the minimum gap by 0.35 to meet the CTQ.

2.4. Statistical Tolerance Analysis

The laws of probability and random chance dominate the component manufacturing process. It is nature to make components with deviations spread out about the target dimensions. Statistical process control (SPC) will make a manufacturing process to output a feature with normal distribution property. Statistical tolerance analysis [11, 16, 17] assumes that all processes are in control. The Root Sum of the Squares (RSS) model is based on the fact that all dimensions are likely to occur at the center of tolerance range rather than at the ends and the parts in an assembly are chosen randomly. Modified Root Sum of the Squares (MRSS) model is used to modify the RSS model because some of the assumption in RSS mode is unreasonable.



2.4.1. The Root Sum of the Squares (RSS) model

The RSS equation is based on statistically principles of combinations of standard deviation. Assume y is the CTQ of a product and the product is assembled by n independent components x_i . The assembly function of the product can be expressed as $y = f(x_1, x_2, \dots, x_n)$. The information we have is the data of x_i . According to the definition in Equation (2-5), the standard deviation of y , or σ_y is

$$\sigma_y^2 = \frac{\sum_{i=1}^r (y_i - \mu_y)^2}{r} \quad (2-20)$$

where

μ_y is the mean of random variable y .

r is the total number of population.

Let $\Delta_y = y_i - \mu_y$,

If Δ_y is small, then

$$\Delta y \approx dy = \frac{\partial f}{\partial x_1} dx_1 + \frac{\partial f}{\partial x_2} dx_2 + \dots + \frac{\partial f}{\partial x_n} dx_n \quad (2-21)$$

Therefore,

$$\sigma_y^2 = \frac{\sum_{i=1}^r dy_i^2}{r} \quad (2-22)$$

From Equation (2-22),

$$\begin{aligned} d_y^2 &= \left(\frac{\partial f}{\partial x_1} dx_1 + \frac{\partial f}{\partial x_2} dx_2 + \dots + \frac{\partial f}{\partial x_n} dx_n \right)^2 \\ &= \left(\frac{\partial f}{\partial x_1} \right)^2 (dx_1)^2 + \left(\frac{\partial f}{\partial x_2} \right)^2 (dx_2)^2 + \dots + \left(\frac{\partial f}{\partial x_n} \right)^2 (dx_n)^2 \\ &\quad + \sum_{j=1}^n \sum_{k=1}^n \left[\left(\frac{\partial f}{\partial x_j} \right) \left(\frac{\partial f}{\partial x_k} \right) (dx_j)(dx_k) \right]_{j \neq k} \end{aligned} \quad (2-23)$$

If all the variables x_i are independent,

$$\sum_{j=1}^n \sum_{k=1}^n \left[\left(\frac{\partial f}{\partial x_j} \right) \left(\frac{\partial f}{\partial x_k} \right) (dx_j)(dx_k) \right]_{j \neq k} = 0 \quad (2-24)$$

The same would hold true for all similar terms. As a result,

$$\sum_{i=1}^r (dy_i)^2 = \sum_{i=1}^r \left[\left(\frac{\partial f}{\partial x_1} \right)^2 (dx_1)^2 + \left(\frac{\partial f}{\partial x_2} \right)^2 (dx_2)^2 + \dots + \left(\frac{\partial f}{\partial x_n} \right)^2 (dx_n)^2 \right]_i \quad (2-25)$$

Each partial derivative is evaluated at its mean value, which is chosen as the nominal. Thus,

$$\frac{\partial f}{\partial x_i} = C_i \quad (2-26)$$

where C_i is a constant for each x_i ,

$$\sum_{i=1}^r (dy_i)^2 = \left(\frac{\partial f}{\partial x_1}\right)^2 \sum_{i=1}^r (dx_1)_i^2 + \left(\frac{\partial f}{\partial x_2}\right)^2 \sum_{i=1}^r (dx_2)_i^2 + \dots + \left(\frac{\partial f}{\partial x_n}\right)^2 \sum_{i=1}^r (dx_n)_i^2 \quad (2-27)$$

Substitute Equation (2-27) into Equation (2-22), the standard deviation is obtained.

$$\begin{aligned} \sigma_y^2 &= \frac{\left(\frac{\partial f}{\partial x_1}\right)^2 \sum_{i=1}^r (dx_1)_i^2 + \left(\frac{\partial f}{\partial x_2}\right)^2 \sum_{i=1}^r (dx_2)_i^2 + \dots + \left(\frac{\partial f}{\partial x_n}\right)^2 \sum_{i=1}^r (dx_n)_i^2}{r} \\ &= \left(\frac{\partial f}{\partial x_1}\right)^2 \frac{\sum_{i=1}^r (dx_1)_i^2}{r} + \left(\frac{\partial f}{\partial x_2}\right)^2 \frac{\sum_{i=1}^r (dx_2)_i^2}{r} + \dots + \left(\frac{\partial f}{\partial x_n}\right)^2 \frac{\sum_{i=1}^r (dx_n)_i^2}{r} \\ &= \left(\frac{\partial f}{\partial x_1}\right)^2 \sigma_{x_1}^2 + \left(\frac{\partial f}{\partial x_2}\right)^2 \sigma_{x_2}^2 + \dots + \left(\frac{\partial f}{\partial x_n}\right)^2 \sigma_{x_n}^2 \end{aligned} \quad (2-28)$$

where $\frac{\partial f}{\partial x_i}$ is the sensitivity. Let $\frac{\partial f}{\partial x_i} = a_i$, Equation (2-28) becomes

$$\sigma_y^2 = a_1^2 \sigma_{x_1}^2 + a_2^2 \sigma_{x_2}^2 + \dots + a_n^2 \sigma_{x_n}^2 \quad (2-29)$$

The independent variables x_i can be considered as a dimension, D_i , with a equal bilateral tolerance, T_i . The nominal dimension, D_i , will be the same as the mean of normal distribution of the tolerance. Apply T_i and D_i to standard normal distribution variable Z in Equation (2-13) as below.

$$Z_i = \frac{USL_i - D_i}{\sigma_i} = \frac{D_i - LSL_i}{\sigma_i} = \frac{T_i}{\sigma_i} \quad (2-30)$$

$$\sigma_i = \frac{T_i}{Z_i} \quad (2-31)$$

Substitute Equation (2-31) into Equation (2-29). We have

$$\left(\frac{T_y}{Z_y}\right)^2 = \left(\frac{a_1 T_1}{Z_1}\right)^2 + \left(\frac{a_2 T_2}{Z_2}\right)^2 + \dots + \left(\frac{a_n T_n}{Z_n}\right)^2 \quad (2-32)$$

If all of the tolerance zones cover the equal numbers of standard deviation, for instance all are

3σ tolerance, then $Z_y = Z_1 = Z_2 = \dots = Z_n$. In addition, let $a_1 = a_2 = \dots = a_n = \pm 1$. Equation (2-32) will reduce to the classical RSS equation

$$T_y^2 = T_1^2 + T_2^2 + \dots + T_n^2 \quad \text{or} \quad T_y = \sqrt{T_1^2 + T_2^2 + \dots + T_n^2} \quad (2-33)$$

From Equation (2-32) we have the general form of RSS equation with sensitivities shown as below.

$$t_{rss} = \sqrt{a_1^2 t_1^2 + a_2^2 t_2^2 + \dots + a_n^2 t_n^2} \quad (2-34)$$

where

t_{rss} is the expected equal bilateral tolerance of RSS model

Now we can evaluate the Root Sum of the Squares tolerance of the gap in Figure 2-8:

$$t_{rss} = \sqrt{(-1)^2 0.25^2 + (-1)^2 0.2^2 + (-1)^2 0.3^2 + (-1)^2 0.1^2 + (1)^2 0.5^2} = 0.673$$

$$\text{Minimum gap} = d_g - t_{rss} = 1 - 0.673 = 0.327$$

$$\text{Maximum gap} = d_g + t_{rss} = 1 + 0.673 = 1.673$$

The positive minimum gap reveals that there is no interference at the “gap.” In a word, we have made the following assumption in the RSS model:

- (1) All manufacturing processes are centered on the midpoint of the dimension, and the distributions are normal. In addition, the tolerances have been converted to equal bilateral tolerances.
- (2) All tolerance zones cover the same number of standard deviations. The unqualified components also include in the assembly.
- (3) All component dimensions are independent.
- (4) The components included in a assembly have been thoroughly mixed and are chosen randomly during assembly process.

However, these are usually not the true situation. Many manufacturing process tend to drift,

the mean of the normal distribution is not on the midpoint of the tolerance zone. Due to the consideration of tool wear compensation, some process is deliberately decentered. Furthermore, it is difficult to make all tolerances with the same number of standard deviations. As a result, the RSS model usually gives an over optimistic analysis result than the real world. The Modified Root Sum of the Squares (MRSS) model is design to compensate for these drawbacks

2.4.2. The Modified Root Sum of the Squares (MRSS) model

A correction factor is used to compensate the shortcomings of RSS mode. The Modified Root Sum of the Squares (MRSS) model is described below.

$$t_{mrss} = C_f \times t_{rss} = C_f \sqrt{a_1^2 t_1^2 + a_2^2 t_2^2 + \dots + a_n^2 t_n^2} \quad (2-35)$$

where

C_f is the correction factor

t_{mrss} is the expected equal bilateral tolerance of MRSS model

Many correction factors have been suggested. The most common correction factor is 1.5, which is recommended by Bender and Levy. Gladman suggested the range as 1.4 to 1.8 [17]. There is a limitation in this method. If the number of components in the assembly is equal to two, the MRSS tolerance is greater than the Worst Case tolerance. The following correction factor will always give a t_{mrss} value that is smaller than t_{wc} [16].

$$C_f = \frac{0.5(t_{wc} - t_{rss})}{t_{rss}(\sqrt{n} - 1)} + 1 \quad (2-36)$$

Therefore, the correction factor of the MRSS tolerance of the gap in Figure 2-8 is:

$$C_f = \frac{0.5(1.35 - 0.673)}{0.673(\sqrt{5} - 1)} + 1 = 1.407$$

$$t_{mrss} = 1.407 \times 0.673 = 0.947$$

$$\text{Minimum gap} = d_g - t_{mrss} = 1 - 0.947 = 0.053$$

$$\text{Maximum gap} = d_g + t_{mrss} = 1 + 0.947 = 1.947$$

2.5. Contribution Analysis

The tolerance sensitivity quantifies the change in the output variable relative to a change in a single input variable. It tells how the arrangement of components and the geometry contribute to assembly variation. The a_i in Equation (2-18) and (2-29) is sensitivity factors corresponding to each tolerance t_i of component x_i . In order to have the ranking of how each tolerance contribute to the assembly tolerance, a proportion contribution value is used to represent the sensitivity. The calculation is different for Worst Case model and RSS model.

For Worst Case model:

$$P_i = \frac{|a_i t_i|}{\sum_{i=1}^n |a_i t_i|} \quad (2-37)$$

where P_i is the percent contribution of the tolerance of i^{th} component in the stack-up.

For RSS model:

$$P_i = \frac{(a_i t_i)^2}{\sum_{i=1}^n (a_i t_i)^2} \quad (2-38)$$

Table 2-2 gives the contribution analysis of the example in Figure 2-8.

Table 2-2 The tolerance contribution analysis of Figure 2-8

Part name	Sensitivity factor (a_i)	Bilateral tolerance (t_i)	$ a_i t_i $	$(a_i t_i)^2$	Worst Case contribution	RSS contribution
A	-1	0.1	0.1	0.01	7.4%	2.2%
B	-1	0.3	0.3	0.09	22.2%	19.9%
C	-1	0.2	0.2	0.04	14.8%	8.8%
D	-1	0.25	0.25	0.0625	18.5%	13.8%
E	1	0.5	0.5	0.25	37.0%	55.2%
		Summation	1.35	0.4525	100.0%	100.0%

2.6. Computer Aided Tolerancing

Since most of the mechanical products are three dimensional and quite complicated, the mathematical model is too complex to formulate. The advances of computer technology have made computer aided tolerancing (CAT) system available. Most of the CAT system uses the CAD geometry to derive the mathematical tolerance model of the product. Due to the mathematical tolerance model subjects to the assembly relationships of the CAD model, some of mathematical tolerance model can not represent the mechanical system exactly. Some software is designed for engineer to program a mathematical tolerance model to simulate assembly tolerance stack-up.

Most of the CAT system calculates the assembly tolerance distribution by Monte Carlo Simulation (MCS) technique. MCS is a statistical technique based on a random number generator. Pradeep [18] have made a comparison of MCS with other tolerance analysis approaches. In general, MCS can be applied to both the linear and nonlinear function of assembly CTQ characteristics, and the distribution of the input variables can be normal or non-normal distribution. MCS outputs the distribution of CTQ characteristics directly that makes the results easy to understand. Simplicity, versatility of application, and unlimited

precision has made MCS the most popular tolerance analysis method. However, MCS needs to generate a large number of random samples simulating the imaginary product assemblies to get the accurate estimate of the CTQ characteristics. Each time, changes are made to all input tolerances, the repeated simulation makes the analysis time consuming. The MCS process is conducted as below:

- (1) Establishing the CTQs as described in Sec. 2.2.1.
- (2) Formulate CTQ functions as described in Sec. 2.2.2. Derive the mathematical tolerance function from the CAD geometry is an easy way. However it is necessary to consider the assembly relationships built in the CAD model.
- (3) Specify the process distribution and the tolerance range corresponding to number of standard deviations to each tolerance. The distribution usually is based on the past experience of manufacturing process or on a sample data. Complex non-normal distribution can be obtained easily by assigning appropriate skew and kurtosis.
- (4) According to the specified process distribution and tolerance range, one set of component dimensions for a sample assembly is selected using a random number generator. The characteristic of CTQ is calculated using the mathematical tolerance model. Then, repeat the sampling and simulation process to get a sufficient large number of the imaginary assemblies.
- (5) Using the simulation data to estimate the statistical characteristic of the CTQ. The histograms can be plotted and the distribution curves can be fitted for each CTQ. The basic statistical characteristic, mean and standard deviation, can be estimated. The production yield rate and the assembly manufacturing process capability index can be calculated.
- (6) Modify the tolerance design. If the yield rate estimated in previous step is not satisfactory, tolerances associated with the individual dimensions may be redesigned. The tolerances with high contribution ranking will be chosen first to modify the tolerance zone. The

manufacturing process also can be reselected by the principle of compensatory control provided by Gerth [19].

The CAT software used in this study is VSA-3D[®]. The simulation results of the gap of the example in Figure 2-8 is shown in Figure 2-10 and Figure 2-11. The output gives the nominal value, mean value, standard deviation, Cp, Cpk, and the histogram of the measurement. In addition, an actual range based on simulated observations, a statistical range, and statistical descriptions of the process also is shown in the output. The contribution analysis is called HLM (Hi-Low-Median) analysis in VSA-3D[®]. The HLM analysis is a one-factor-at-a-time study with the factor levels set at the upper, lower, and nominal specification limits of the tolerance distributions while holding the other factors at their nominal dimensions.

The result in Figure 2-10 assumes that all manufacturing processes are centered on the midpoint of the dimension, the distributions are normal, and all tolerances are with 3 sigma points at the tolerance limit. The gap at 3 sigma point is 0.6696mm that is almost the same as the result of RSS model. The HLM analysis also gives the same result of RSS contribution analysis. In Figure 2-11, it is assumed that the mean of the manufacturing process drifts 1.5 sigma uniformly. The gap at 3 sigma point is 0.8847mm that is close to the result of MRSS model.

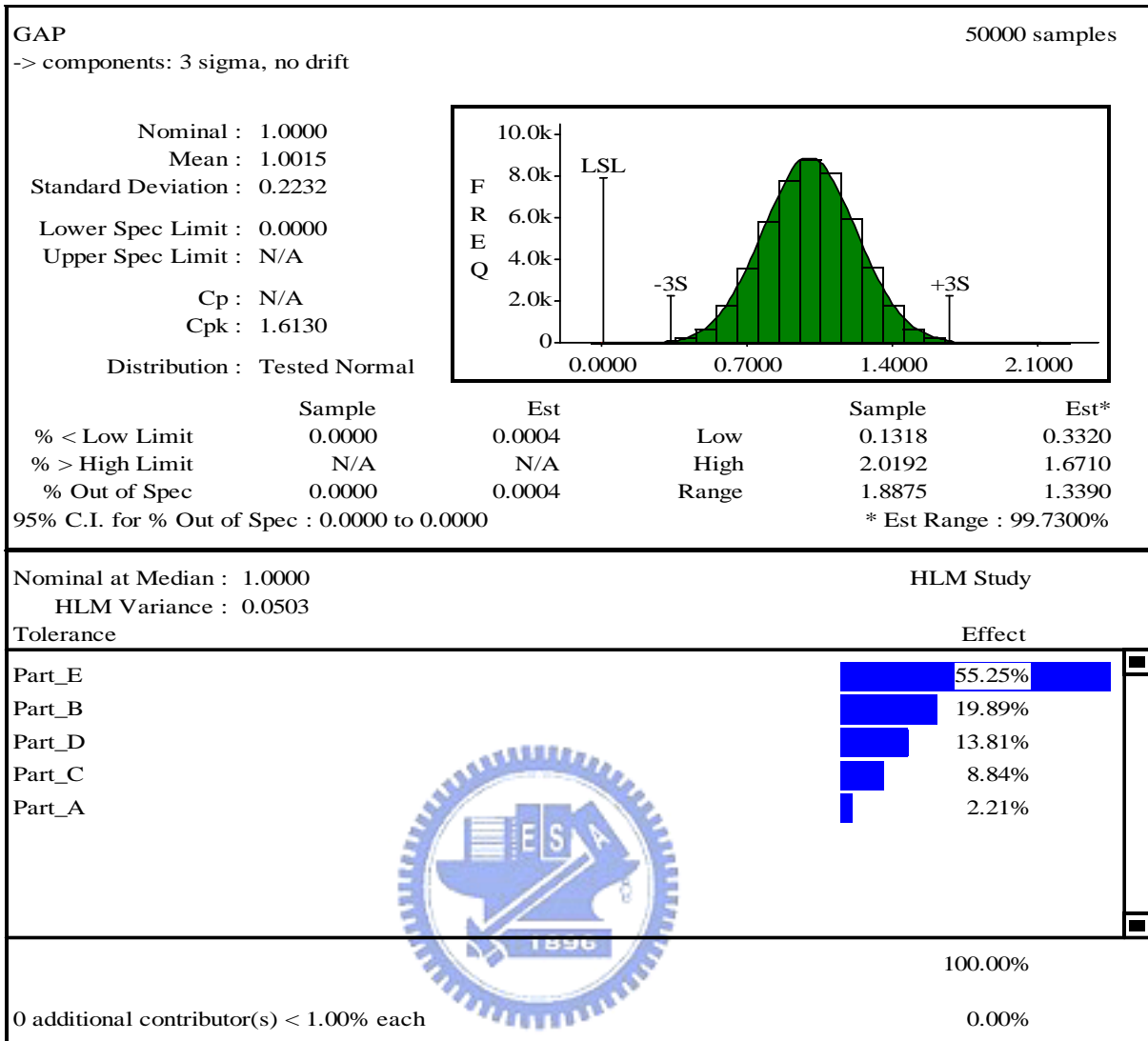


Figure 2-10 The gap in Figure 2-8 analyzed by CAT without process drift

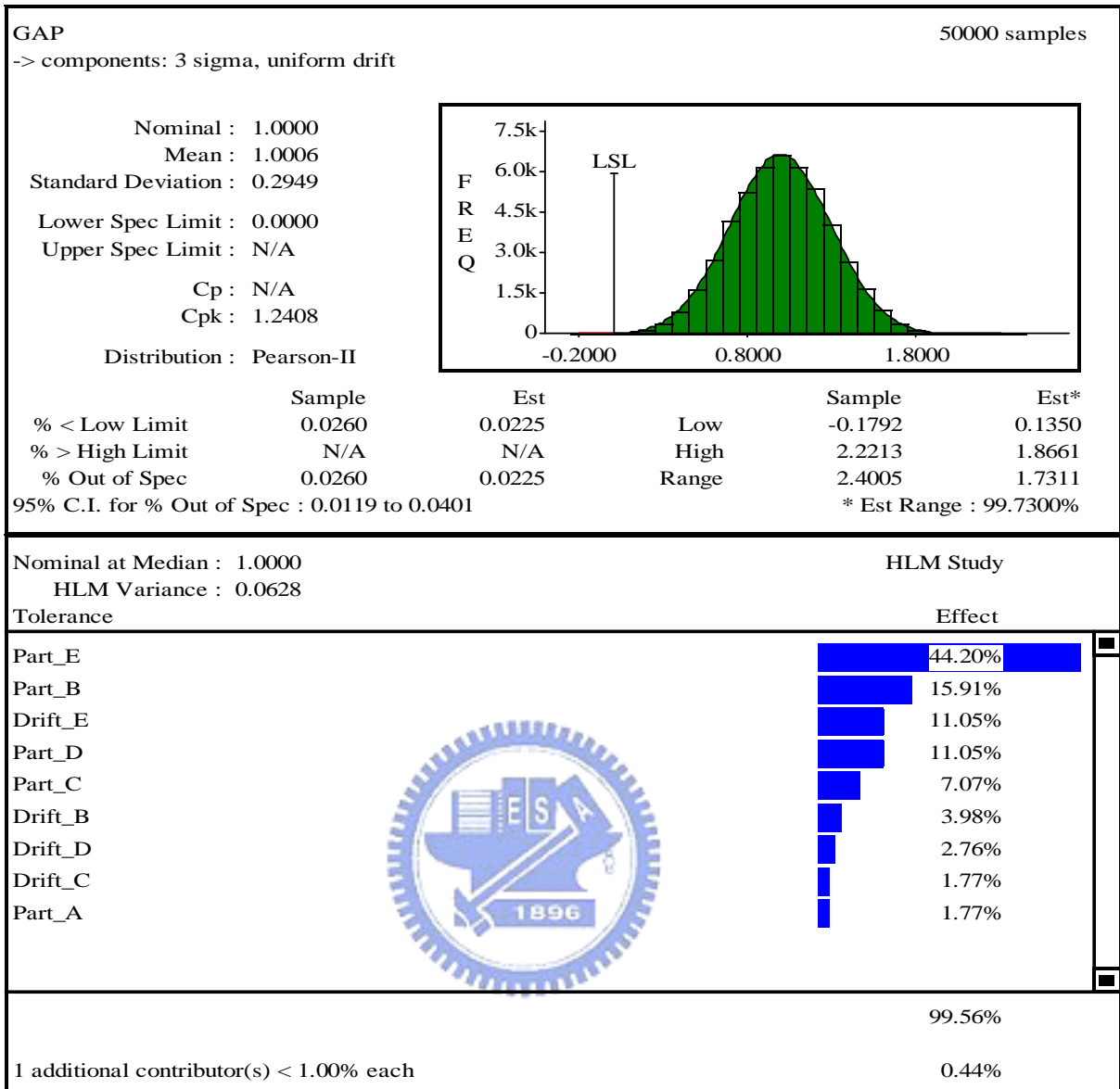


Figure 2-11 The gap in Figure 2-8 analyzed by CAT with process drift

Chapter 3. Lens System

Usually one or several optical elements are mounted together to construct an opto-mechanical subassemblies or assemblies. Lens is a typical opto-mechanical assembly. Optical elements are lenses, prisms, mirrors, windows and etc. First, the perfect centered optics and mounting principle will be described in this chapter. Afterwards, the mounting principle and assembly method is discussed. Finally, how the tolerances of optical elements and mechanical components cause element tilt, decenter, and despace which lead to extra aberration is described in detail. The discussion emphasizes on the lenses of optical axis symmetric whether it is spherical or aspheric.

3.1. Centered Optics

Yoder [20] stated that the ultimate usefulness of the opto-mechanical device depends on having the right optics in the right places and keeping them in the operating condition. It means that centering and spacing dimensions are most critical in lens mounting. Yoder [21] also describe the centered optics. Because of the rotationally symmetrical properties of the optical surfaces and their aberrations, it is easy to image that there is a straight line in space and to locate all surfaces having optical power symmetrically about the line. If the all centers of curvature of the surfaces lie on this line, we define the line as the optical axis, and the system has been centered. In the case of flat surfaces with nominal centered design, they are generally assumed to be normal to the optical axis and hence also symmetric about that axis. Figure 3-1 (a) illustrates a centered biconvex lens with centers of curvature $C1$ and $C2$ of the surfaces $R1$ and $R2$. Figure 3-1 (b) shows a plano-convex lens with optical axis passing through the curvature center $C2$ and perpendicular to $R1$.

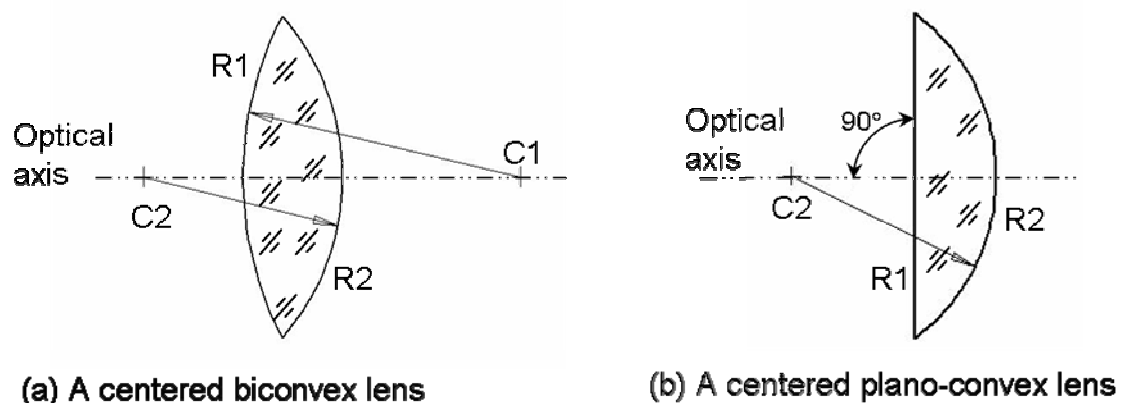


Figure 3-1 Perfect centered optical lens

Manufacturing or assembly errors that cause one or more surface center to move away from the optical axis produces asymmetric aberrations. In addition, the lack of symmetry about the axis leads to off-axis aberrations. The optical designer will define the sensitivity of the optical system to these errors. Then tolerances can be assigned to the components and the locating condition of the components. If the variations of resultant assembly characteristics fall within the allowable range of tolerances then the system performance is acceptable.

3.2. Lens Mounting Principles

A perfect centered optical system, such as shown in Figure 3-1, has the centers of curvature of all the surfaces lying on a single axis. Cade [22] discussed the basic principle of mounting a lens. Figure 3-2 illustrates a sphere setting on a ring. The Z-axis of the ring is perfect aligned with the geometric center of the sphere C_s . A plano convex lens can be made by slicing the sphere on any plane. If the optical axis of the plano convex lens would like to coincide with the Z-axis of the ring, the sliced plane must be perpendicular to the Z-axis. This plane can be mounted perfectly square with the lens barrel if the barrel is provided with an accurately shoulder or ring.

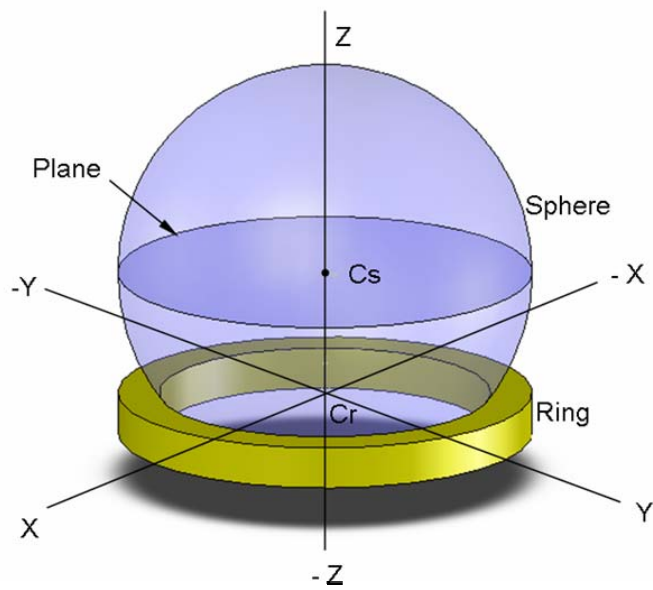


Figure 3-2 Centering principle

Hopkin [23] pointed out the fact that the overall thickness of the lens assembly is a minimum when all the lenses are perfectly centered. The lens will tend to center itself if the lens is assembled with the optical axis vertical. When slightly tapping the lens, it will encourage the assembly to settle into the centered position. Figure 3-3 shows a perfectly centered lens that has the centers of curvature of all surfaces lying on a single axis. The spacer has matching curved surfaces with the same curvature as the contacted lens. The overall thickness of the assembly is a minimum.

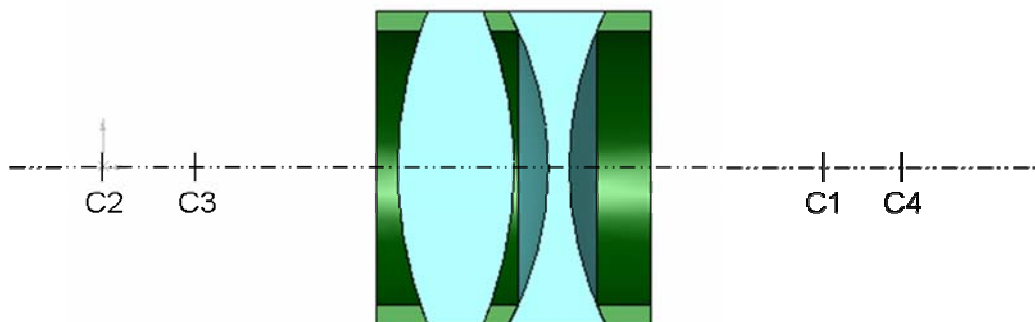


Figure 3-3 A perfectly centered lens and spacer

However, the self-centering does not always occur and residual misalignment always exists. The lens illustrated in Figure 3-4 will not self-center because the centers of curvature of surface 2 and surface 4 are coincide. The second lens and spacer may rotate on surface 2 without changing the overall lens thickness. Therefore, when two centers of curvature are close together, the self-centering condition is weak. It is necessary to have some other ways to locate the lenses in a centered position. The method is to use the edges of the lenses. Each lens and spacer is edged to a specific diameter. The cylindrical edge surface must be generated on an axis concentric with the optical axis. If the cell used to mount the lens and spacer is a true cylinder and intimate contact occurs between the lens rim and the cell inside diameter (ID), the optical assembly will be centered as shown in Figure 3-5.

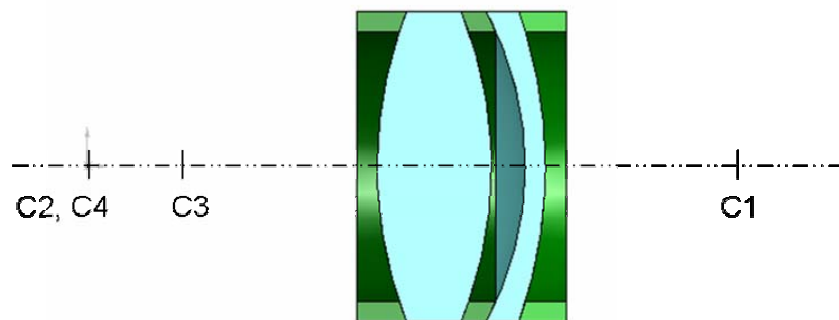


Figure 3-4 A special case which self-centering will not occur

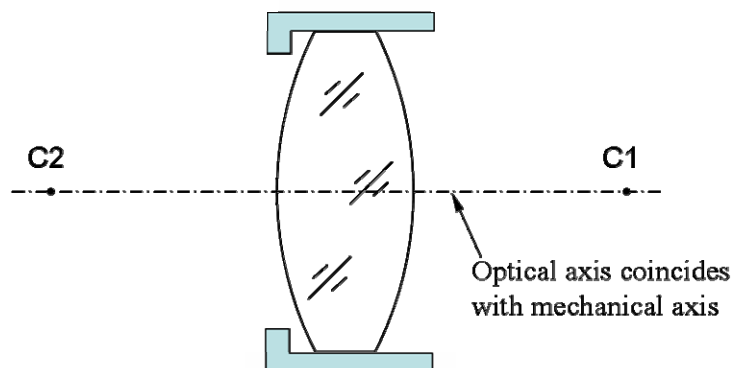


Figure 3-5 A perfectly centered and edged lens mounted in a perfect cell

A Z number is used to estimate the self-centering condition of a lens. As shown in Figure 3-6, the Z number is defined as:

$$Z \text{ number} = \frac{Y_1}{2R_1} - \frac{Y_2}{2R_2} \quad (3-1)$$

where Y_1 and Y_2 are the contact heights from the optical axis. R_1 and R_2 are the surface radii. Radius R is positive when the center of the curvature is to the right of the surface. Radius R is negative when the center of the curvature is to the left of the surface. When the Z number of a lens element is bigger than 0.07, the lens element has good self-centering condition [21].

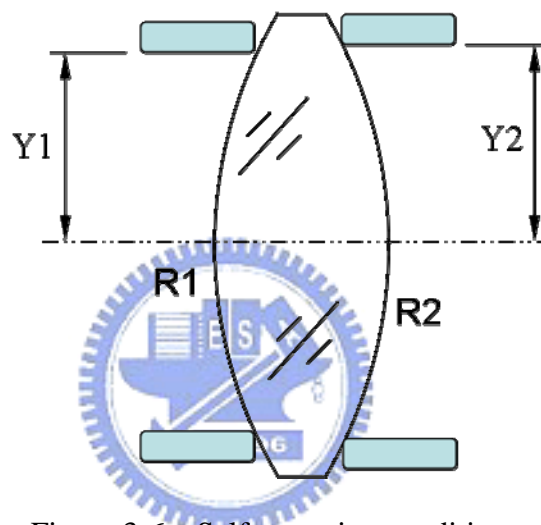


Figure 3-6 Self-centering condition

In practice, because lenses are never perfectly centered and edged to true cylinders and diameters, surface tilt always exists in lenses. Variation also exists in mechanical components such as spacer, cell and barrel. There must be clearance between the lenses and the cell (or barrel) that will lead to element tilt and decenter. Therefore, it is necessary to specify tolerances to each component and to analyze the opto-mechanical tolerance stack-up.

3.3. Lens Assemblies Design

Yoder [24] have introduced the lens assembly designs usually adopted by engineers.

“Drop-In” Assembly

The “drop-in” assembly design concept is widely used in commercial applications. The lens elements and the mounting components are manufactured to specified dimensions within specified tolerances. The lens is assembled without further machining and with a minimum of adjustment. Low cost and ease of assembly make “drop-in” design suitable for high volume production. Because all parts are selected randomly from the stock, it is expected that a small percentage of end products will not meet the performance requirement. Figure 3-7 illustrates an example of “drop-in” assembly. The threaded retainer holds the lens components and spacer in place. Sharp corner interfaces are used throughout. The centering accuracy depends primarily on the edge of lenses. The axial preload exerted by retainer will squeeze out the total edge thickness difference before the rims of the lenses touch the ID of cell. The axial space between the lenses depends on the spacer dimensions and the radius errors of the lenses.

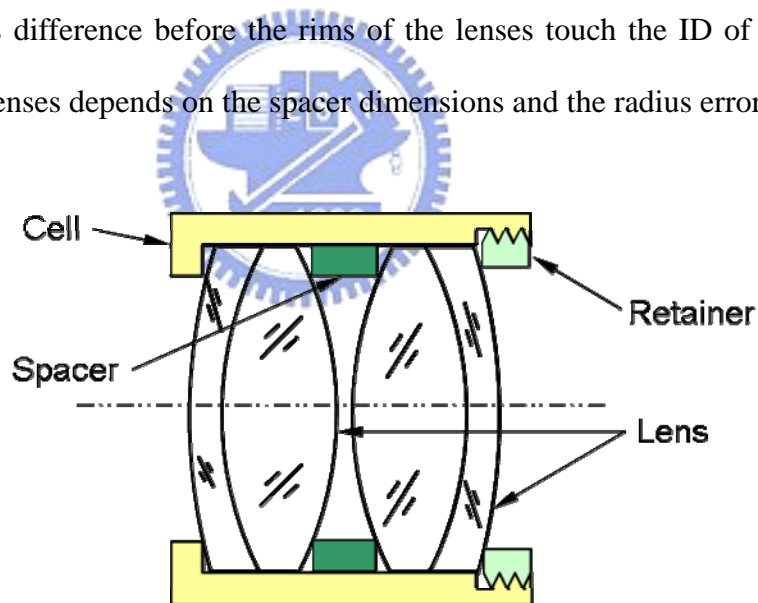


Figure 3-7 A optical subsystem assembled by “drop-in” technique

“Lathe” Assembly

“Lathe Assembly” technique is often used in the assembly of lenses for high performance aerial reconnaissance and space science payload. The lens seats in the mount are

custom machined on a lathe to fit closely to the measured outside diameters (ODs) of a specific lens or specific set of lenses. Axial position of each seat is also determined during this operation. The lenses should be precision edged to a high degree of roundness. Sufficient material is provided at the corresponding seat IDs for the ensuing fitting and removing process. Radial clearances between lens and mount are usually ranging from 1.5 μ m to 5 μ m.

Subcell Assembly

Subcell assembly design have the lenses mounted and aligned precisely within individual subcells. These subcells inserted in sequence into precisely machined IDs of outer barrel. The thicknesses of subcells and spacers are precisely machined so that the air spaces between lenses are within design tolerances without adjustment. Figure 3-8 illustrates an example of subcell assembly lens barrel design.

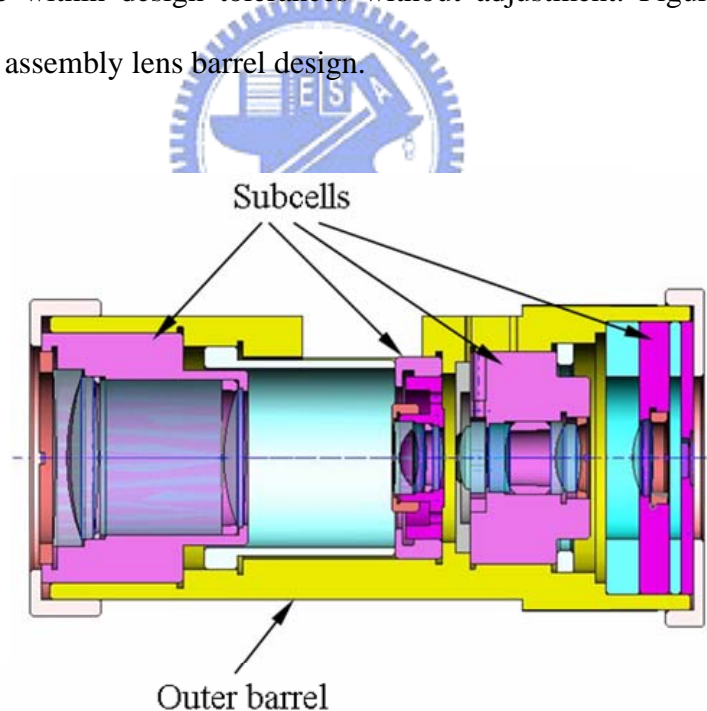


Figure 3-8 Subcell assembly lens barrel design

3.4. Variations in Lens Element

ISO 10110 Standard [25] had defined the specification in drawing of the characteristics, especially the tolerances, of optical elements and system. First, there are the purely optical specifications which are primarily materials related. Second, there are opto-mechanical specifications such as surface form, radius, thickness, and centering. Third, there are surface texture and surface imperfections specifications. Finally, there are surface treatment and coating specifications. The opto-mechanical specifications are the items that will cause lenses positions errors in an assembly. They are described as following.

Radii of Curvature

Spherical surfaces are defined by starting the radius of curvature with a dimensional tolerance. This tolerance shall indicate the range within which the actual surface must be contained. As most optical parameters in a system are proportional to changes in curvature rather than radius, the radius tolerance is obtained by converting the tolerance of curvature to the tolerance of radius. Thorburn [26] noted that setting a fixed tolerance of the sagitta is a more reasonable method of radius tolerancing. Sagitta error results from the test surface having a radius of curvature different from the specified radius [25]. The surface form deviation is to be specified in “fringe spacings”. One fringe spacing is a distance equal to one half the specified light wavelength. Unless otherwise specified, the wavelength is that of the green spectral line of mercury, 546.07nm. The number of fringe spacings is corresponding to a dimensional radius of curvature tolerance. The relationship between sagitta error tolerance and radius of curvature tolerance can be obtained by the following formula, assume the ration $\Delta R/R$ is small.

$$N = \frac{2\Delta R}{\lambda} \left\{ 1 - \sqrt{1 - \left[\frac{\phi}{2R} \right]^2} \right\} \quad (3-2)$$

If the ration ϕ/R is small, this formula may be simplified as:

$$N \approx \left[\frac{\phi}{2R} \right]^2 \cdot \frac{\Delta R}{\lambda} \quad (3-3)$$

where

N is the maximum permissible number of fringe spacings,

R is the radius of curvature,

ΔR is the dimensional radius of curvature tolerance,

ϕ is the diameter of test area, and

λ is the wavelength (normally, 546.07nm).

Center Thickness

Due to the special optical fabrication process, the thicknesses are difficult to measure and maintain to a close tolerance. Parks [27] recommended keep the center thickness tolerance as loose as possible. The variation of the lens center thickness will lead to the position shift of the following optical surfaces that are attached to it as shown in Figure 3-9. The translation of optic along the optical axis is called element despace. The thickness shall be indicated as a nominal size with a (preferably symmetrically) tolerance.

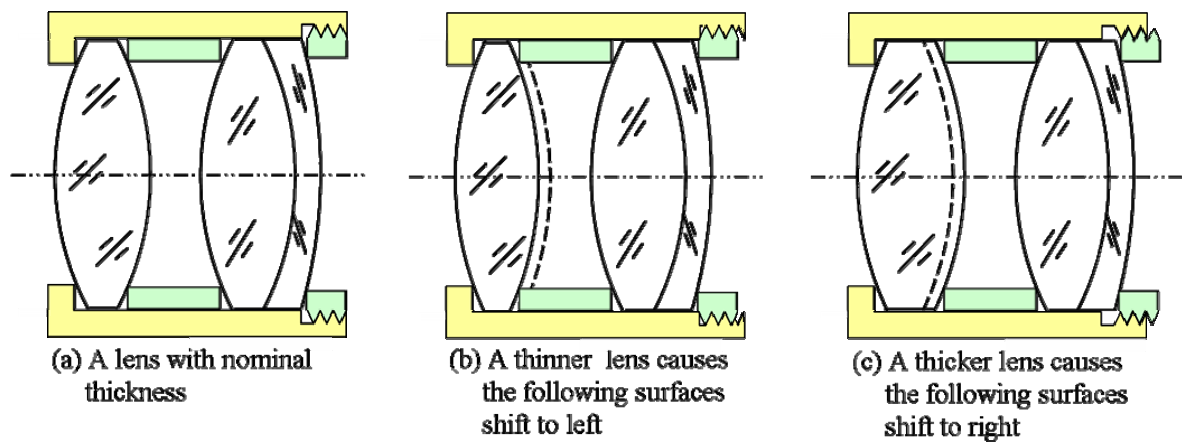


Figure 3-9 Center thickness variation causes surfaces despace

Diameter

The ID of lens cell is always designed to be larger than the OD of lens. The variation of OD of a lens element will alter the clearance between the rims of the lenses and the ID of lens cell. “Floating” assembly may occur based on how the lens cell and the lens locate to one another. The lens cell and the lens will probably not assembly concentric to each other. Therefore potential element tilt and decenter occur as illustrated in Figure 3-10.

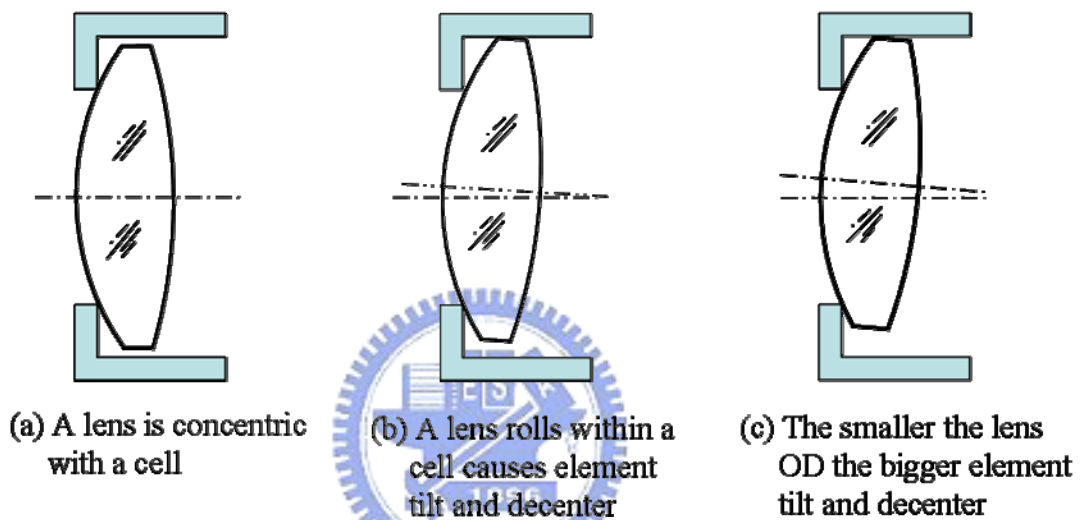


Figure 3-10 Lens OD variation causes element tilt and decenter

Centering

Centered optics has been described in Section 3.1. Besides the optical axis, the datum axis is as important as the optical axis. The datum axis [25] is an axis selected by consideration of specific features of an optical system. It serves as a reference for the location of surfaces, elements and assemblies. For a lens element, the datum axis is usually referencing the cylindrical rim. The datum axis is also called the mechanical axis. A centering error exists when an optical surface is not perpendicular to the mechanical axis at the intersection point. The tilt angle of an optical element is the angle between the mechanical axis and the optical axis. Thorburn [26] interpreted the centering tolerances as shown in Figure 3-11. A centered

lens is shown in Figure 3-11 (a). A decentered lens is illustrated in Figure 3-11 (b). In which the optical axis has shifted an amount of ε_s from the mechanical axis. A tilted lens with a tilt angle τ_s is shown in Figure 3-11 (c). In Figure 3-11 (d), the center of curvature of surface #2 does not lie on the mechanical axis. That surface can be designated as either tilted or decentered. There is no difference between tilt and displacement of a single spherical surface. The result of centering error is usually called as surface tilt. It must be noted that centering error is different from the element tilt and decenter which are the position variation of a lens within a cell.

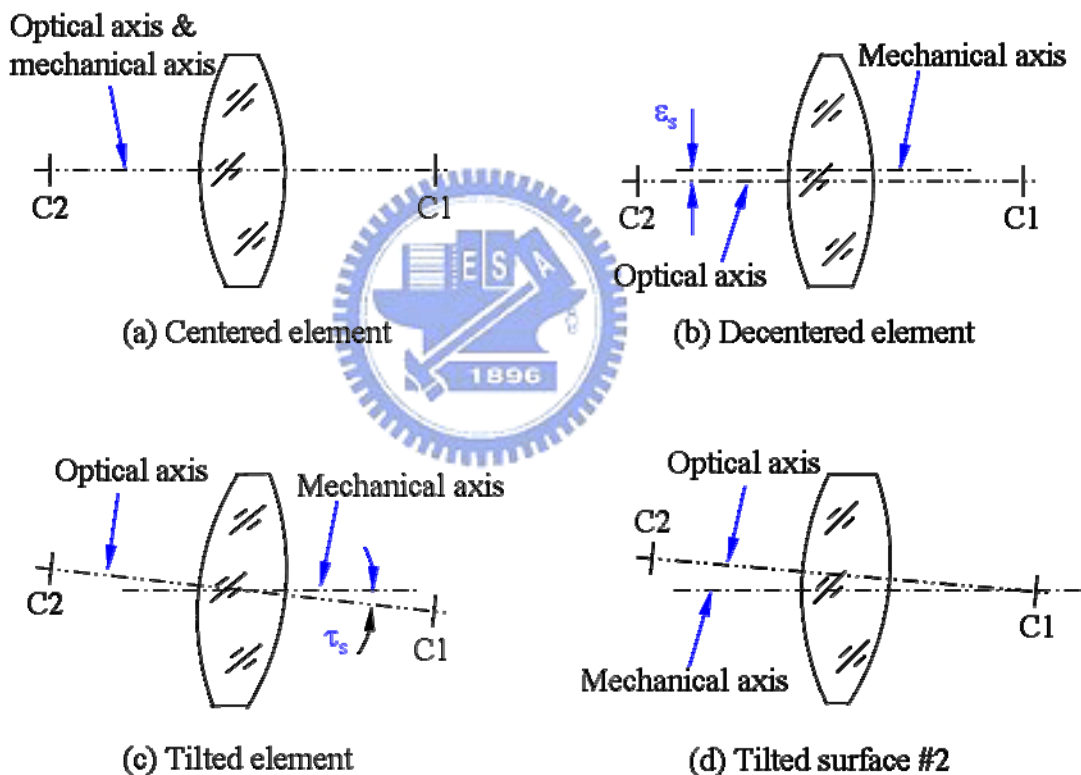


Figure 3-11 Centering tolerances

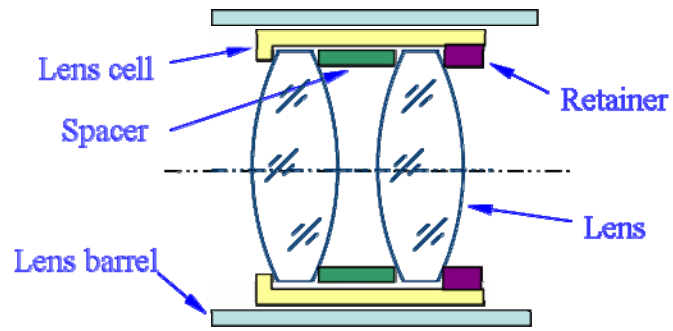
The mechanical axis of a lens element is determined by the edge grinding process after surface polishing. Edge grinding makes the lens having cylinder rim. This cylinder defines a mechanical axis of the lens element. Whether the mechanical axis coincides with the lens' optical axis or not, that depends on how the optical axis is oriented during the lens edge grinding process. In fact, an actual element with centering surface tilt will be a mixed mode of

the four simple cases in Figure 3-11. The two centers of curvature will lie at arbitrary distances from the mechanical axis. When a group of lenses are stack up, the centers of curvature will not fall on a single line. Centering errors cause extra aberrations that degrade the optical performance substantially.

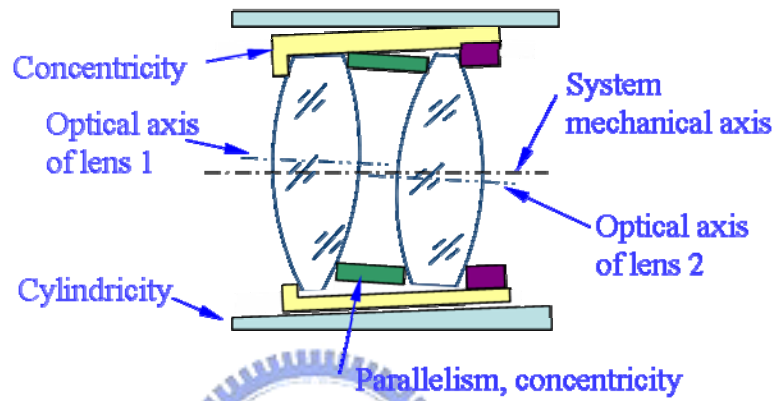
3.5. Variations in Lens Assembly

A typical lens mounting assembly is illustrated in Figure 3-12. Lens element is mounted inside the lens cell and rest on the shoulder of cell. Lens elements are separated by a carefully machined spacer to obtain the required air space between surface vertices. Then a retainer is inserted into the cell to hold the lenses. The optical designer assumes that individual lenses are centered on the imaginary straight line which coincides with the axis of cell and lens barrel as shown in Figure 3-12(a). However there are several places where variations may occur [28]. The major assembly variation sources consist of lens-to-cell clearances, cell-to-barrel clearances, concentricity between the ID and OD of the cell, the cylindricity of the inside bore of lens barrel, and the geometrical accuracy of the spacer as shown in Figure 3-12(b). The mechanical engineer must control the tolerances stack-up attributed to the individual component variations to meet the requirements specified in optical design. The mechanical engineer must also provide the resultant tolerance stack-up distribution information to optical designer.

Manufacturing and assembly variations that make one or more surface centers move away from the optical axis will cause extra aberrations. It is the reasons for optical performance degradation. There are many factors causing variations. The resultant position variations of optical elements can be classified as element tilt, decenter and despace. These are the major CTQs which will be modeled and simulated in this study.

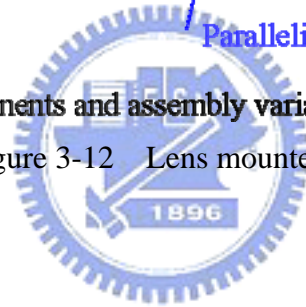


(a) Idea case of lens assembly



(b) Components and assembly variation in real world

Figure 3-12 Lens mounted in barrel



Chapter 4. Opto-mechanical tolerance model

4.1. Tolerance modeling

Tolerances on linear and angular dimensions may be expressed in several ways. Plus and Minus Tolerancing will be used in this study. The dimension is given first and followed by a plus and minus expression of tolerances. Converting dimensions to equal bilateral tolerance has been discussed in Section 2.2. It is assumed that the tolerance is in normal distribution, and the tolerance spans a $\pm 3\sigma$ range distribution with its mean value at the midpoint of the range. Then, the dimensions can be expressed as:

$$\text{Dimension} \pm \text{tolerance} = \text{Dimension} + \frac{Z}{3} \times \text{tolerance} \quad (4-1)$$

where the random variable Z is defined in Equation (2-13) and is subjected to the probability density function, Equation (2-14).

Geometric dimensioning and tolerancing (GD&T) is a system of symbols defined in ASME Y24.5M-1994 Standard [13]. It is used to specify geometric characteristics and other dimensional requirements of the features of a part. There are five tolerance types: form, profile, orientation, location, and runout. The tolerance value describes how the features deviate from the true positions. Where a diameter symbol is preceded to the tolerance value, the specified tolerance value represents the diameter of a cylindrical tolerance zone. Identification is unnecessary where the tolerance zone is other than a diameter, the specified tolerance value represents the distance between the two parallel straight lines or planes, or the distance between two uniform boundaries.

Since the component is represented as the point geometry in this study, geometrical tolerance can be modeled by varying the points from true positions. The GD&T symbols can be modeled by two basic types of the tolerance zone. They are perpendicular tolerance zone

and circular tolerance zone. In a perpendicular tolerance zone the position of points are varied along a direction normal to the feature surface within a specified total width zone. Table 4-1 illustrates some of the GD&T symbols applied in this study that are modeled by perpendicular tolerance zone. In a circular tolerance zone the position of points are varied radially on the feature surface within a specified total diameter zone. Table 4-2 shows the GD&T symbols applied in this study that are modeled by circular tolerance zone. It must be noted that Table 4-1 and Table 4-2 do not include all the symbols and the applications in ASME Y24.5M-1994 Standard.

Table 4-1 GD&T symbols represented as the perpendicular tolerance zone


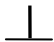
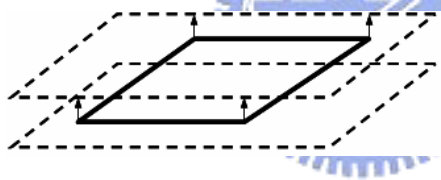
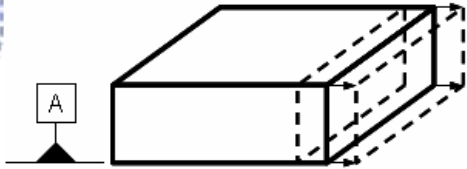


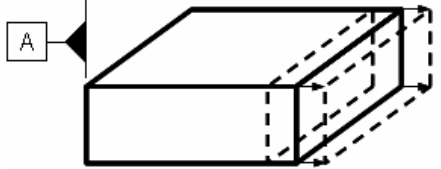
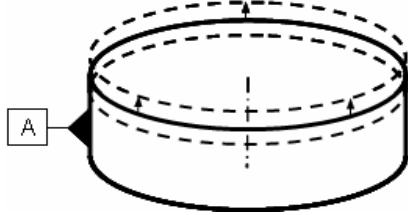



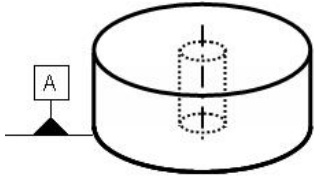


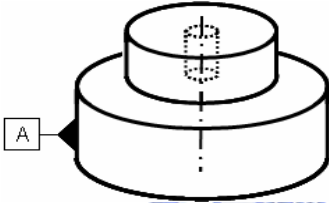

Symbol		
Characteristic	Flatness	Perpendicularity
Feature	Surface	Surface
Diagram		
Symbol		
Characteristic	Parallelism	Runout
Feature	Surface	Not parallel to datum axis
Diagram		

Table 4-2 GD&T symbols represented as the circular tolerance zone

Symbol		
Characteristic	Position	Perpendicularity
Feature	Line, Axis	Axis
Diagram		
Symbol		
Characteristic	Concentricity	Straightness
Feature	Axis	Axis
Diagram		

4.2. Opto-mechanical tolerance model on optical components

4.2.1. Spherical lens

The engineering specification and variation of a sphere lens has been discussed in Section 3.4. In order to have a proper tolerance model for a spherical lens, it is necessary to review the centering and the edge ground process of a lens after the surface polishing process. The tilt of optical elements is caused by the centering and edging process. A biconvex singlet is the basic shape of a lens. Figure 4-1 depicts the misalignment of an optical lens during centering and edging process. The typical setup for centering and edging a lens element is shown in Figure 4-1(a). Several methods have been developed to detect the alignment error of a lens during centering [21]. If the lens is perfectly centered and the spindle of the grinding

wheel is perfectly parallel to the spindle of bell cup, a perfect centered lens is fabricated. In Figure 4-1(b), the lens is in intimate contact with the bell cup, the centering error or surface tilt is caused by the methods of centering and the accuracy of centering detecting. Therefore, the tilt between the optical axis and mechanical axis exists after the edging process. In Fig. 4-1(c), a gap exists between the bell and the lens because of a burr, a particle dirt, or the adhesive hardened on the bell edge. Again, the surface tilt is built in the lens. Fig. 4-1(d) shows another situation. The lens is well centered; however, the spindle of the grinding wheel is not parallel to the spindle of the bell cup. The wear of grinding wheel also results in the misalignment of optical axis and mechanical axis.

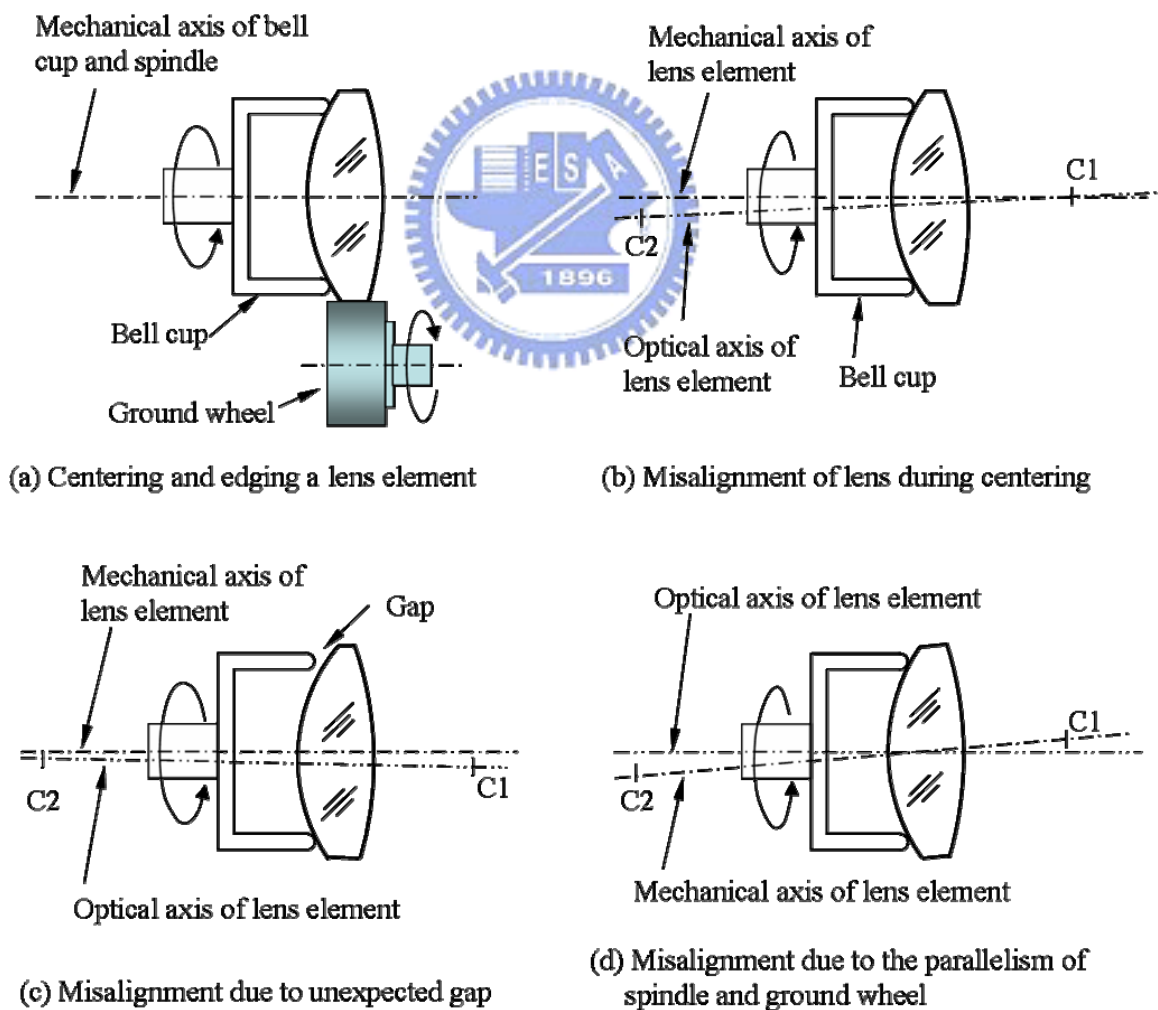


Figure 4-1 Misalignment of lens during centering and edging

According to the surface tilt variation of a lens element in the edging process, it is appropriate to simulate the surface tilt tolerance of a biconvex lens by varying the vertex of a surface. Another reason to vary the position and angle of the vertex of an optical surface is that the optical design software uses them to create the tilt and decenter of an optical surface. Figure 4-2 illustrates the opto-mechanical tolerance model of a sphere biconvex lens. The engineering specification of a biconvex sphere lens is shown in Figure 4-2(a). The tolerance model of a biconvex sphere lens is described below:

Step 1: Set up a local Cartesian coordinate system for the opto-mechanical system as shown in Figure 4-2(b). The origin of the coordinate system will coincide with the vertex of surface one of a perfect lens. The z-axis of the coordinate system is not only the mechanical axis of a lens but also coincides with the optical axis of a perfect lens. The y-axis lies on the vertical direction. The x-axis penetrates into the figure perpendicularly. The mechanical constraints of the lens are expressed as a straight line which is parallel to the z-axis.

Step 2: Define the tolerance zone for lens tilt. In Figure 4-2(c), the first circular tolerance zone CTZ_S1 is created on X-Y plane at point M (0, 0, 0) and the second circular tolerance zone CTZ_S2 is created at point N (0, 0, T) on a plane parallel to X-Y plane. The diameter of circular tolerance zone CTZ_S1 and CTZ_S2 is determined by the following equation:

$$CTZ_{tilt} = T \tan \tau_s \quad (4-2)$$

where

CTZ_{tilt} is the diameter of the circular tolerance zone,

T is the nominal central thickness of the lens,

τ_s is the surface tilt tolerance specification of the lens.

Step 3: Determine the optical axis randomly. In Figure 4-2(d), a point P is selected randomly within CTZ_S1 and another point Q is chosen randomly within CTZ_S2. Point P and

point Q can be expressed by the vector notation as below:

$$\vec{r}_P = x_P \vec{i} + y_P \vec{j} + z_P \vec{k} \quad (4-3)$$

$$\vec{r}_Q = x_Q \vec{i} + y_Q \vec{j} + z_Q \vec{k} \quad (4-4)$$

The normalized vector along the optical axis of the lens is

$$\vec{o} = \frac{\vec{r}_Q - \vec{r}_P}{|\vec{r}_Q - \vec{r}_P|} \quad (4-5)$$

Step 4: Determine the centers of curvature of surface 1 and surface 2. In Figure 4-2(e), the vertex point V1 of surface 1 is the same as point P. The vertex V2 of surface 2 can be determined by the following equation:

$$\vec{r}_{V2} = \vec{r}_P + (T \pm t) \vec{o} \quad (4-6)$$

The center of curvature of surface 1 will be determined by:

$$\vec{r}_{C1} = \vec{r}_P + (R1 \pm r1) \vec{o} \quad (4-7)$$

The center of curvature of surface 2 will be determined by:

$$\vec{r}_{C2} = \vec{r}_{V2} - (R2 \pm r2) \vec{o} \quad (4-8)$$

Step 5: Determine the two surfaces of the lens. In Figure 4-2(f), let \vec{r} be an arbitrary point of surface 1, surface 1 can be expressed as Equation (4-9).

$$|\vec{r} - \vec{r}_{C1}| = R1 \pm r1 \quad (4-9)$$

Similarly, surface 2 can be expressed as Equation (4-10).

$$|\vec{r} - \vec{r}_{C2}| = R2 \pm r2 \quad (4-10)$$

Step 6: Determine the other points which are necessary for ensuing tolerance analysis on the lens. For instance, the edge of the lens can be determined by solving the equations of the surface and the straight line which represents the rim of the lens.

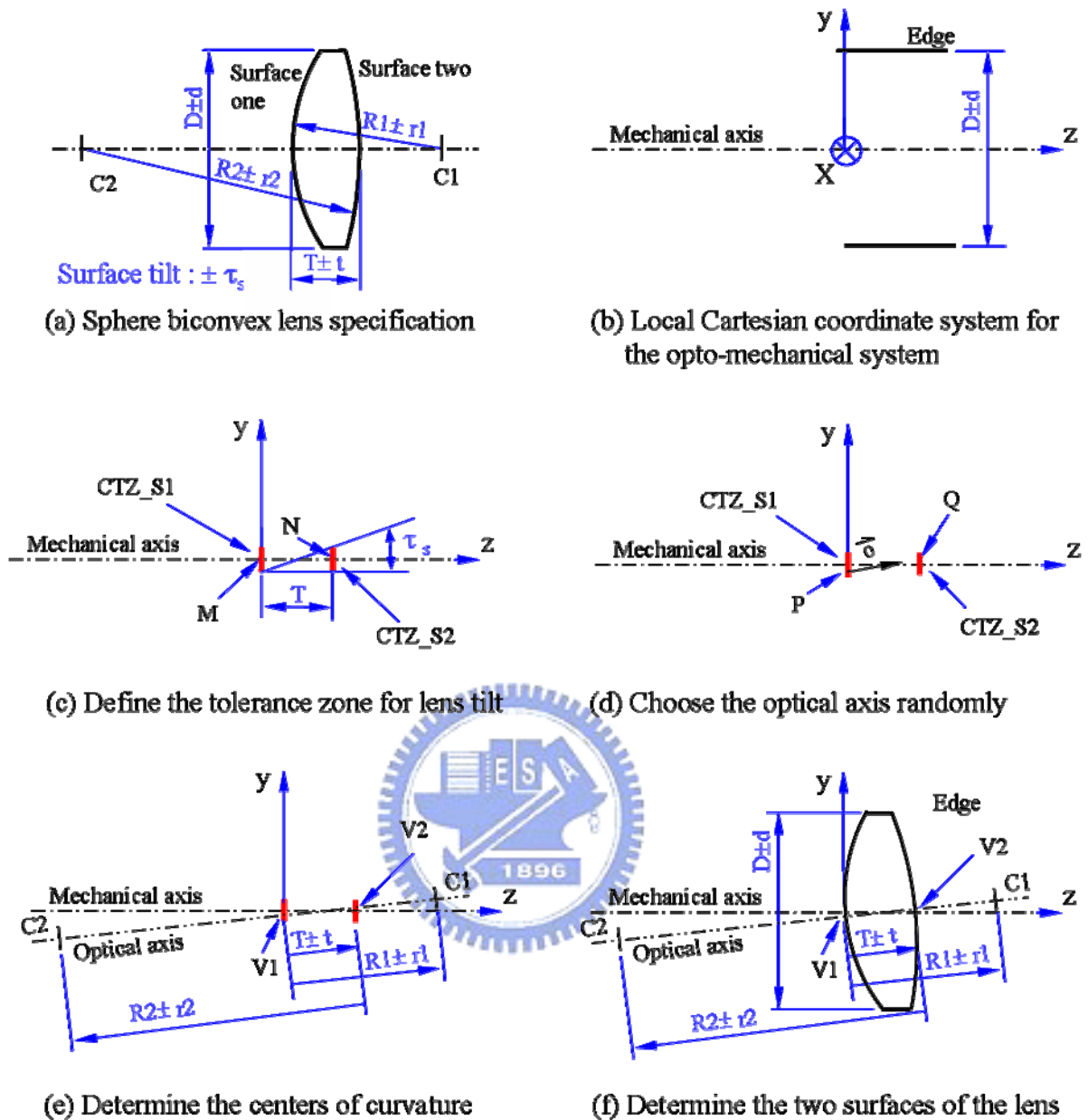


Figure 4-2 Opto-mechanical tolerance model of biconvex sphere lens

Different kind of surface tilted lens will be generated depends on the step 3 of the tolerance model. If both point P and Q are chosen on the Z axis then a centered lens, as shown in Figure 3-11(a) is generated. If both P and Q are varied almost the same distance away from the z- axis along the same direction, then a decentered element as shown in Figure 3-11(b) is acquired. If point P and point Q are varied in such a way that they separate away from each other, then a tilted lens, as shown in Figure 3-11(c) is obtained. The lens with single tilted

surface in Figure 3-11(d) will be simulated by varying both point P and Q away from Z axis with the same direction but different distance. In Figure 4-3, a similar procedure is applied to meniscus convex lens, biconcave lens and meniscus concave lens. Plano-convex lens and plano-concave lens is shown in Figure 4-4, the planar surface of the lens is perpendicular to the optical axis vector. As a result, a proper three dimensional tolerance model is created for spherical optical lens.

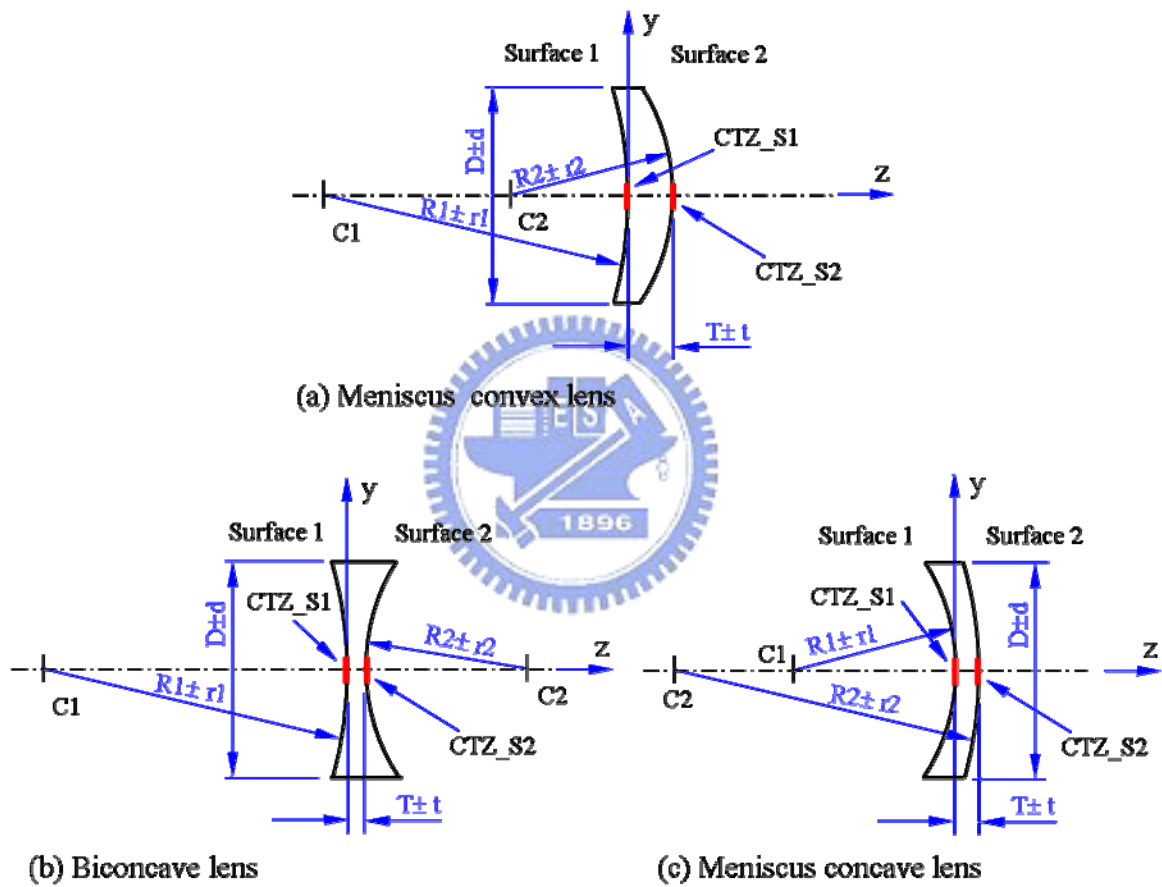


Figure 4-3 Opto-mechanical tolerance model of meniscus convex lens, biconcave lens and meniscus concave lens

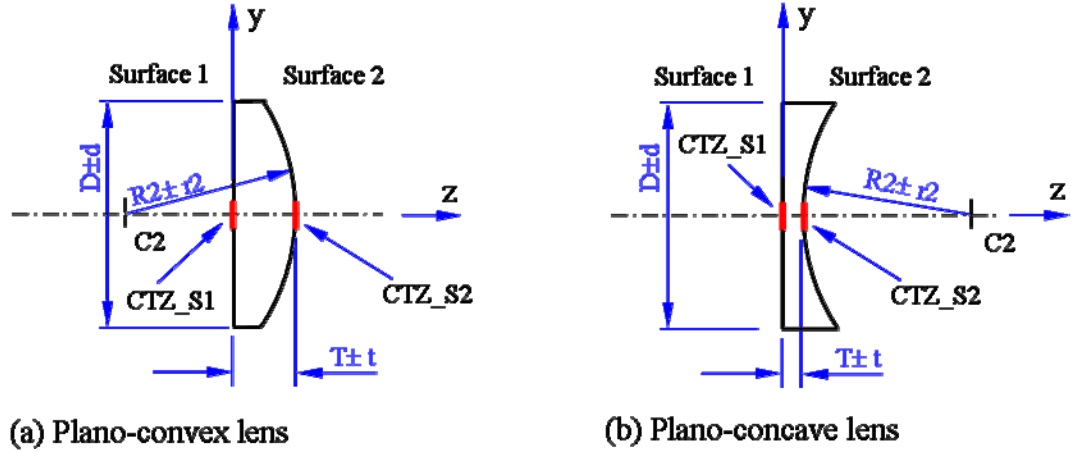


Figure 4-4 Opto-mechanical tolerance model of plano-convex lens, and plano-concave

4.2.2. Aspheric lens

Plastic aspheric lens is fabricated by the plastic injection process while glass aspheric lens is fabricated by the molding process. The aspheric lens discussed here is rotational symmetrical optical elements. The most common form of a aspheric surface is a surface with the sag defined in Equation (4-11) [29], the Cartesian coordinate system is defined the same as Figure 4-2(b).

$$z = f(s) = \frac{cs^2}{1 + \left(1 - (1+k)c^2s^2\right)^{1/2}} + \sum A_j s^{2j} \quad (4-11)$$

where

c is the base curvature of at vertex,

k is a conic constant,

z is the sag of aspheric surface,

s is a radial distance from z axis. $s^2 = x^2 + y^2$

$A_j s^{2j}$ are the higher-order aspheric terms.

The optical axis of an aspheric element is formed by joining all the centers of curvature

together. The center of curvature at a certain radial distance is necessary for the following assembly simulation. The radial distance is usually the supporting diameter of the mounting shoulder or the contacting circular diameter of the spacer. As the surface is rotational symmetrical about the optical axis, the center of curvature at arbitrary s value can be determined by selecting a cross section, for example $x = 0$, as illustrated in Figure 4-5. The radial distance from the z axis is $s^2 = y^2$. Therefore, the slope of the curve at $(y1, z1)$ is

$$\tan \theta = \frac{2\Delta y}{f(y1 + \Delta y) - f(y1 - \Delta y)} \quad (4-12)$$

where Δy is an infinitesimal increments of $y1$. As a result, the coordinates of center of curvature is $(0, 0, z1 + y1 \cdot \tan \theta)$.

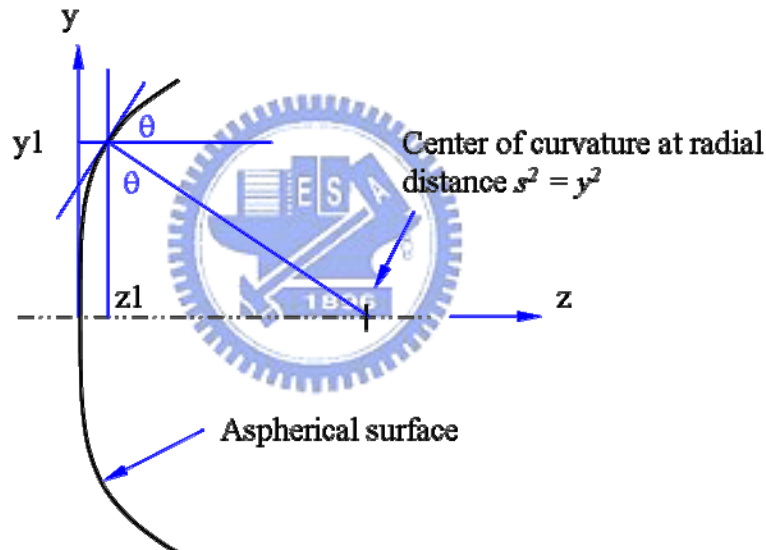


Figure 4-5 Center of curvature of aspheric surface at radial distance $y1$

As each aspherical surface has its own optical axis, the surface tilt and decenter are defined separately in the specification list. A biconvex aspheric lens is shown in Figure 4-6(a), the opto-mechanical tolerance model is described as below:

Step 1: Set up a local Cartesian coordinate system for the opto-mechanical system as shown in Figure 4-6(b). The coordinate system is set up the same as the coordinate system for the sphere lens described in Sec. 4.2.1.

Step 2: Define the surface decenter tolerance. In Figure 4-6(c), the first circular tolerance zone CTZ_S1 with diameter ε_s is created on the x-y plane at the origin, and the second circular tolerance zone CTZ_S2 with diameter ε_s is created at point $(0, 0, T \pm t)$ on a plane parallel to x-y plane. The diameter of the circular tolerance zone CTZ_S1 and CTZ_S2 equals to the surface decenter specification of the lens.

Step 3: Define the surface tilt tolerance. In Figure 4-6(d), a point P is chosen randomly within CTZ_S1 as the vertex of surface one, and another point Q is chosen randomly within CTZ_S2 as the vertex of surface two. Create an optical axis vector \vec{o} with the surface tilt tolerance for surface two by similar techniques discussed in the step 2 and step 3 of Sec. 4.2.1.

Step 4: Create centered aspheric surfaces. In Figure 4-6(e), surface 1 is created on an independent sub-local coordinate system, and surface 2 is created on another independent sub-local coordinate system. Both surfaces are centered about the z axis of the sub-local coordinate systems. The centers of curvature at a certain radial distance from the optical axis are also calculated.

Step 5: Move the aspheric surfaces to their vertex point on the local coordinate system. In Figure 4-6(f), surface 1 is moved to the local coordinate system by locating the origin of the sub-local coordinate system on point P and paralleling the coordinate axes to each other. Surface 2 is move to the local coordinate system by locating the origin of the sub-local coordinate system on point Q and aligning the sub-local z axis with vector \vec{o} .

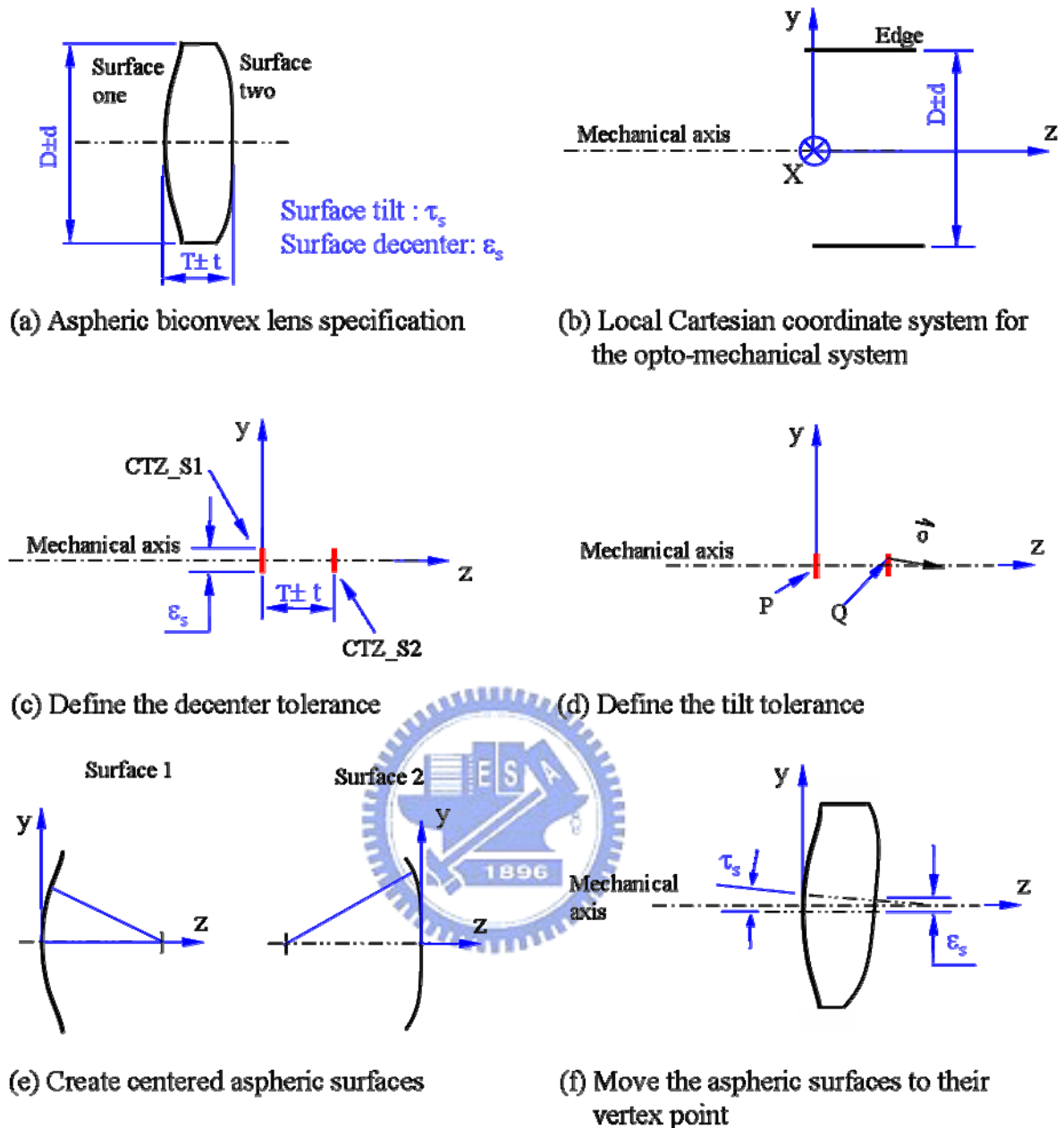


Figure 4-6 Opto-mechanical tolerance model of biconvex aspheric lens

4.3. Assembly variations in lens assembly

4.3.1. Rolling center in assembly

For a “drop-in” assembly, the real position of optical elements and mechanical elements within a cell are random. The determination of element tilt and decenter due to assembly variation is described as following. In Figure 4-7, a typical centered bi-convex lens is

mounted on the shoulder of an ideal cell perfectly. The optical and mechanical axis of the bi-convex lens coincides with the axis of the bore of cell. The dotted line depicts the lens in a maximum tilted condition due to the assembly variation. The motion of lens caused by assembly variation seems that the element rolls on its surface again the shoulder of cell. The center of curvature of surface one C1 is also the rolling center of lens element. That is the only point belongs to the coordinate system of the lens remains stationary in the coordinate system of the cell despite how much tilt the lens is. As a result, the resultant element tilt τ_m and element decenter ϵ_m of the lens can be calculated. In the same way, a lens with concave front surface mounted on the shoulder of a cell is shown in Figure 4-8. The center of curvature of the concave surface is the rolling center of the lens and is a stationary point belongs to lens when assembly variation occurs. Because the lenses in Figure 4-7 and Figure 4-8 are centered lens, the resultant tilt and decenter of the optical axis are the same as the element tilt and decenter of the mechanical axis. In case of lens with fabrication error they are different.

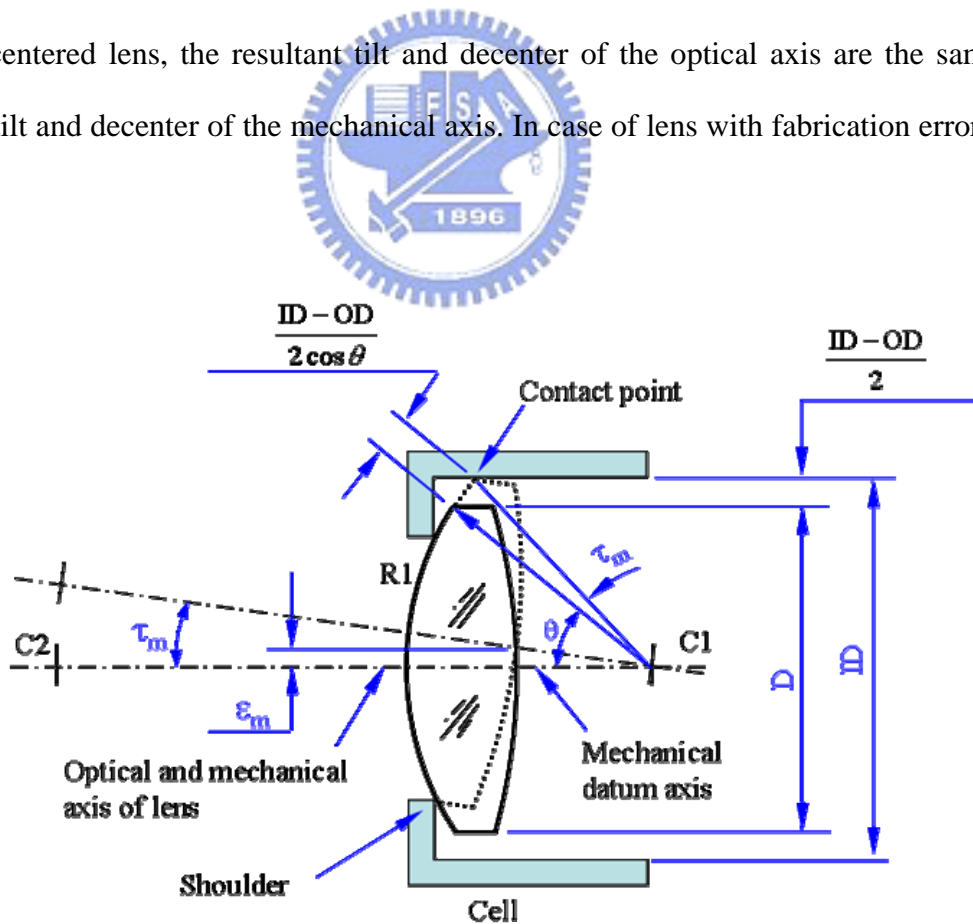


Figure 4-7 Rolling center of convex surface on cell shoulder

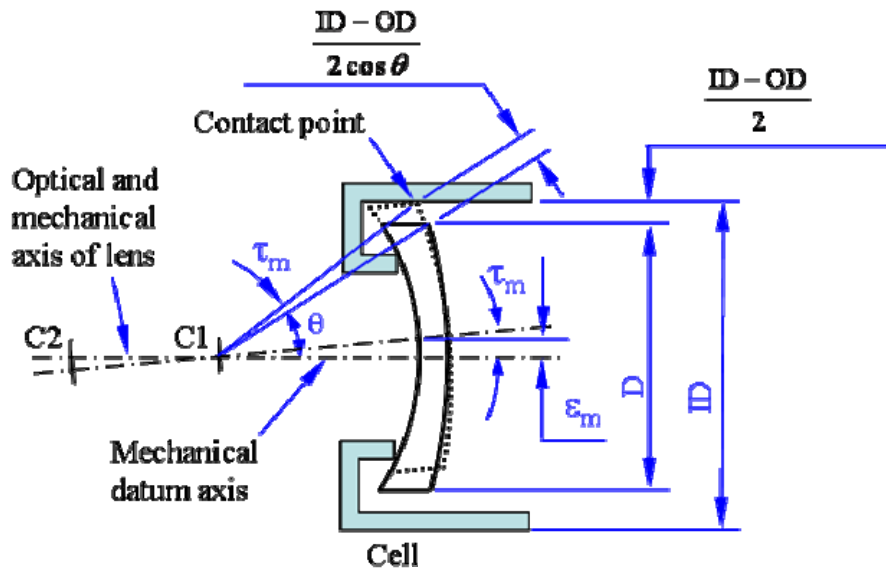


Figure 4-8 Rolling center of concave surface on cell shoulder

In the real world, manufacturing variation exists in all components; even so, the rolling center still remains stationary. As long as all the dimensions and geometrical tolerances of the lens and mounting cell are determined, the position of the rolling center of the lens is determined by the geometric relationships of the lens and the cell. In Figure 4-9, a surface tilted biconvex lens is mounted on a cell which the height of shoulder is uneven. The lens may roll against the shoulder until its rim contact with the cell. The rolling center C1 may or may not locate on the center axis of the cell. The element tilt τ_m which equals to the mechanical axis tilt of the lens is the angle between mechanical axis of lens and the mechanical datum axis of lens system. The resultant optical axis tilt τ_o of the lens is the angle between optical axis of lens and the mechanical datum axis of lens system. The element decenter ϵ_m is the normal distance from mechanical center of surface two to the mechanical datum axis of lens system. The resultant decenter ϵ_o is the normal distance from optical vertex of surface two to the mechanical datum axis of lens system. τ_m and ϵ_m usually are the tolerance analysis outputs of optical design software.

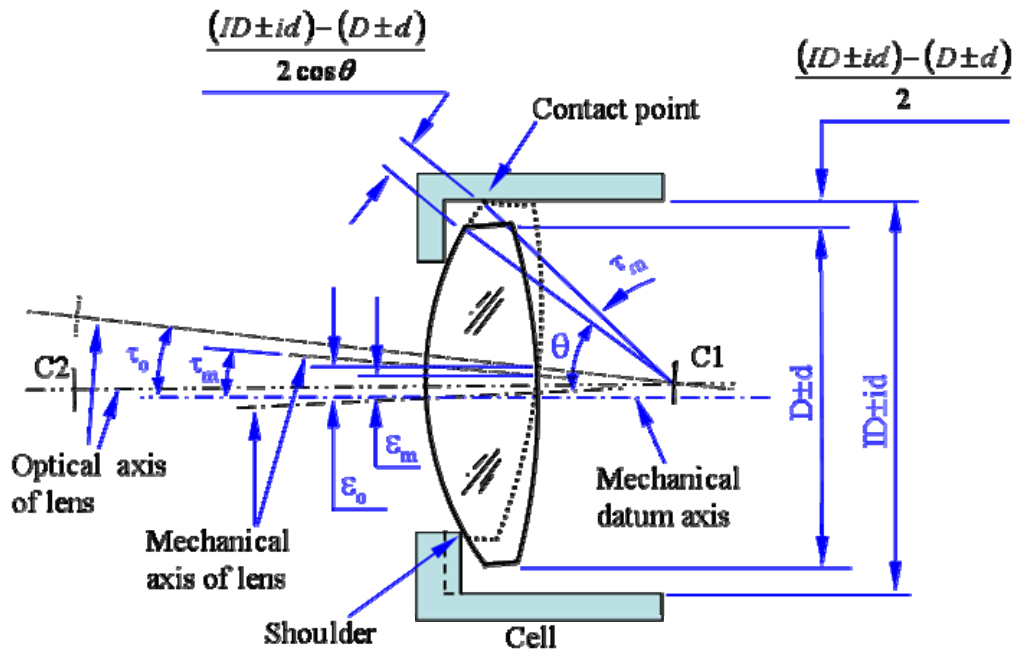


Figure 4-9 Manufacturing variation and rolling center

In “drop-in” assembly design, spacer is usually loaded between two lenses to have the designed air space. The determination of the position of the spacer in a lens assembly system is straightforward. In Figure 4-10, a typical spacer is attached to a biconvex lens within a cell. The dotted line depicts the spacer in maximum element tilted situation due to the assembly variation. The motion of the spacer caused by assembly variation is that the spacer rolls on the surface which it attaches on. The center of curvature of surface 2 of the lens is the rolling center of the spacer. Again, this is the only point belongs to the coordinate system of the spacer retains stationary in the coordinate system of the lens or cell despite how much element tilt the spacer is. Similarly, the assembly variation of a spacer which is attached to a concave surface of a lens in a cell is shown in Figure 4-11.

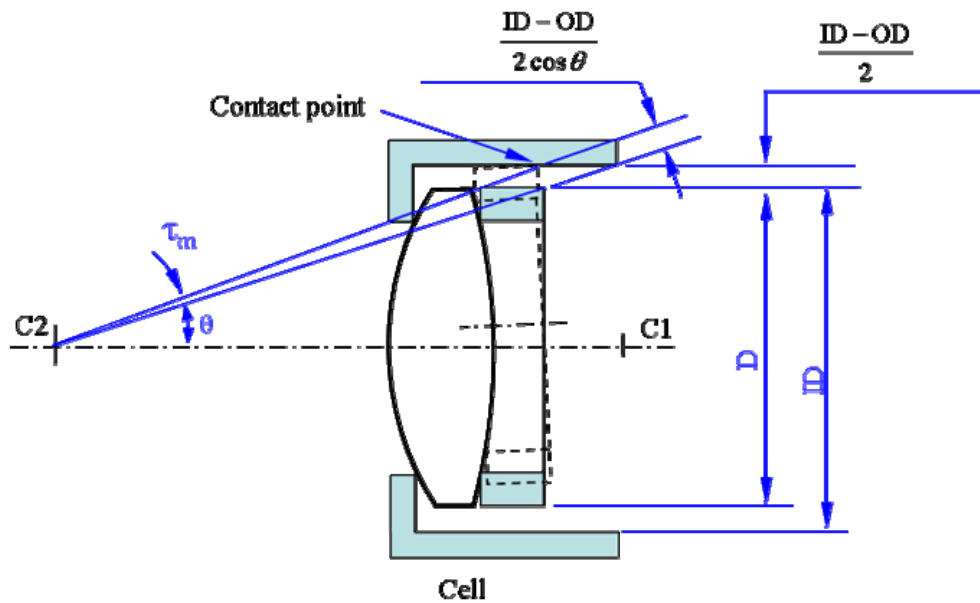


Figure 4-10 Rolling center of spacer on convex surface

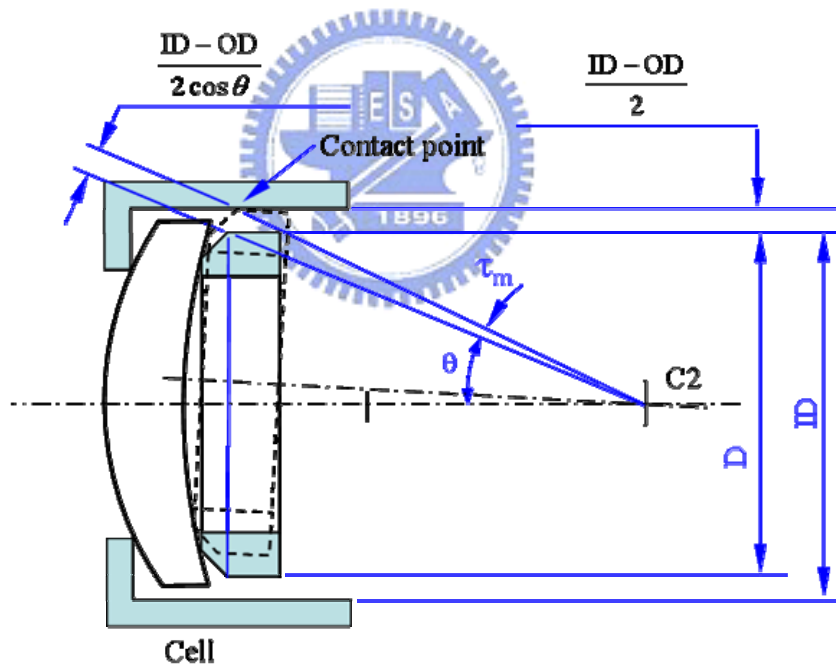


Figure 4-11 Rolling center of spacer on concave surface

The lens loaded in the assembly after the spacer can be considered as mounting a lens on the shoulder of the spacer. This is the same situation as a lens mounted on the shoulder of the cell. As a result, the rolling center of each component in a cell can be determined. The

4.4. Tolerance model of mechanical components

The mechanical components in a lens assembly are spacers, retainers, cells, and lens barrels. The dimensional and geometrical tolerances are simulated by the techniques discussed in Section 4.1. In addition, some virtual points must be added into the tolerance model according to the dimensions and tolerances of the optical elements which are attached to the mechanical components. For instance, the opto-mechanical tolerance model of the cell in Figure 4-7 is shown in Figure 4-13. The first virtual point C is the stationary rolling center for the attached optical element. The position of point C is determined by the dimensions and tolerances of the attached optical element and cell itself. The second virtual point U is the radial variation center of the attached optical element. Point U is located on the bore axis of the cell and is at a distance R1 from point C. A circular tolerance zone parallel to x-y plane with radius $(ID-OD)/2\cos\theta$ is created on point U as the locating point of the attached optical element. During the execution of Monte Carlo simulation, all the dimensions are generated randomly according to the specifications of tolerances; the position of point C or point U of each observation is different in the sample.

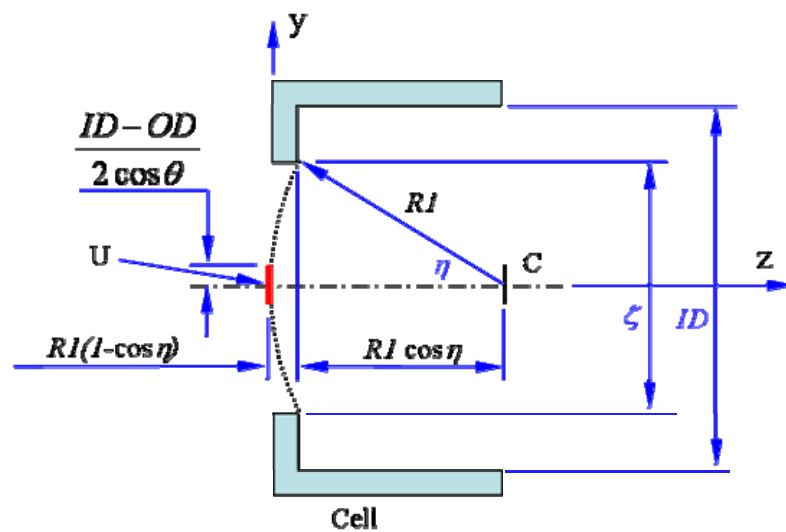
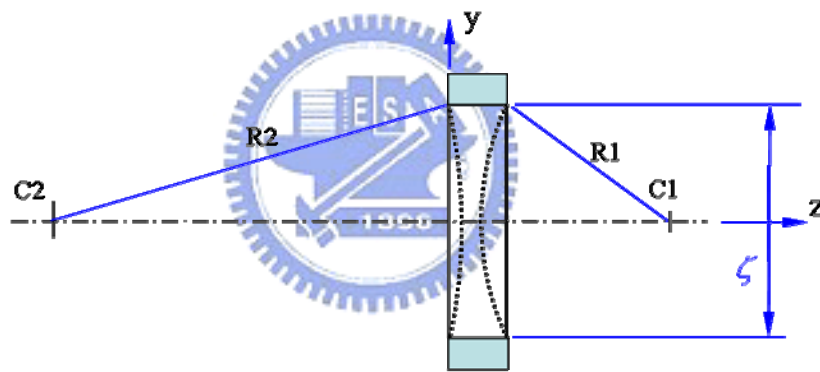
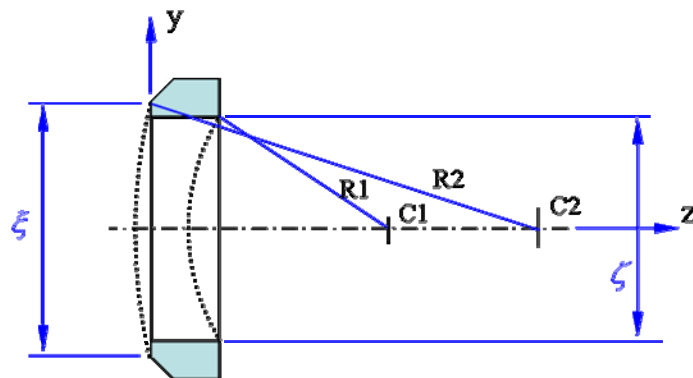


Figure 4-13 Tolerance model of cell

In the same way, the virtual point of stationary rolling center is necessary to add into the mechanical tolerance model of spacers. Figure 4-14(a) shows the mechanical tolerance model of the spacer in Figure 4-10. It is assumed that the optical element attached on the right side of the spacer is a convex surface. Point C2 is the stationary point in the coordinate frame of the space when it is assembled within a cell. The position of point C2 is determined by the dimensions of the spacer and the lens that the spacer is attached on. Point C1 is the rolling center for the lens attached to the right side of the spacer. The position of point C1 is determined by the dimensions of the spacer itself and of the lens which is attached on the spacer. The tolerance model of spacer in Figure 4-11 is shown in Figure 4-14(b). It also assumed that the optical element attached on the right side of the spacer is a convex surface.



(a) Spacer between two convex surfaces



(b) Spacer between concave and convex surfaces

Figure 4-14 Tolerance model of spacers

4.5. Assembly model

The assembly model is the method to position and orient parts in space with respect to each other. The mathematical models of assemblies make use of the matrix transformation [30]. The point geometry model of each component has a base coordinate frame. The point geometry model of each mating part has its own coordinate frame as well. A 4×4 matrix transformation can represent both the relative position of two components and their relative orientation. The matrix represents the location and orientation of an entire coordinate frame of a part, not simply a point. Figure 4-15 shows the transformation containing a translational part represented by vector p and a rotational part represented by R . Vector p is expressed in the coordinates of frame 1. Matrix R rotates frame 1 into frame 2. The mathematical form of the transform is

$$T_r = \begin{bmatrix} R & p \\ 0^T & 1 \end{bmatrix} \quad (4-13)$$



where p is a 3×1 displacement vector indicating the position of the new frame relative to the old one, R is a 3×3 rotation matrix indicating the orientation of the new frame relative to the old one, Superscript T transpose a conventional column vector to a row vector. Therefore, if q is a vector in the second frame, its coordinates in the first frame are given by q' :

$$q' = \begin{bmatrix} R & p \\ 0^T & 1 \end{bmatrix} \begin{bmatrix} q \\ 1 \end{bmatrix} = Rq + p \quad (4-14)$$

An assembly is a chain of coordinate frames on parts designed to achieve certain dimensional relationship, the CTQ characteristics, between some of the components or between features on these parts. This connective model is valid only under the situation of statically determinate or kinematically constraint. It is assumed that all components are rigid. The motion of a rigid body can be described by six parameters, three linear motions and three

related to rotational motions. Such a body is said to have six degrees of freedom. The six degrees of freedom of a simple cube is depicted in Figure 4-16. X, Y, and Z represent translations along the respective axes, α , β , and γ represent rotation about these axes. An object's position and orientation are completely specified with respect to a reference frame when the six degrees of freedom of the object are known relative to the reference frame.

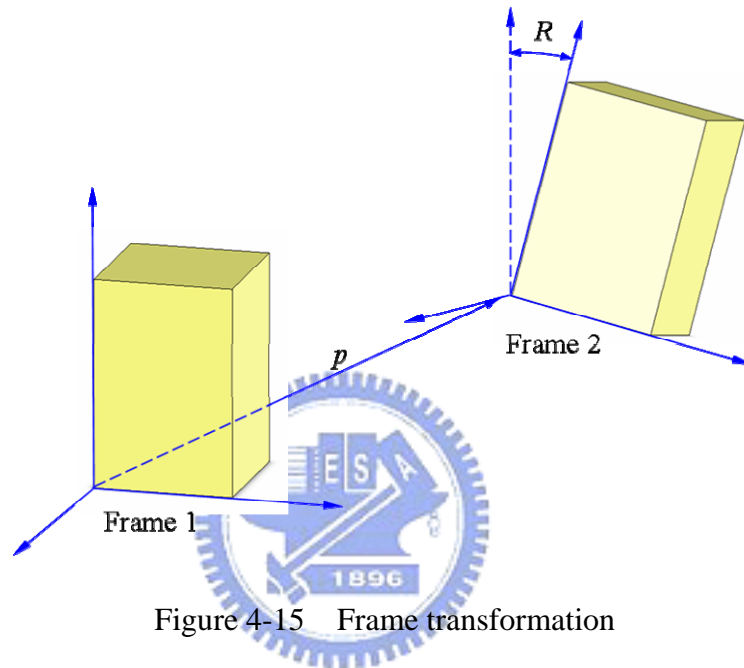


Figure 4-15 Frame transformation

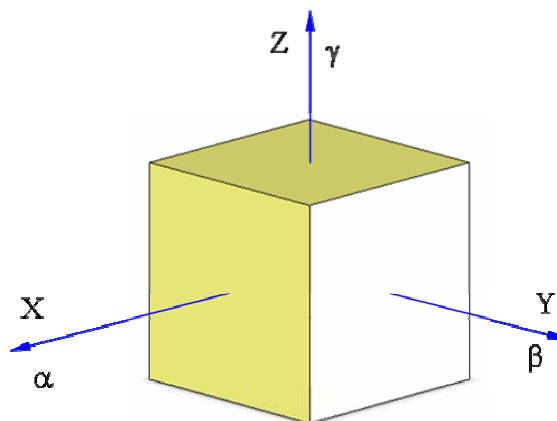


Figure 4-16 Degrees of freedom of a rigid body

Figure 4-7 is the assembly of the lens in Figure 4-2 and the cell in Figure 4-13. The

frame relationship can be defined by the following procedures. First, move the frame of the lens and let the center of curvature $C1$ of the lens coincides with the virtual point C of the cell. Now three translational degrees of freedom, X , Y , and Z , of the lens are constrained. Second, align point M of the cell with point U of the cell. Then additional two rotational degrees of freedom α and β of the lens are constrained. Finally, because the components within the cell are rotational symmetric about the z axis, the rotational degree of freedom γ of the lens can be constrained by defining extra virtual points on both lens and cell at proper position and making them coplanar. As a result, the frame of lens is fully constrained with respect to the frame of cell. Similar procedure can be applied to the assembly of spacers.

After all of the components are assembled, the point geometry belongs to the coordinate frame of each component has been transformed to the datum coordinate frame which is usually set on the first component in the assembly. The CTQs of the assembly can be calculated directly referring the points of each component. Figure 4-9 can be treated as an observation of the lens assembly in Figure 4-7 during Monte Carlo simulation. The element tilt τ_m , decenter ε_m and optical axis tilt τ_o , decenter ε_o can be calculated according to the definition discussed in Section 4.3.1. The despace of a lens is the position variation of a lens relative to the preceding one.

Chapter 5. Case Study

The opto-mechanical tolerance model developed in Chapter 4 is effective especially in the “drop-in” assembly. The “drop-in” design is widely used in commercial applications due to the low cost and easy assembly. The CTQs of assembly will meet the system requirements without further adjustment. Therefore, a design of 10X zoom lens for a digital video camera is chosen for the case study.

5.1. Portion of a zoom lens design

Most of the optical construction of high ratio zoom lens consists of four or five lens groups. Some groups are fixed and others are movable independent to each other during zooming. Figure 5-1 shows the optical and opto-mechanical design of the second group and the third group of a 10X zoom lens. There are three lenses in Group II. Lens L5 contacts with lens L6 directly, lens L6 and lens L7 are separated by a spacer S2. All components are assembled from the left side of cell C2. There are four lenses in Group III. L8 is a lateral compensating lens and have to be attached from the left side of the cell C3. Lens L9, lens L10, lens L11 and spacer S3 are loaded from the right side of the cell C3. L10 and L11 are separated by spacer S3. L10 and L11 comprise a doublet lens. Both groups are the “drop-in” design assembly. The optical element tilt, decenter and despace within the cell caused by the variation of manufacturing and assembly process will be calculated by the tolerance model developed in Chapter four.

The fabrication data of the lens design and the tolerance requirements from the optical software are given in Table 5-1. The mechanical drawings of cell C2 and spacer S2 are shown in Figure 5-2. Figure 5-3 gives the mechanical drawings of cell C3 and spacer S3. These drawings define the initial dimensional and geometrical tolerance of the opto-mechanical

interface. The initial tolerances are determined by the experience of mechanical engineer and some preliminary estimation. The assembly tolerance requirements from optical software are given in Table 5-2. For element tilt, decenter and despace, all lenses have the same tolerance specification.

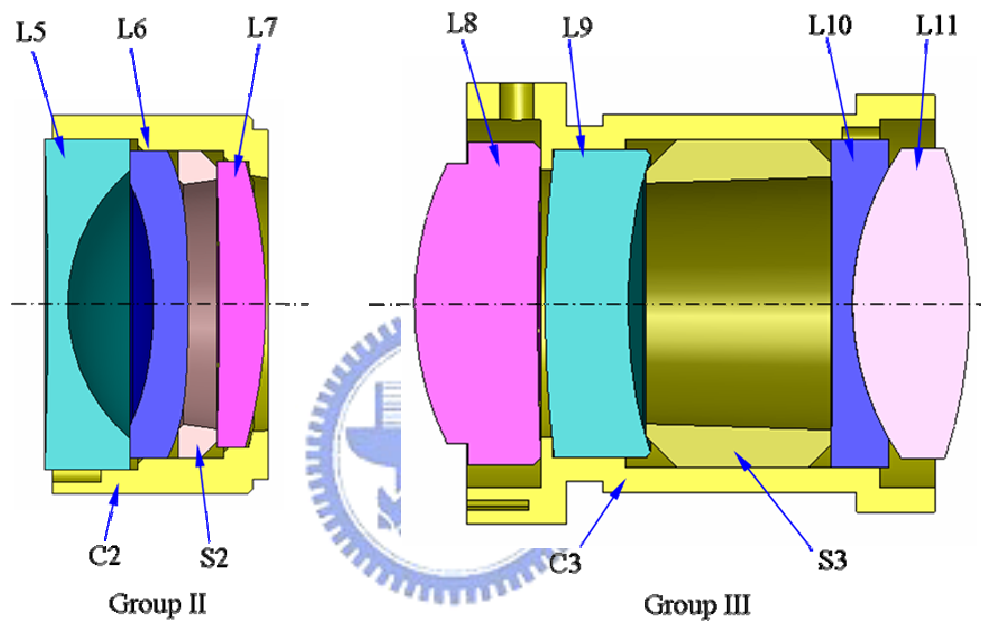
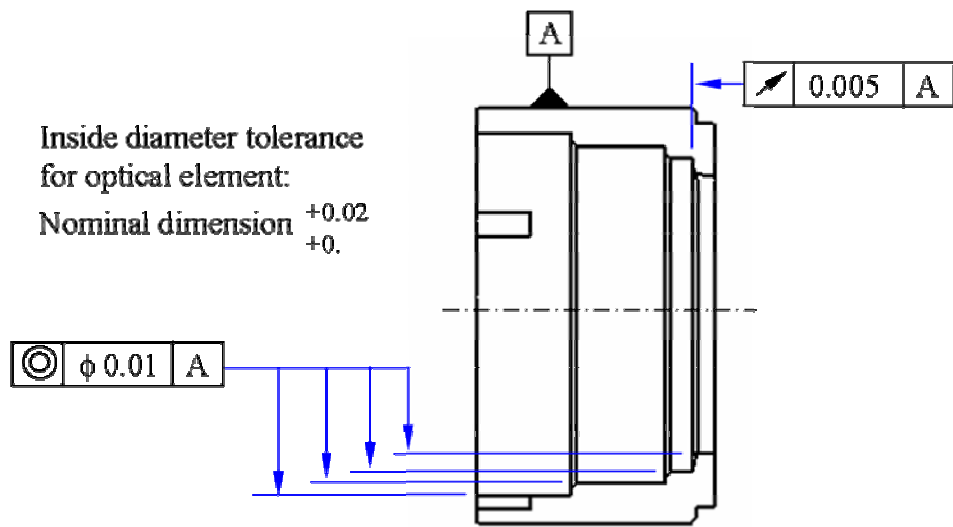


Figure 5-1 Portion of a zoom lens design

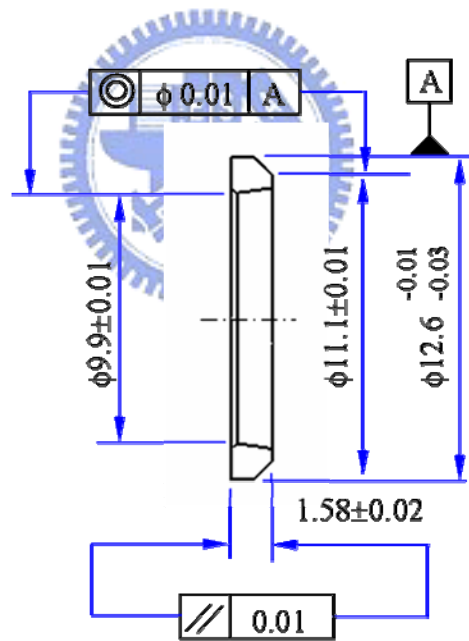
Table 5-1 The fabrication data and tolerance of optical elements

Lens	S1 radius (mm)	S2 radius (mm)	Thickness (mm)	Spacing to next lens	S1: Fringes of radius tolerance	S2: Fringes of radius tolerance	Surface tilt (min.)	Thickness tolerance (mm)	Surface decenter (mm)	OD tolerance (mm)
L5	-182.06	7.20	0.80	3.500	3	3	2'	±0.05		-0.01 -0.03
L6	Asphere	Asphere	1.40	1.270	4	5	5'	±0.02	±0.01	-0.01 -0.03
L7	-177.40	-20.95	1.90		3	3	2'	±0.05		-0.01 -0.03
L8	12.94	130.54	5.00	0.303	3	3	2'	±0.05		-0.01 -0.03
L9	53.56	Asphere	3.38	8.318	3	4	5'	±0.04	±0.01	-0.01 -0.03
L10	-284.25	11.04	0.80	0.000	3	3	2'	±0.05		-0.01 -0.03
L11	11.04	-20.29	4.767		3	3	2'	±0.05		-0.01 -0.03

Note: The cemented decenter tolerance of L10_L11 doublet: 6'

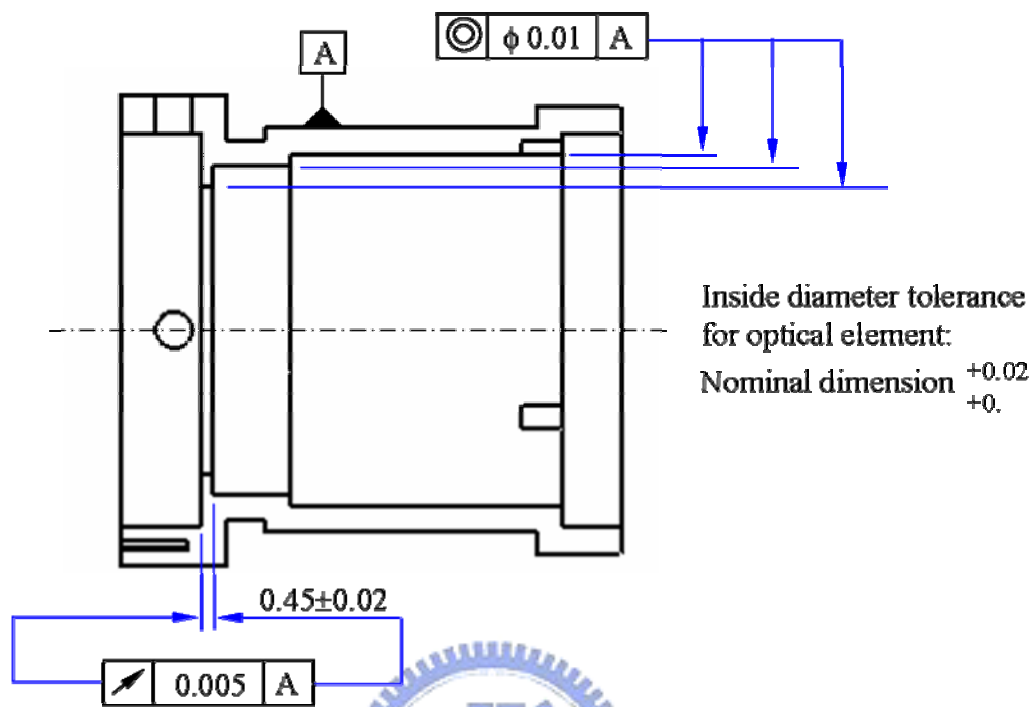


(a) Cell C2

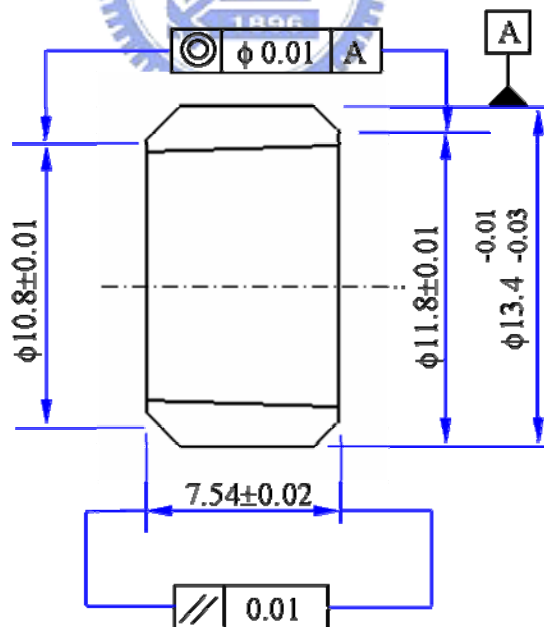


(b) Spacer S2

Figure 5-2 Drawing of opto-mechanical interface of Group II



(a) Cell C3



(b) Spacer S3

Figure 5-3 Drawing of opto-mechanical interface of Group III

Table 5-2 The assembly tolerance requirements

Element tilt	± 4 min.
Element decenter	± 0.025 mm
Element despace	± 0.03 mm

5.2. Programming flow chart

The opto-mechanical tolerance model developed in this study is implemented by VSA-3D® software. The software performs variation analysis by Monte Carlo simulation. Users have to define the mathematical relationship between input variations and output measurements. The input variations are the component geometry, tolerances and assembly variations. The output measurements in this study is the element tilt, decenter and position of a lens in an assembly. VSA-3D® shows an actual range based on Monte Carlo simulated observations, a statistical range, statistical descriptions of the process, and contributors to the variation. The validation of the tolerance model can be checked by the following ways. First, check the nominal dimensions of the output measurements, because the nominal dimension is usually the design target. For instance, the element tilt or decenter of any lens should be zero whether the lens is assembled or not. Second, check the position of some points on component before and after assembly. Engineers should know the exact coordinate of these points before and after assembly. Finally, check the statistical range and distribution of the output measurement. According to the input variations, engineers can roughly estimate the statistical range of the output measurement and evaluate the rationality of the results. Furthermore, the user's experience is importance in reading the data of output measurements. The programming flow charts are shown in Figure 5-4 to Figure 5-7. The assembly flow diagram is illustrated in Figure 5-8.

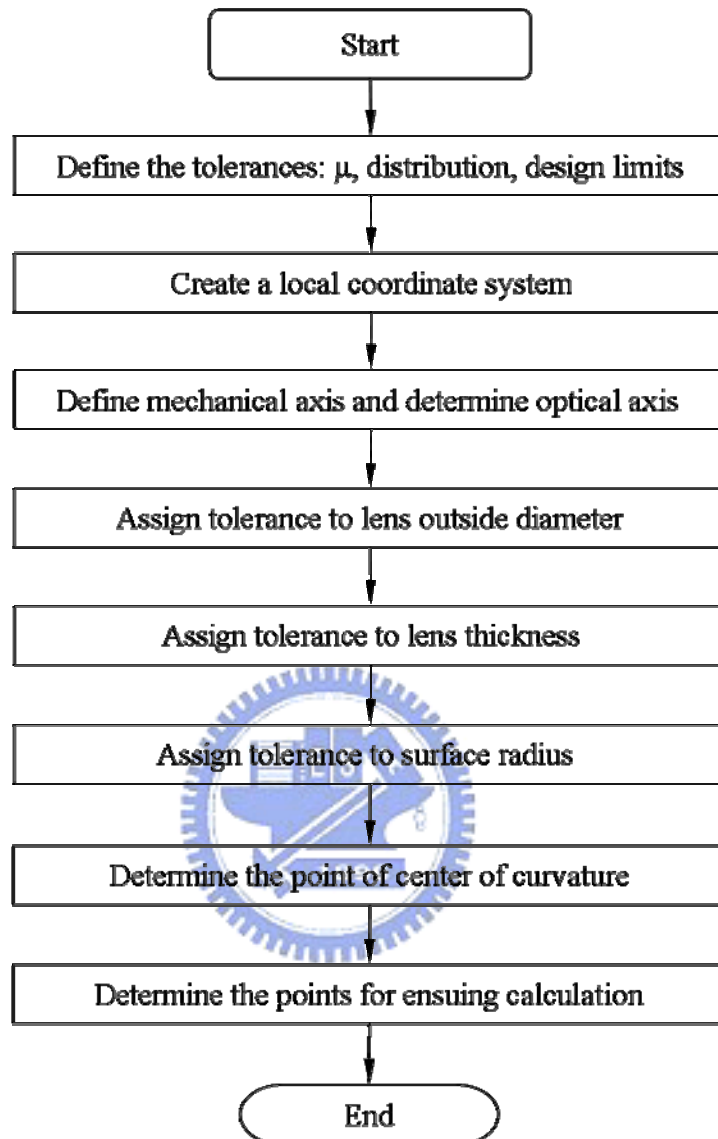


Figure 5-4 Flow chart of sphere lens tolerance model

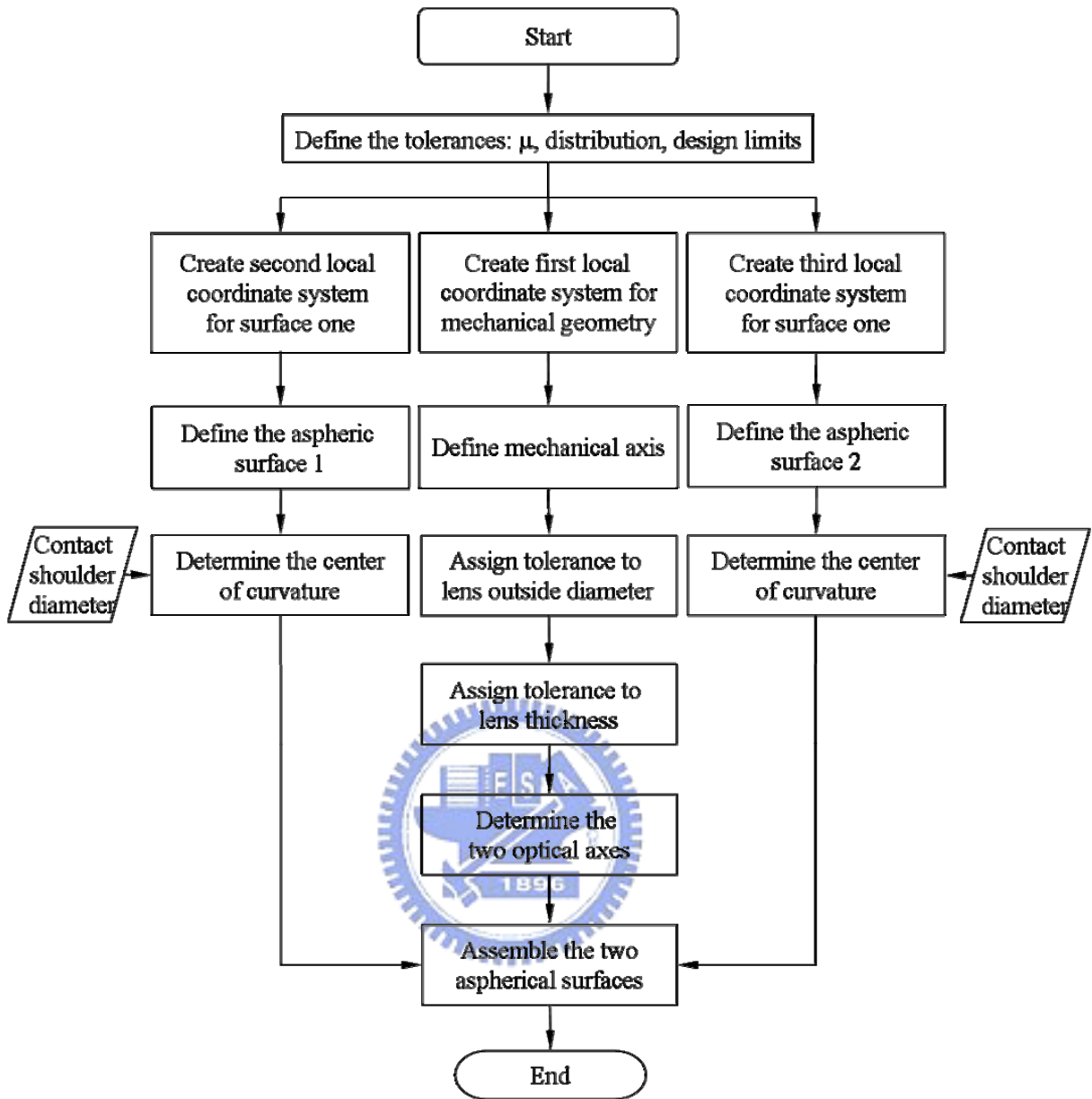


Figure 5-5 Flow chart of aspherical lens tolerance model

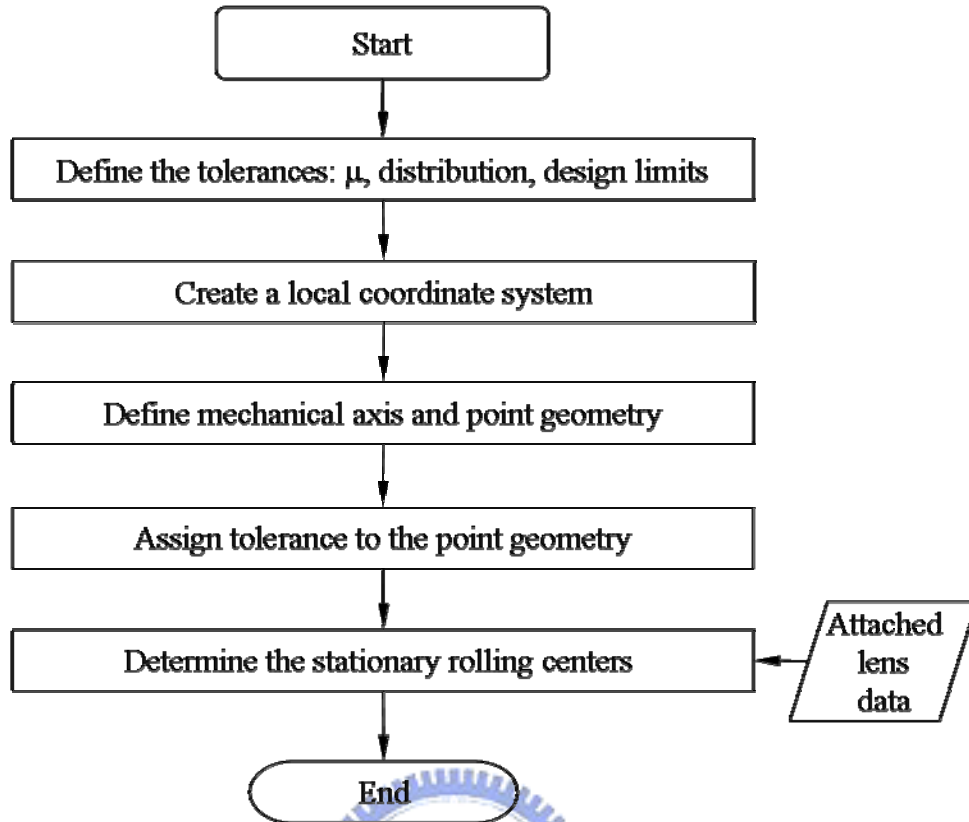
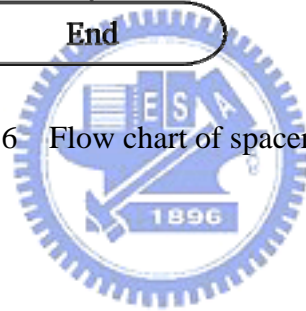


Figure 5-6 Flow chart of spacer tolerance model



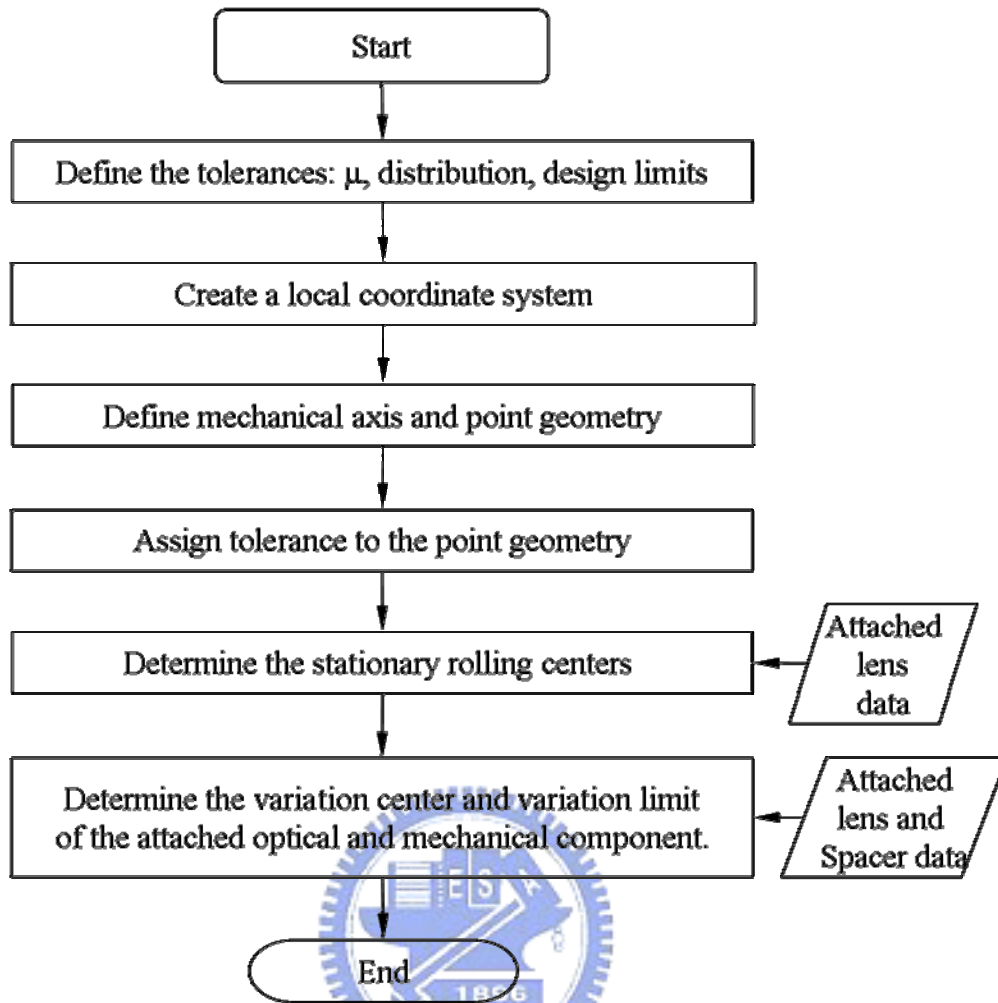
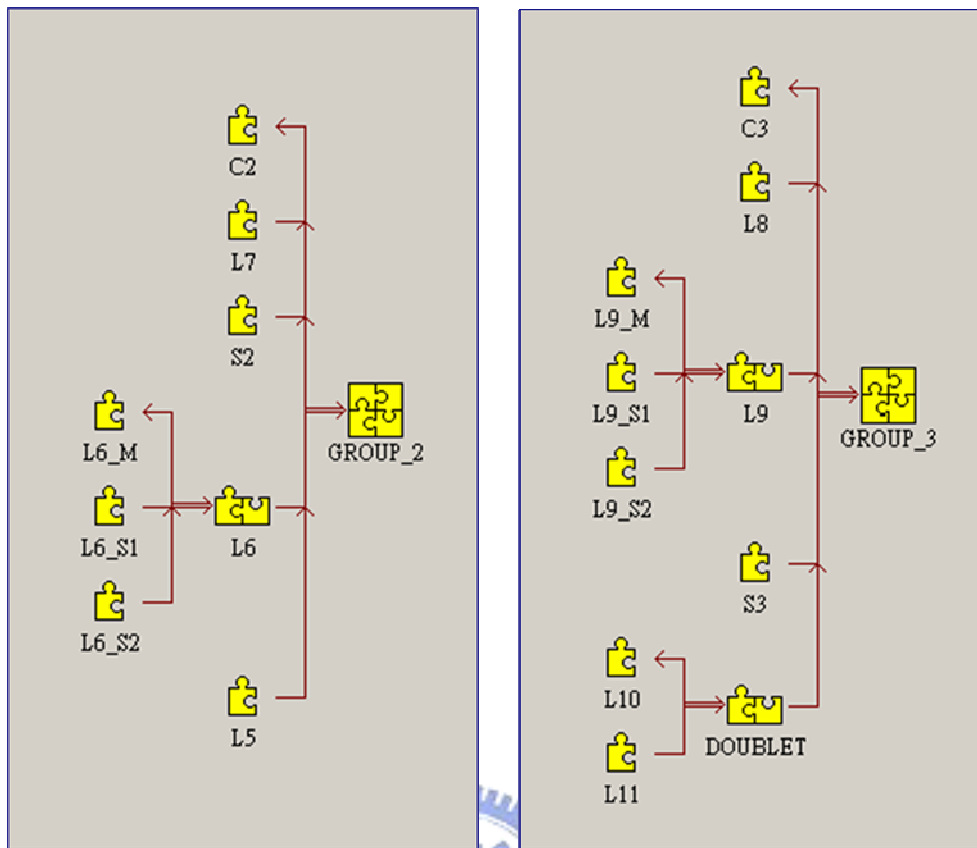


Figure 5-7 Flow chart of cell tolerance model



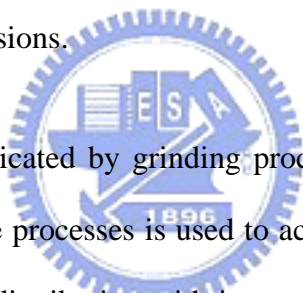
(a) Assembly flow diagram of group II

(b) Assembly flow diagram of group III

Figure 5-8 Assembly flow diagram

5.3. The statistical distribution of the tolerances

Section 2.1.2 has discussed the importance of the characteristic of a distribution to the Monte Carlo simulation. Table 5-2 lists the statistical distributions of the opto-mechanical parameters in the tolerance model. Generally speaking, the dimension variation of the manufacturing process approximates to be a normal distribution. The statistical distributions of the tolerances of mechanical dimensions and geometrical symbols are assumed to be normal with 3 sigma points at the tolerance limit and without truncation. This means that there is no inspection for these parts before assembly; therefore, approximately 0.26% of the parts do not meet the tolerance requirements. Due to the machining process of the forming mold for aspheric lens, the tolerance distribution of the aspheric molded lens parameters will be treated as mechanical dimensions.



For optical elements fabricated by grinding process, a particular distribution which is determined by the nature of the processes is used to achieve the desired value [31]. First, the center thickness of a lens is a distribution with its peak at 50% point from nominal value to the high side tolerance. Furthermore, the distribution is truncated to reject 0.26% of unqualified parts. Second, the optical surface polishing processes are usually fitted to test plates to check the surface radius. Because there is a strong tendency to go toward a “hollow” test glass fit where contact is at the edge of the surface, the radii of convex surfaces tend to be bigger and the radii of concave surfaces tend to be smaller. The distribution is a displaced normal distribution. The peak is at 40% point from nominal value to the hollow side and 3 sigma points at the tolerance limited value on the hollow side. Finally, the surface tilt and decenter of a lens are assumed to have a normal distribution with the one sigma points at the tolerance limits. Truncation is necessary to reject the unqualified optical elements.

Table 5-3 Statistical distributions of tolerance

Tolerance	Distribution	Sigma	Peak position	Skew	Kurtosis	Truncation	Figure
Mechanical dimension	Normal	3	0%	0	0	No	
Lens center thickness	Pearson	3	50%	-0.9	0.9	Yes	
Convex surface radius	Normal	3	40%	0	0	No	
Concave surface radius	Normal	3	-40%	0	0	No	
Surface tilt & decenter	Normal	1	0%	0	0	Yes	

5.4. The simulation results

The simulation results from VSA-3D[®] software are shown as the following:

Element tilt: Figure 5-9 to Figure 5-15.

Element decenter: Figure 5-16 to Figure 5-21.

Element despacer: Figure 5-22 to Figure 5-25.

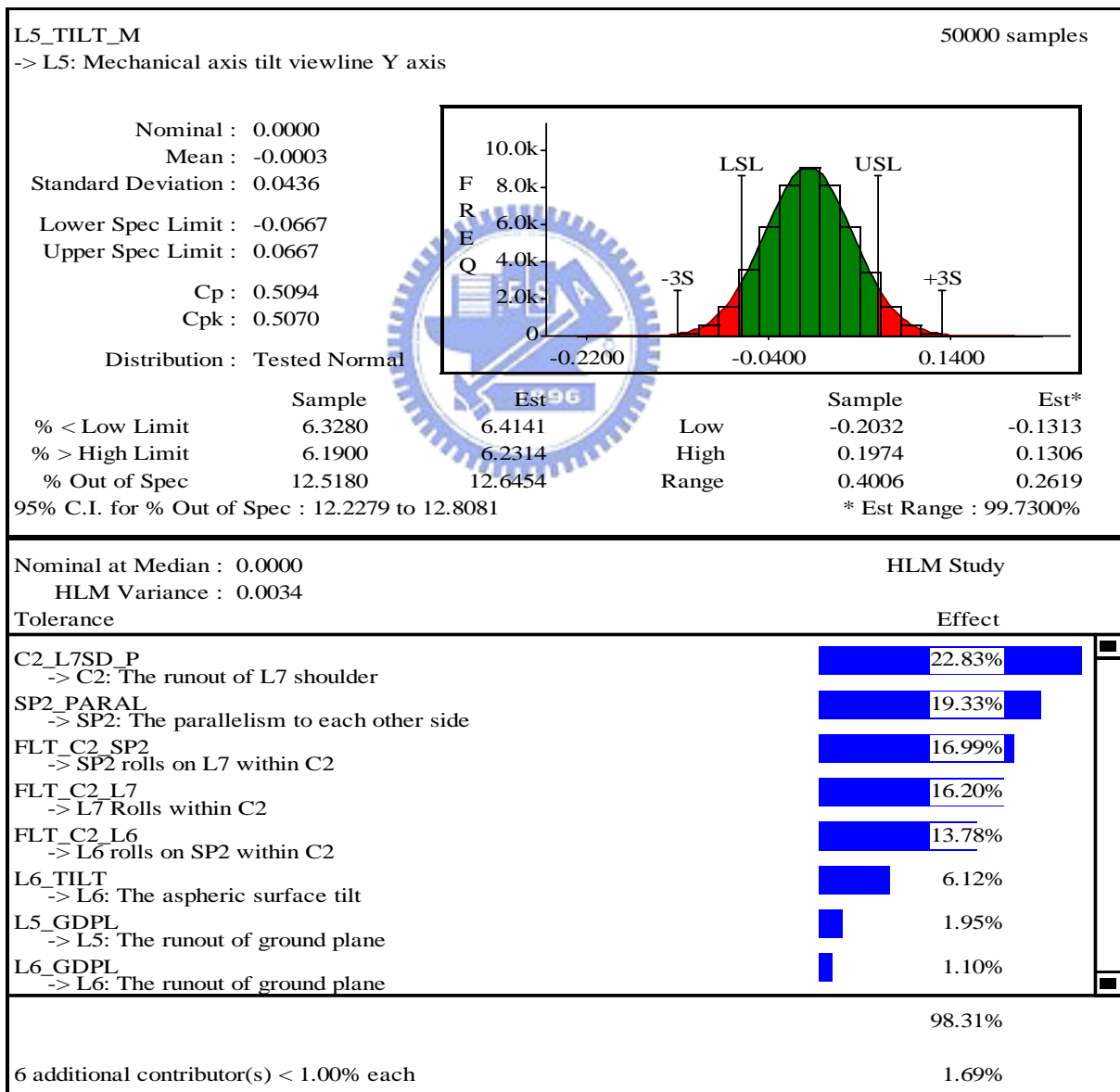


Figure 5-9 The element tilt of L5

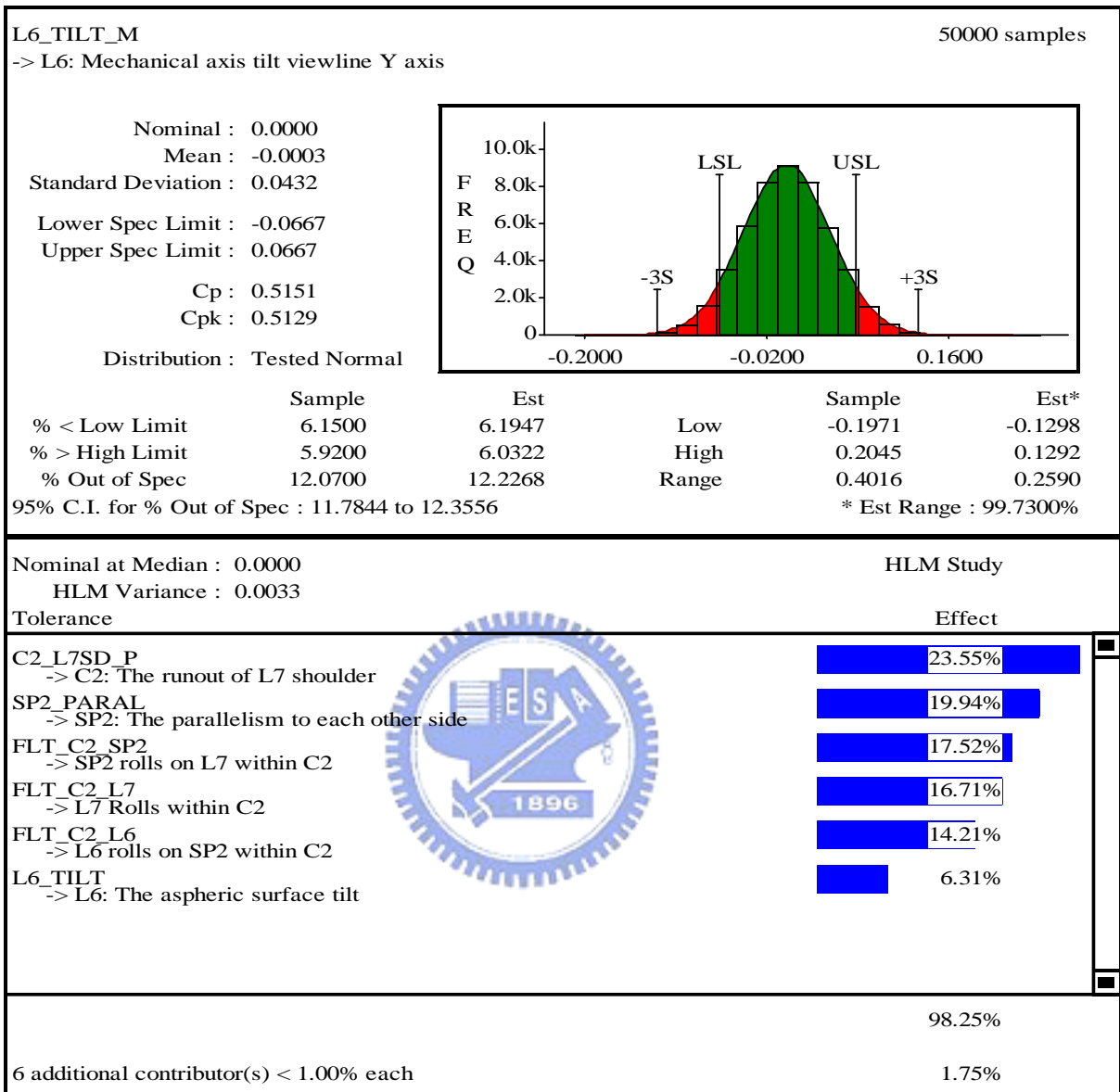


Figure 5-10 The element tilt of L6

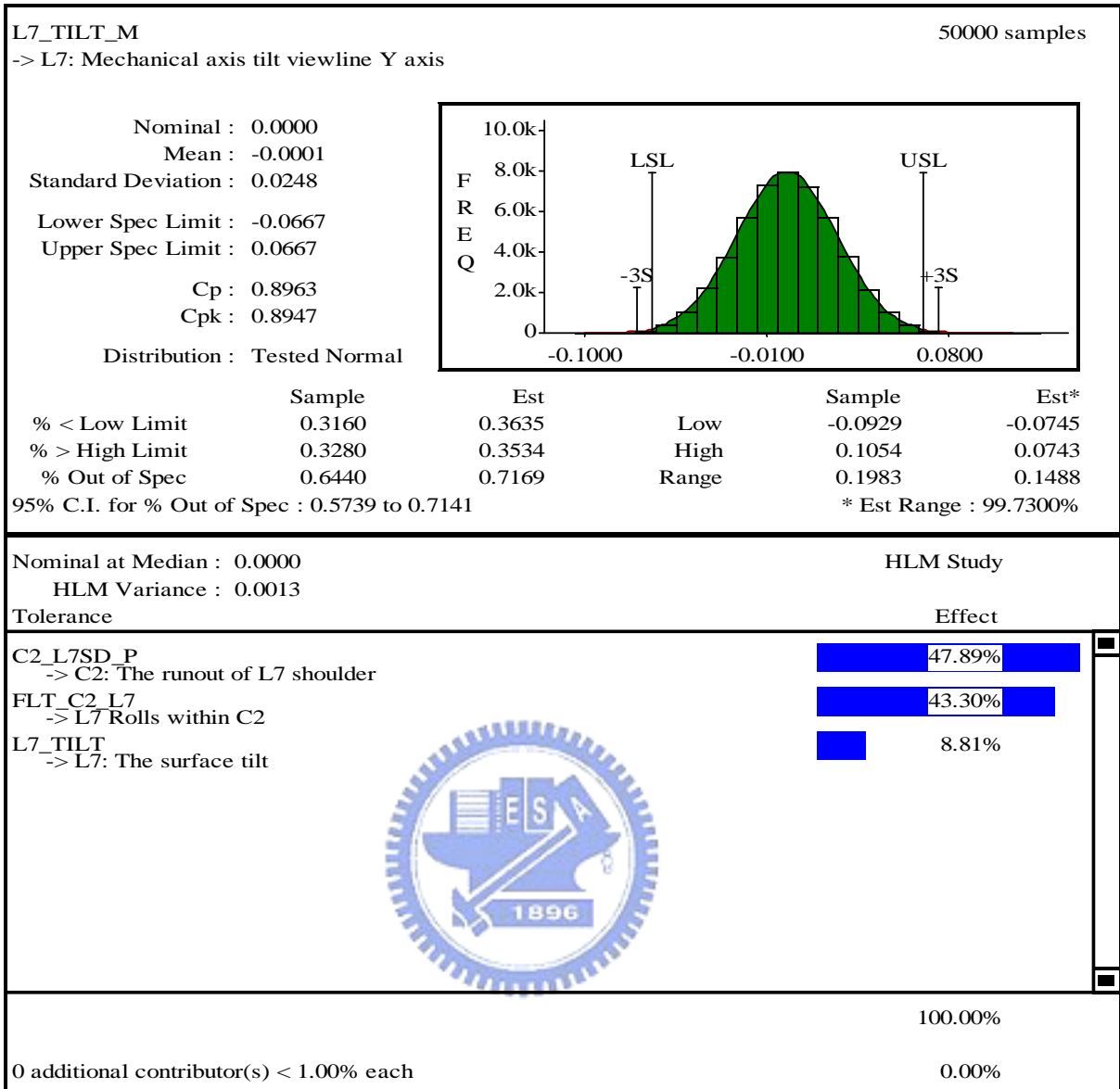


Figure 5-11 The element tilt of L7

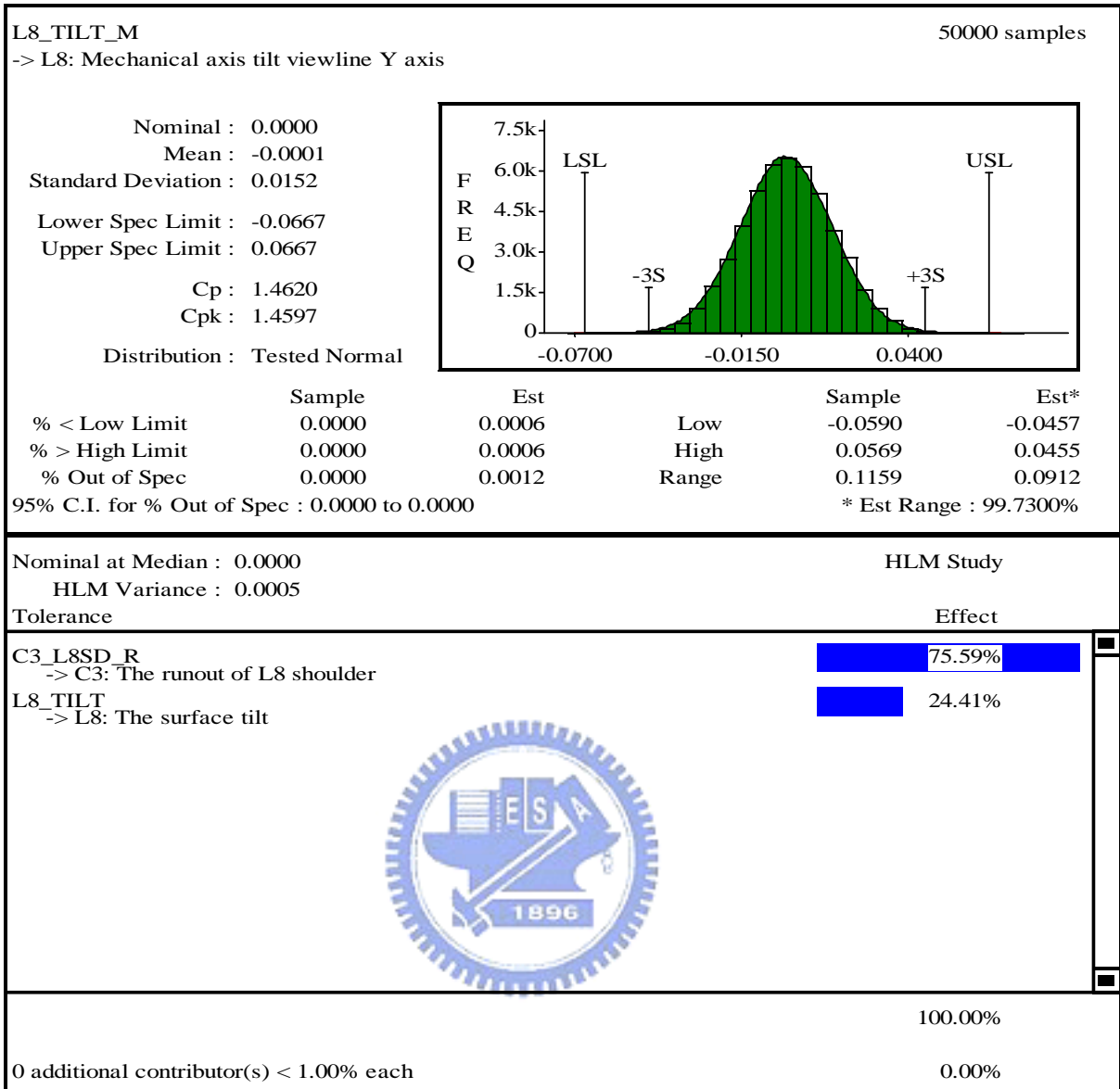


Figure 5-12 The element tilt of L8

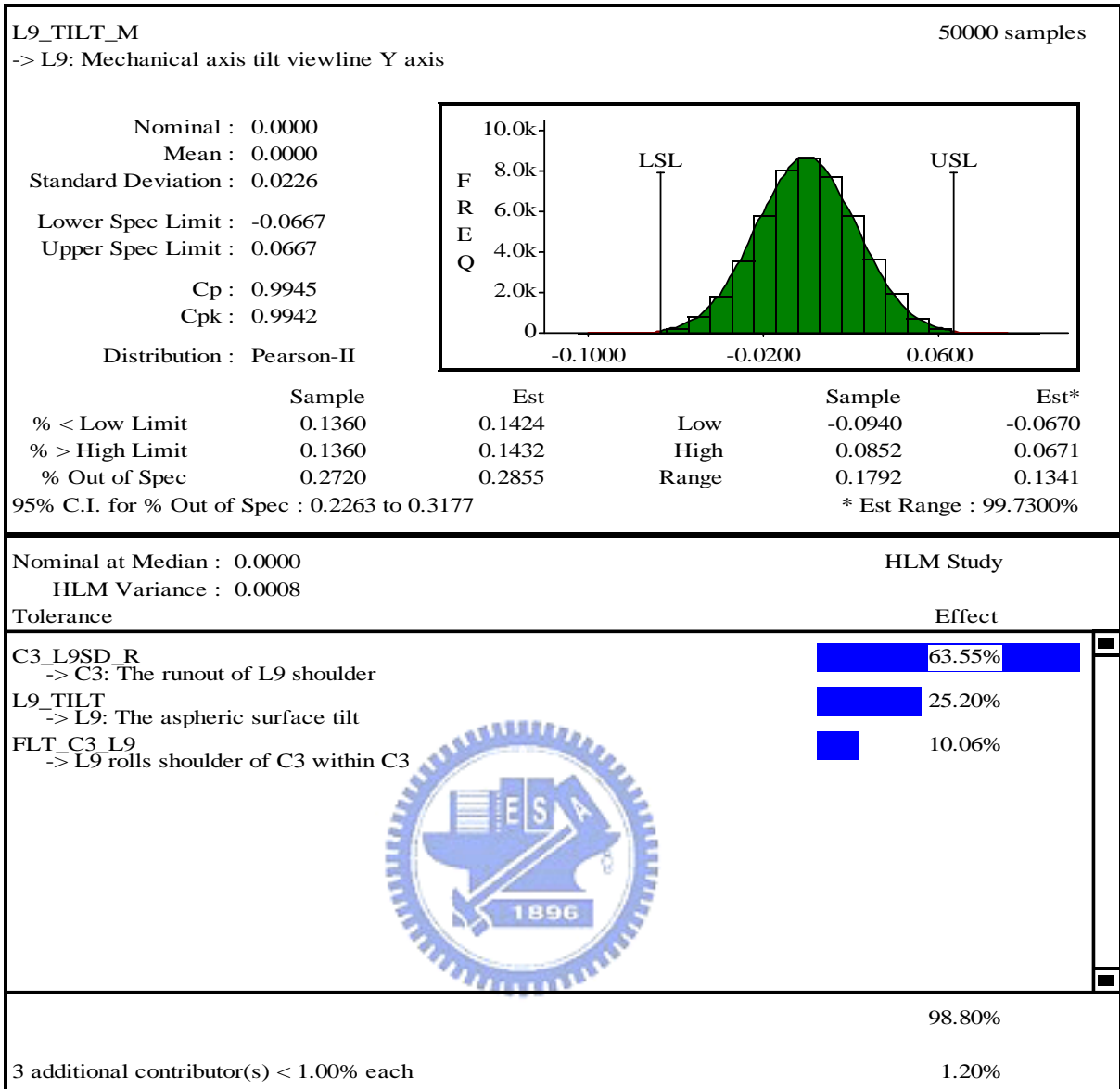


Figure 5-13 The element tilt of L9

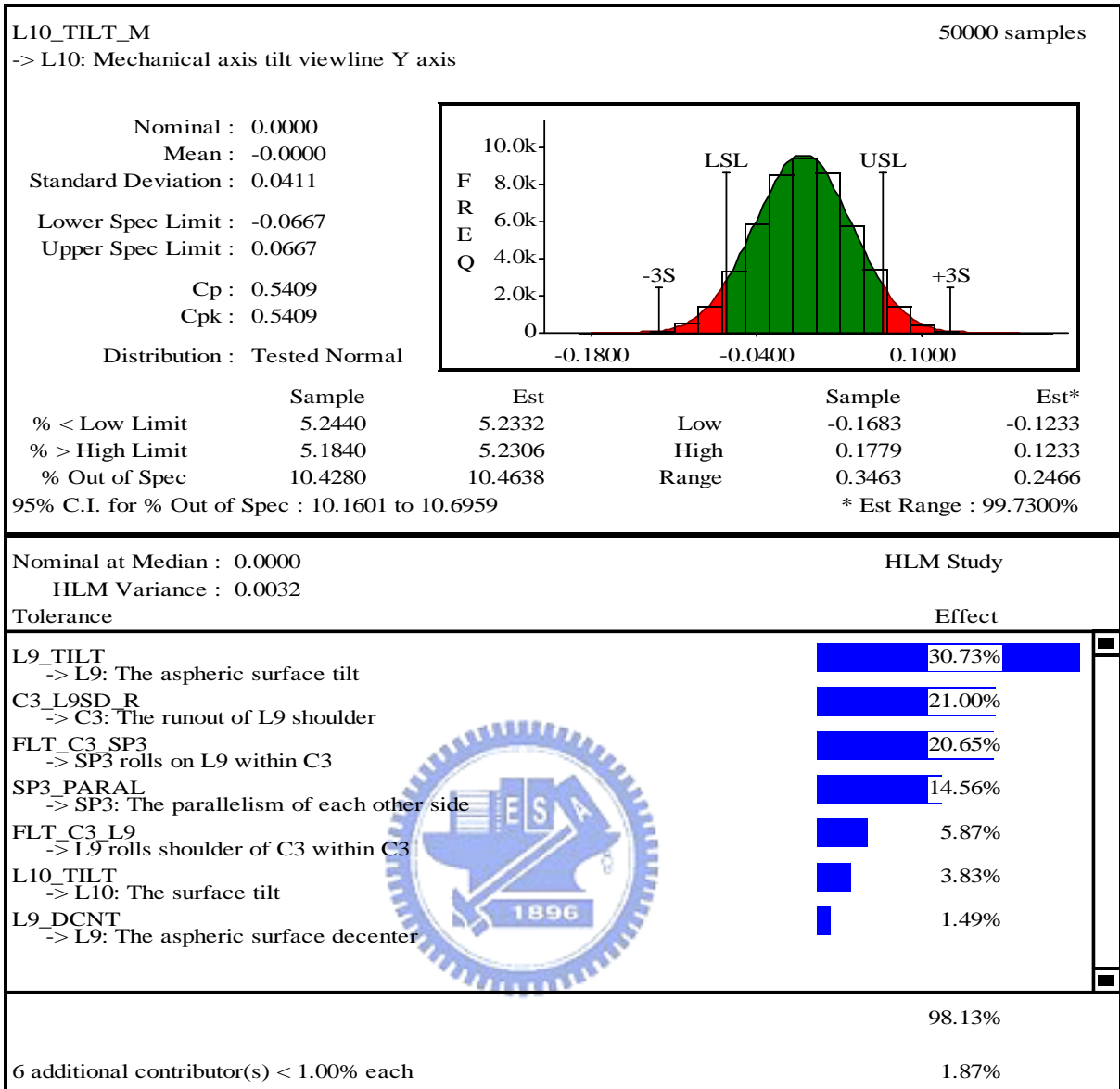


Figure 5-14 The element tilt of L10

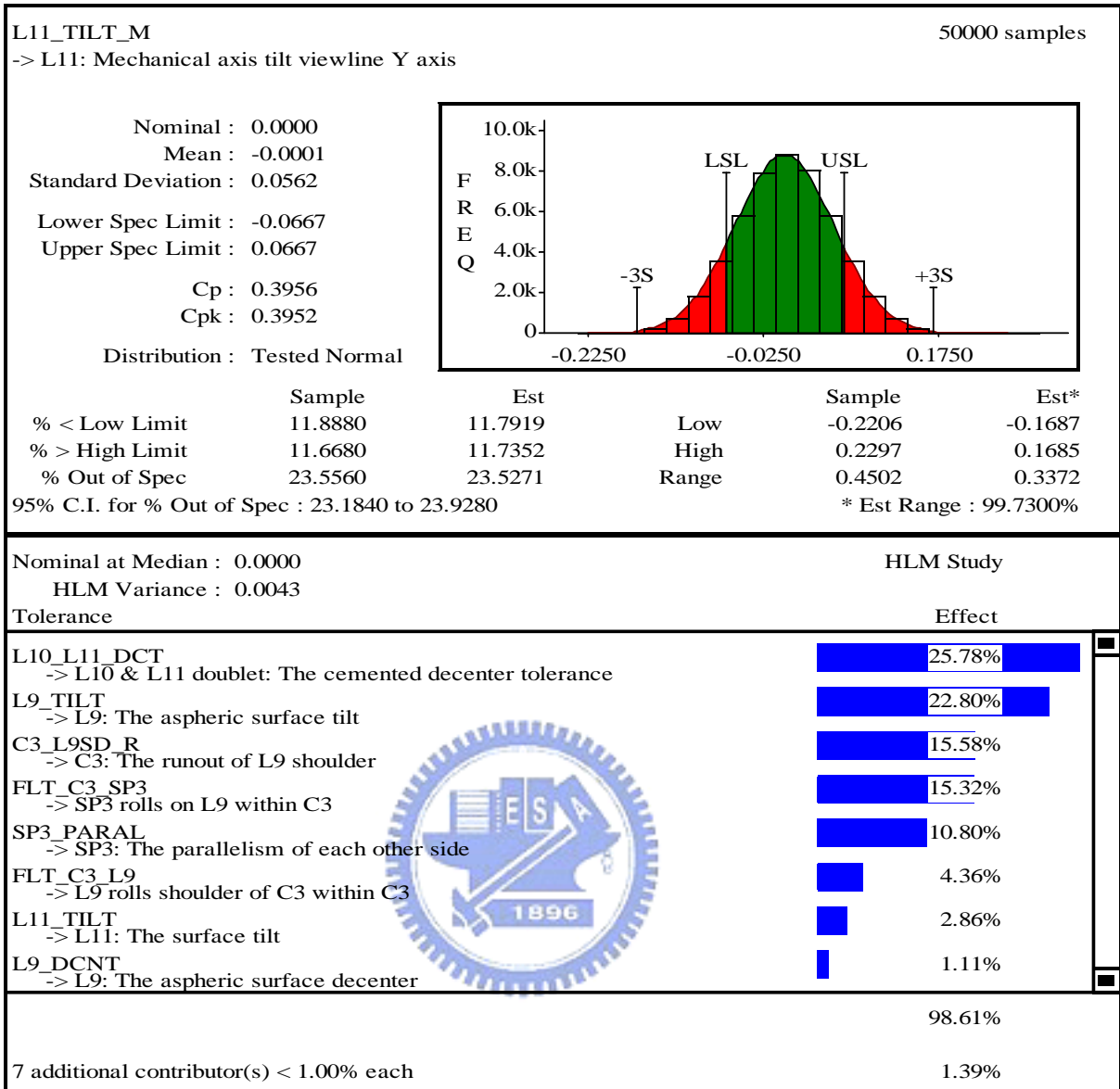


Figure 5-15 The element tilt of L11

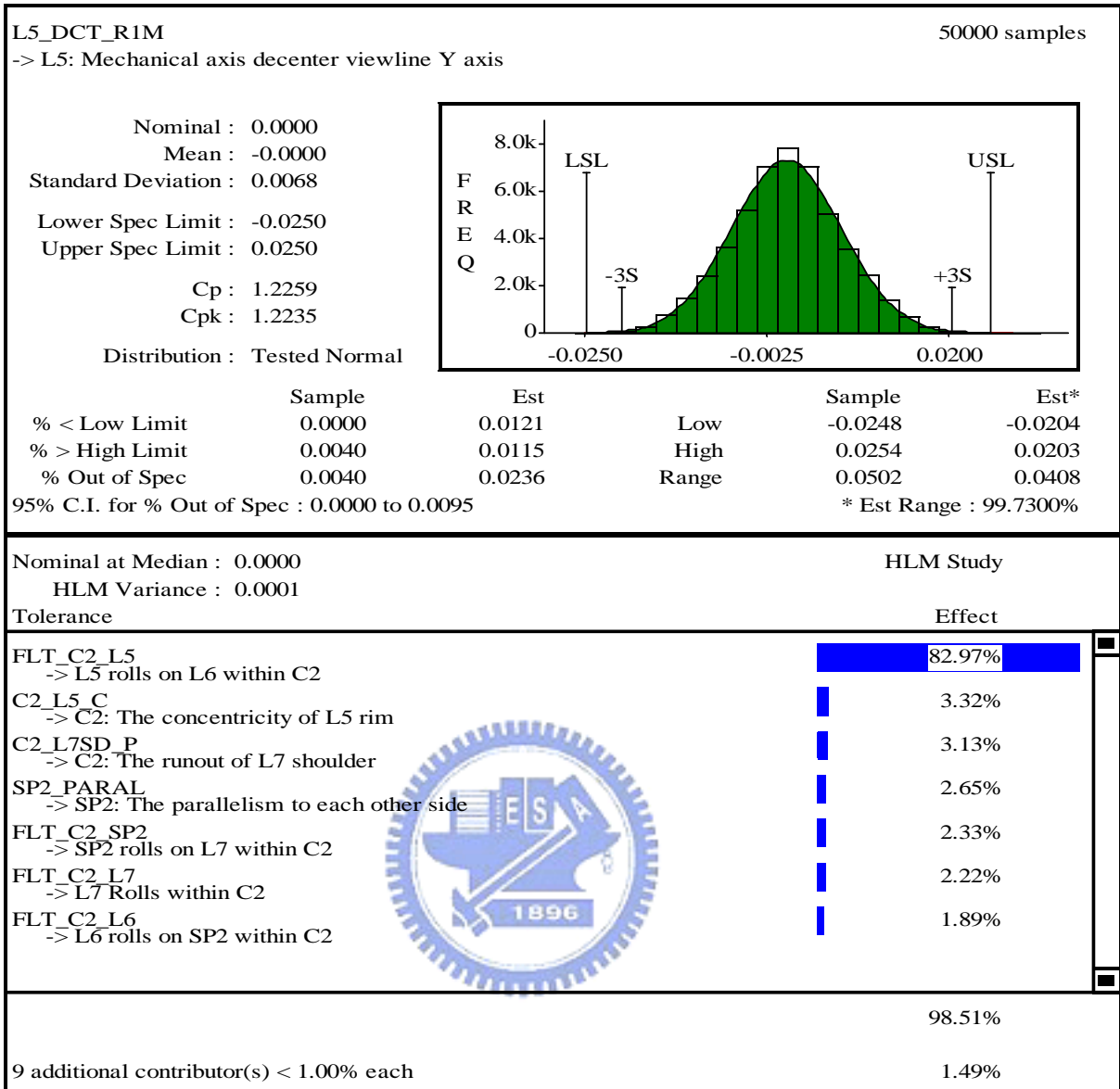


Figure 5-16 The element decenter of L5

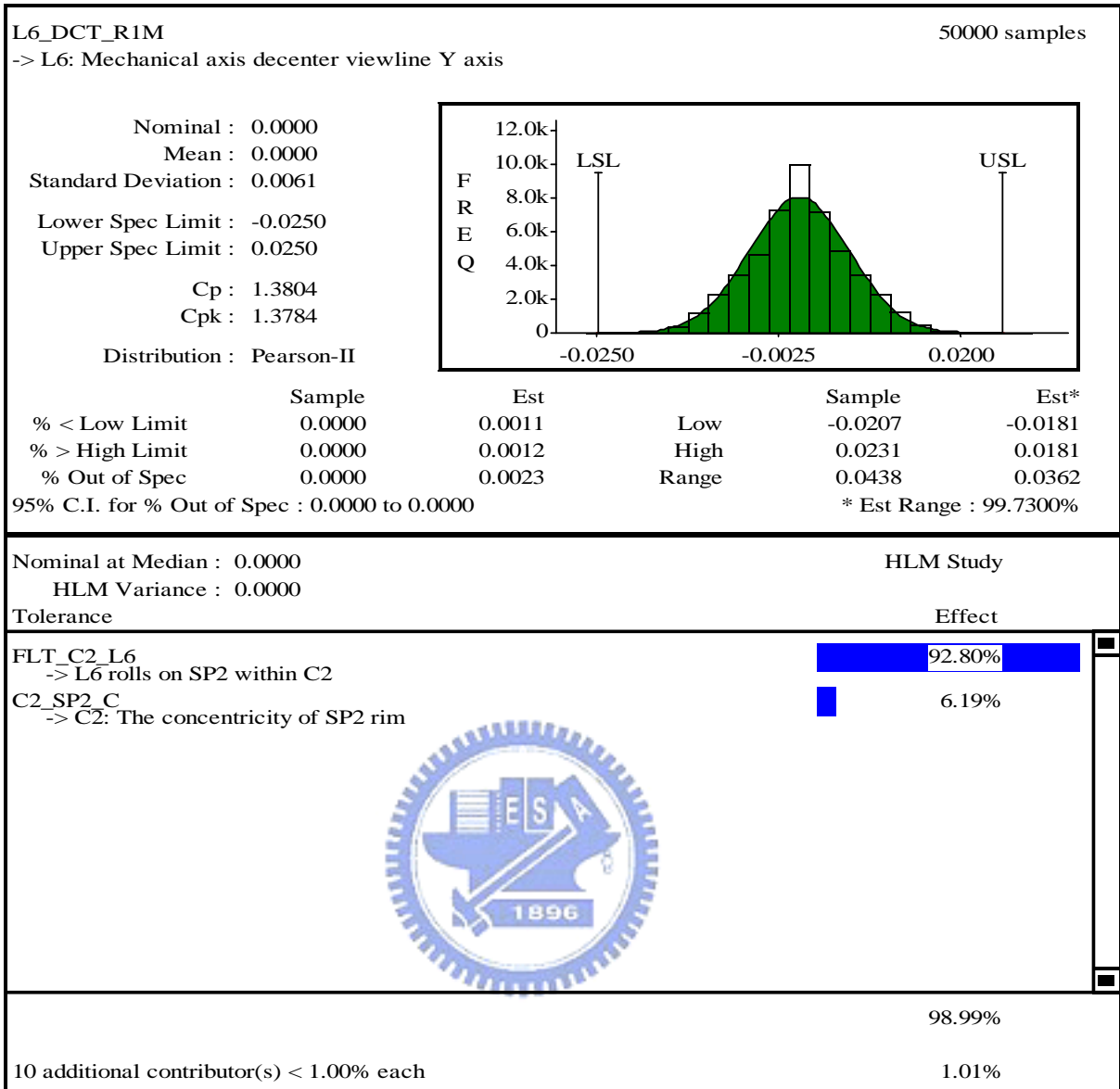


Figure 5-17 The element decenter of L6

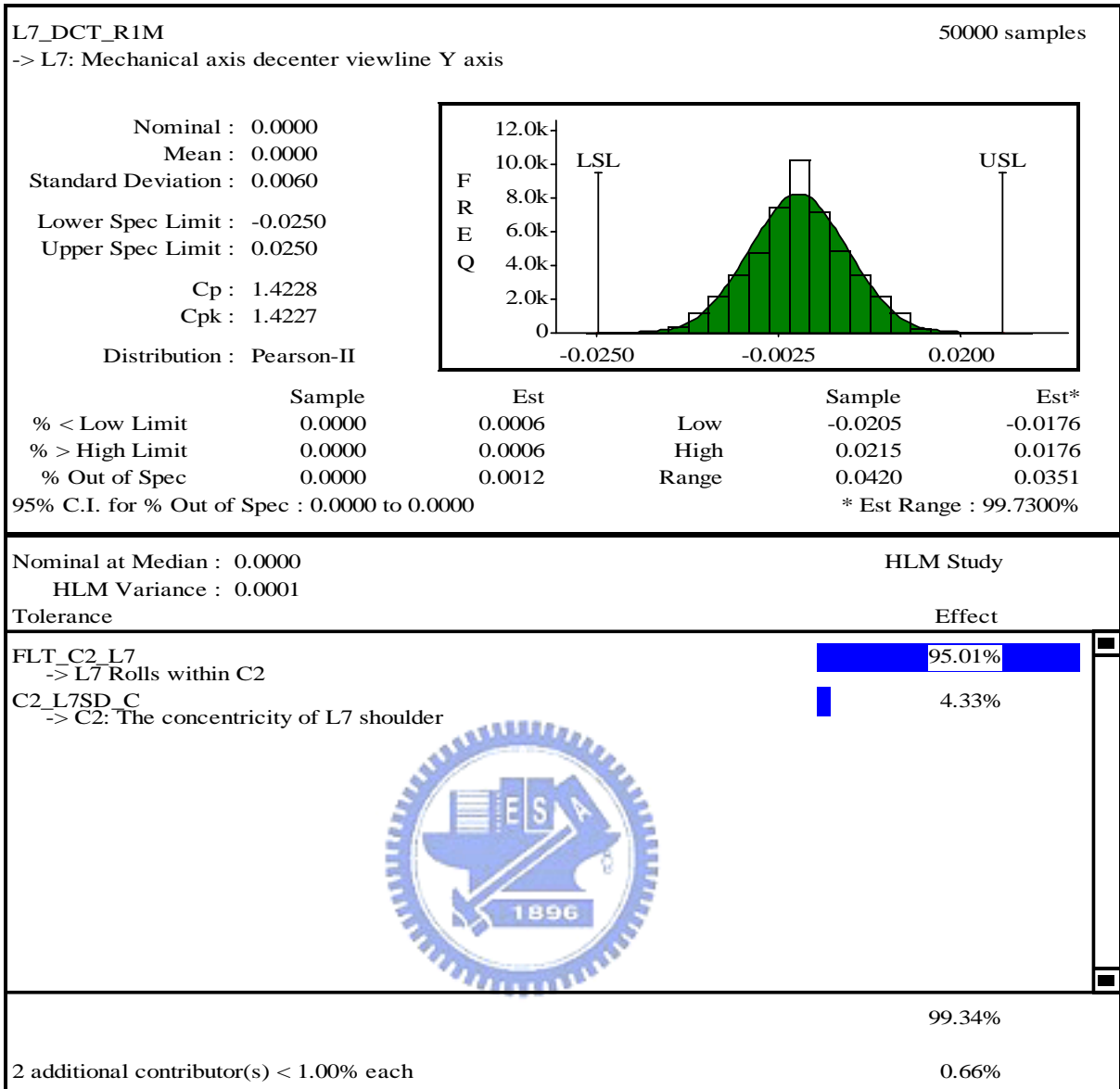


Figure 5-18 The element decenter of L7

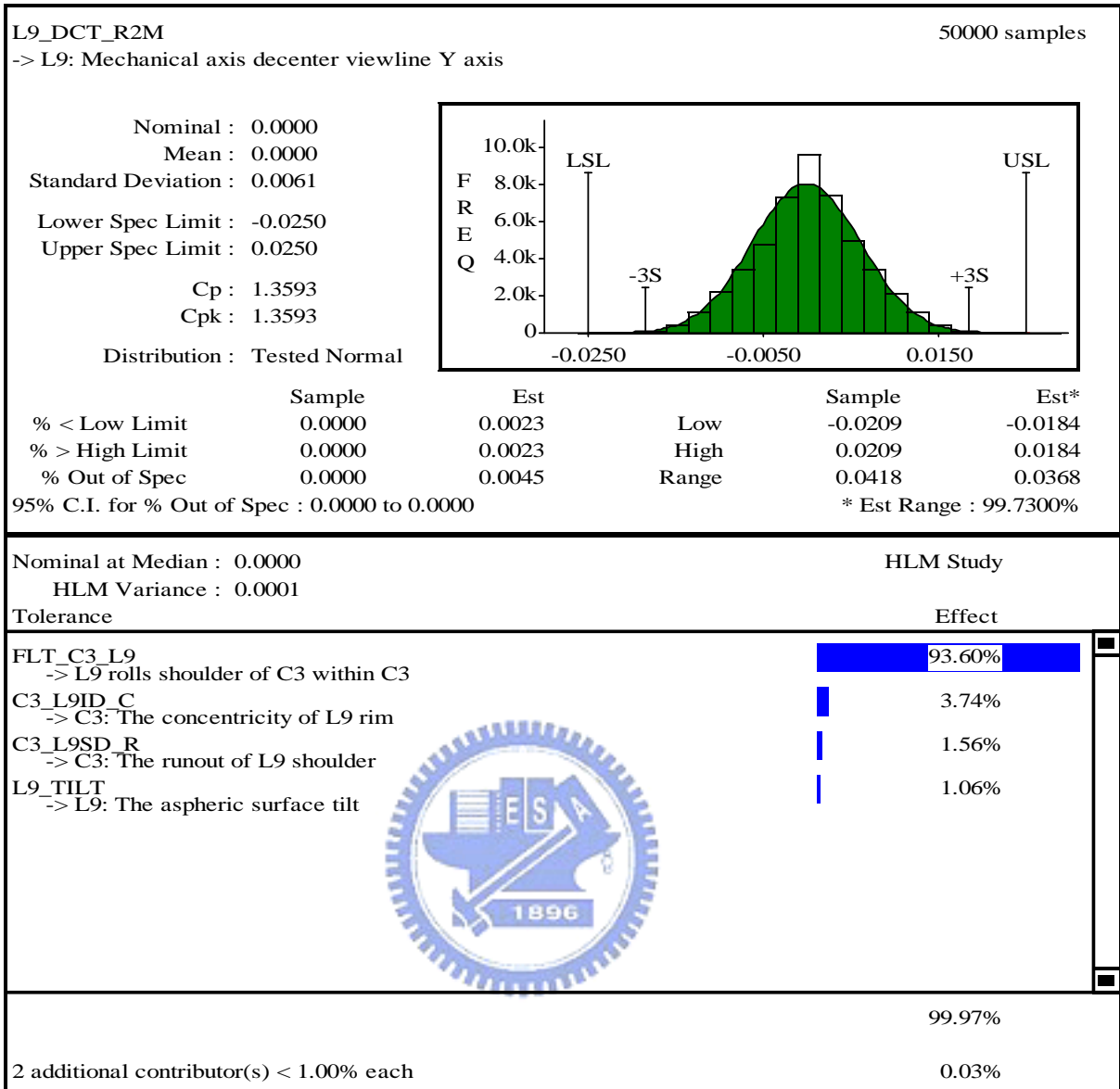


Figure 5-19 The element decenter of L9

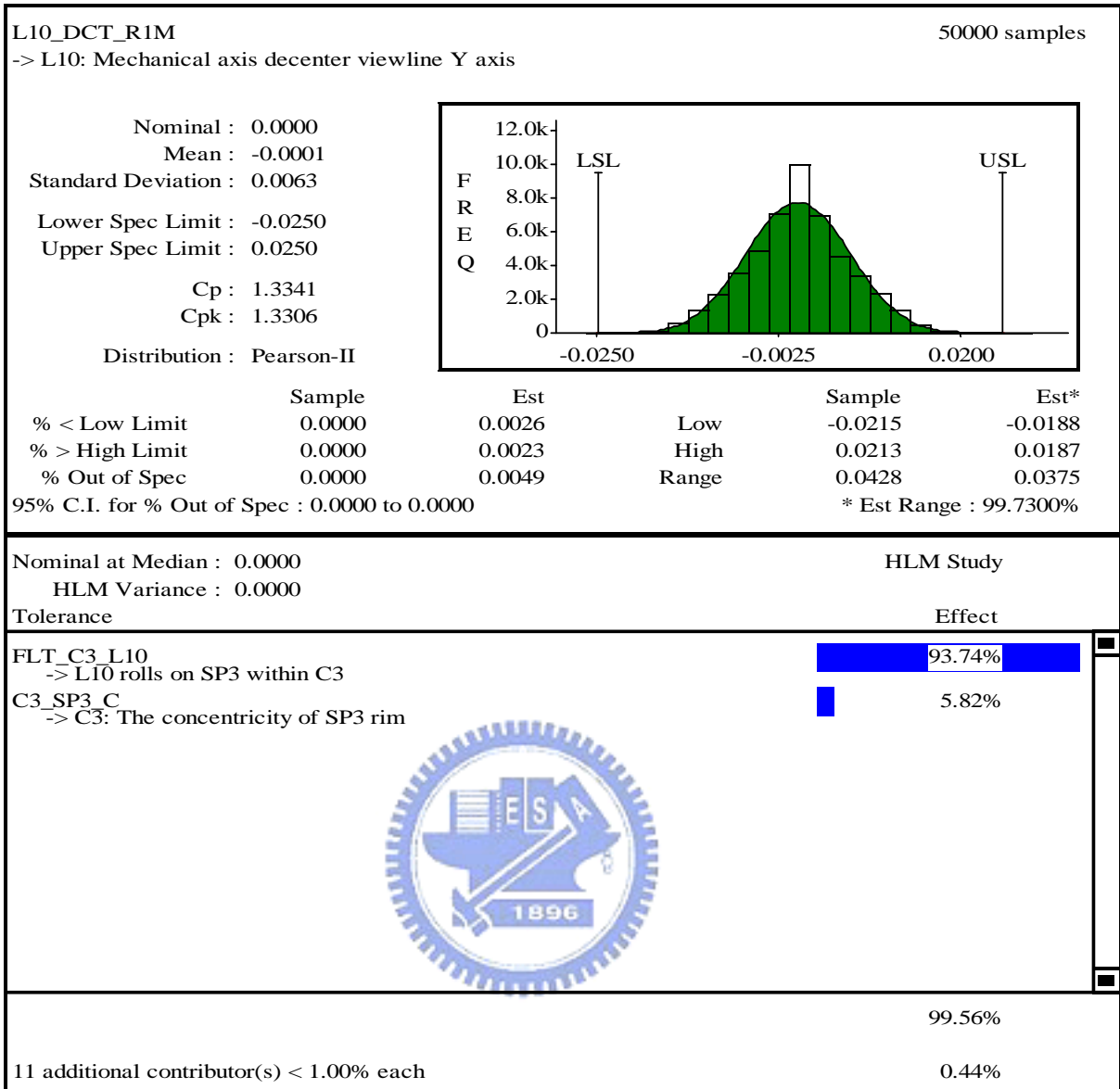


Figure 5-20 The element decenter of L10

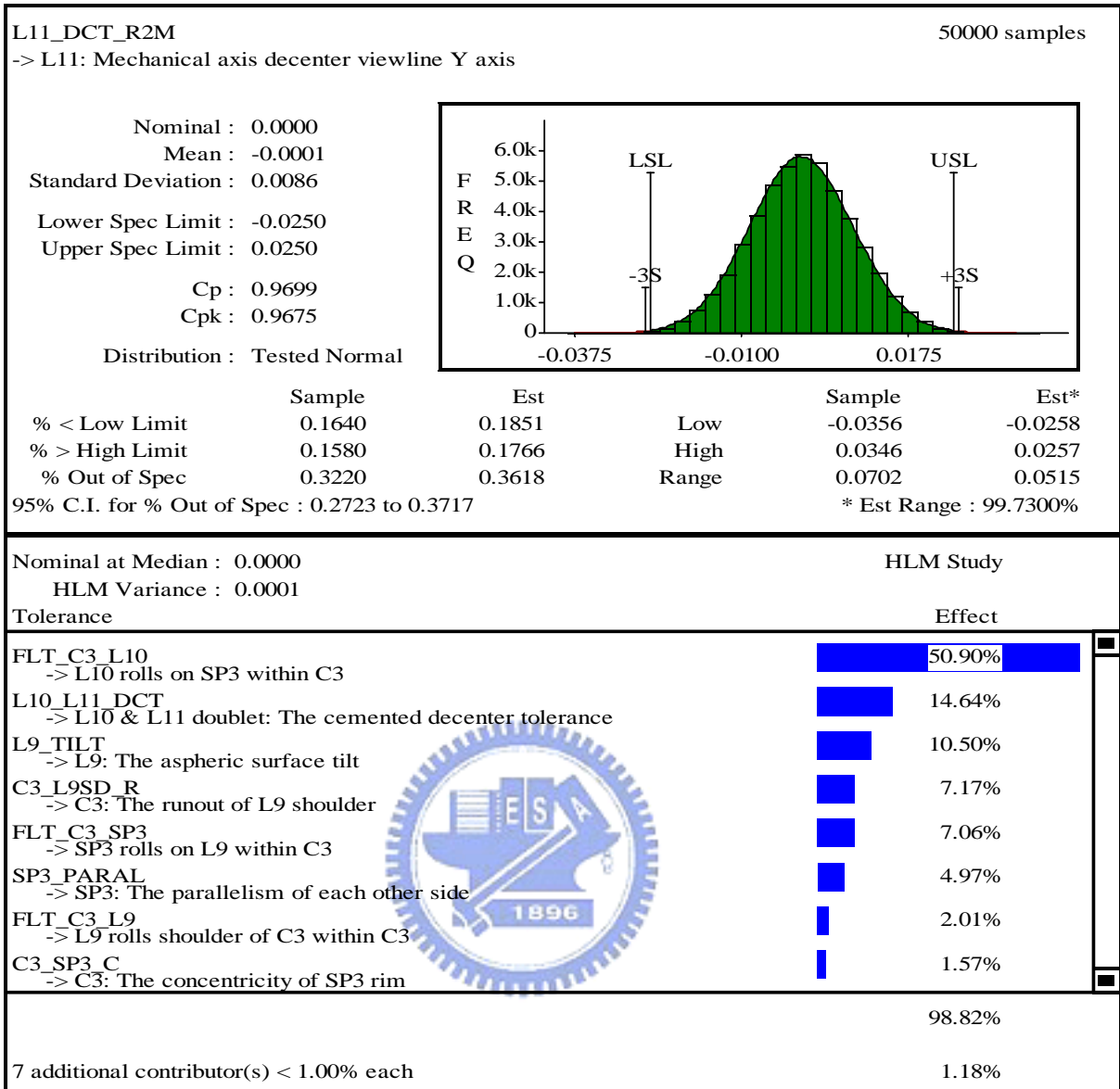


Figure 5-21 The element decenter of L11

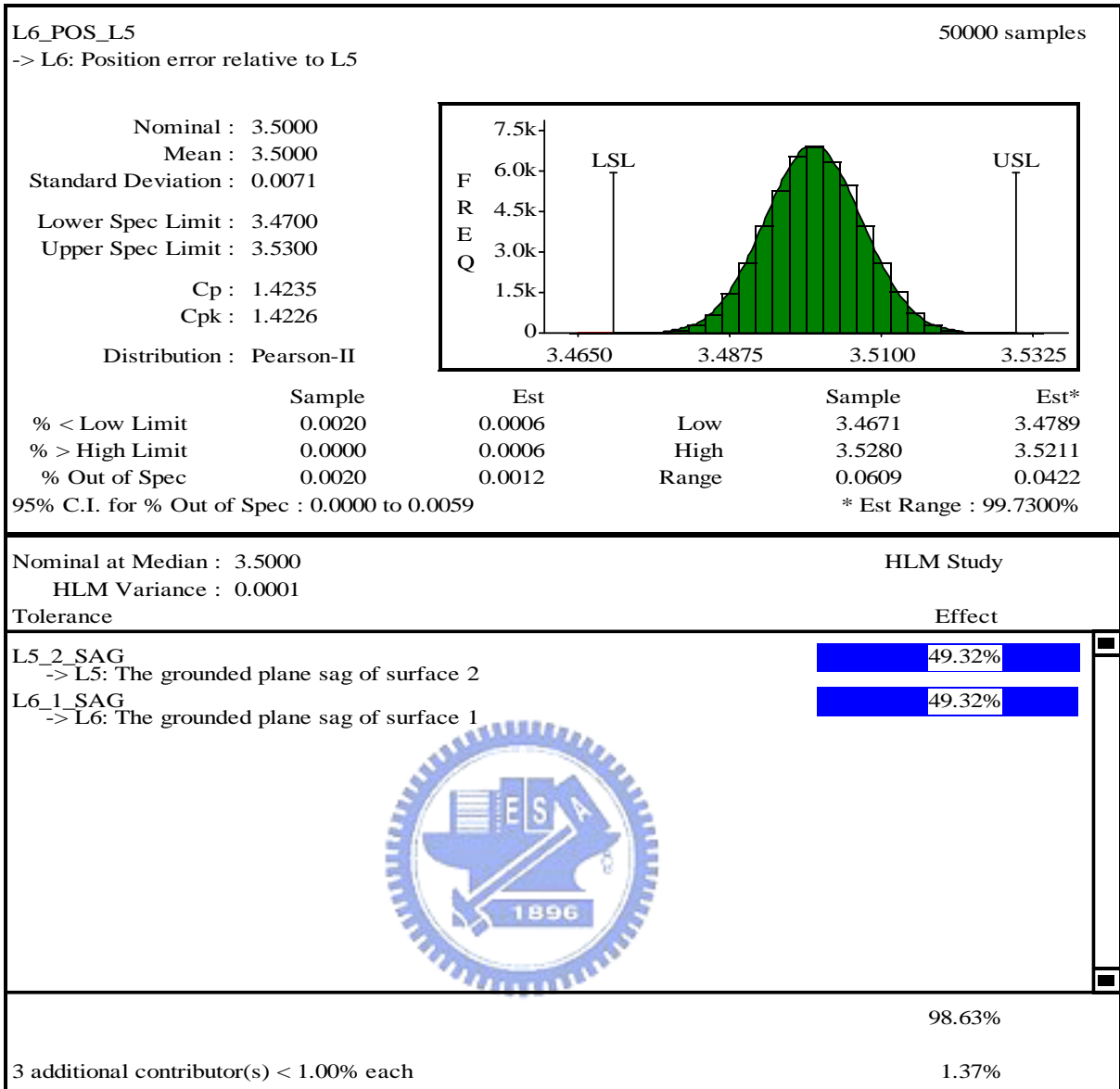


Figure 5-22 Despace of L6

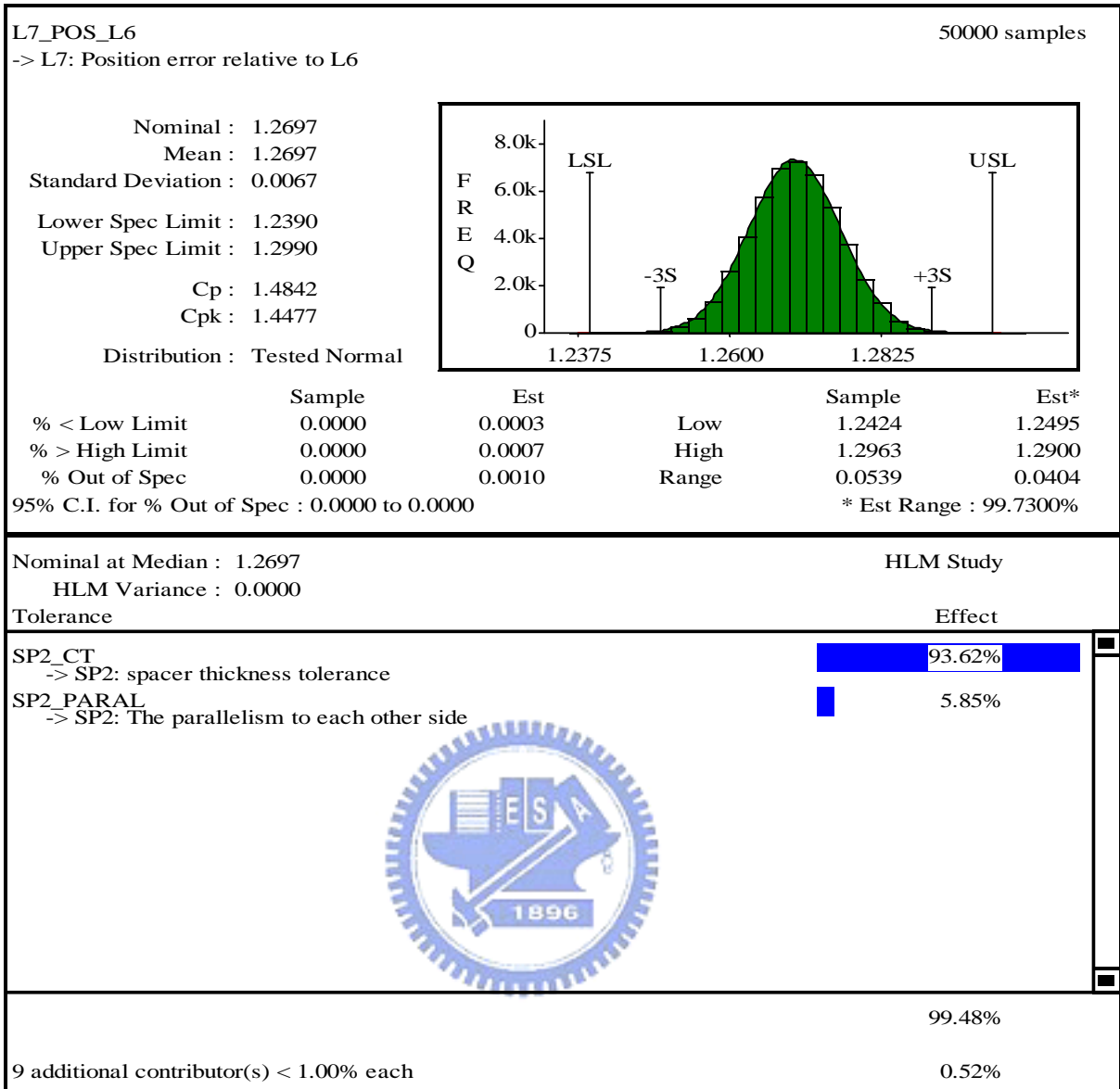


Figure 5-23 Despace of L7

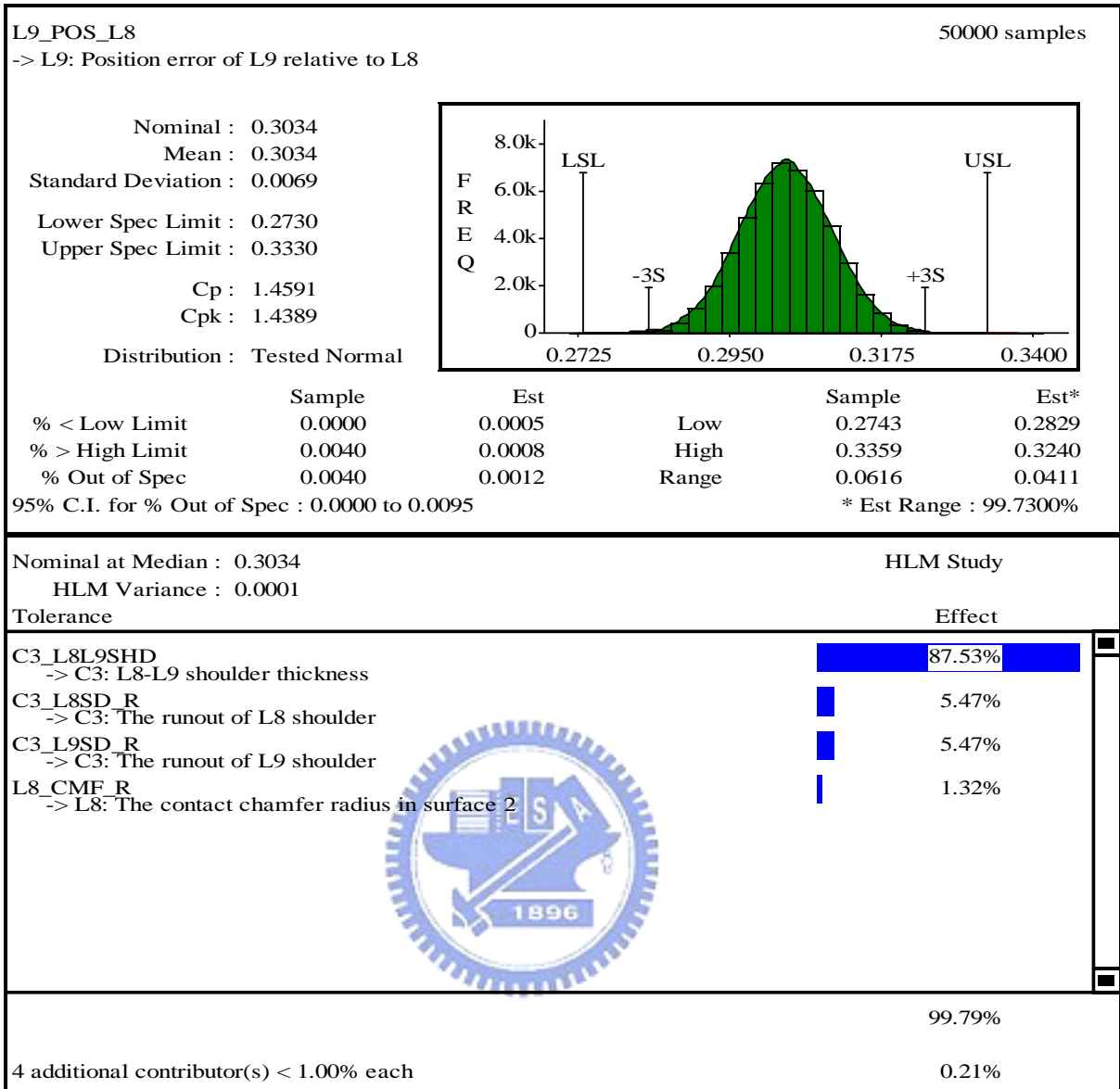


Figure 5-24 Despace of L9

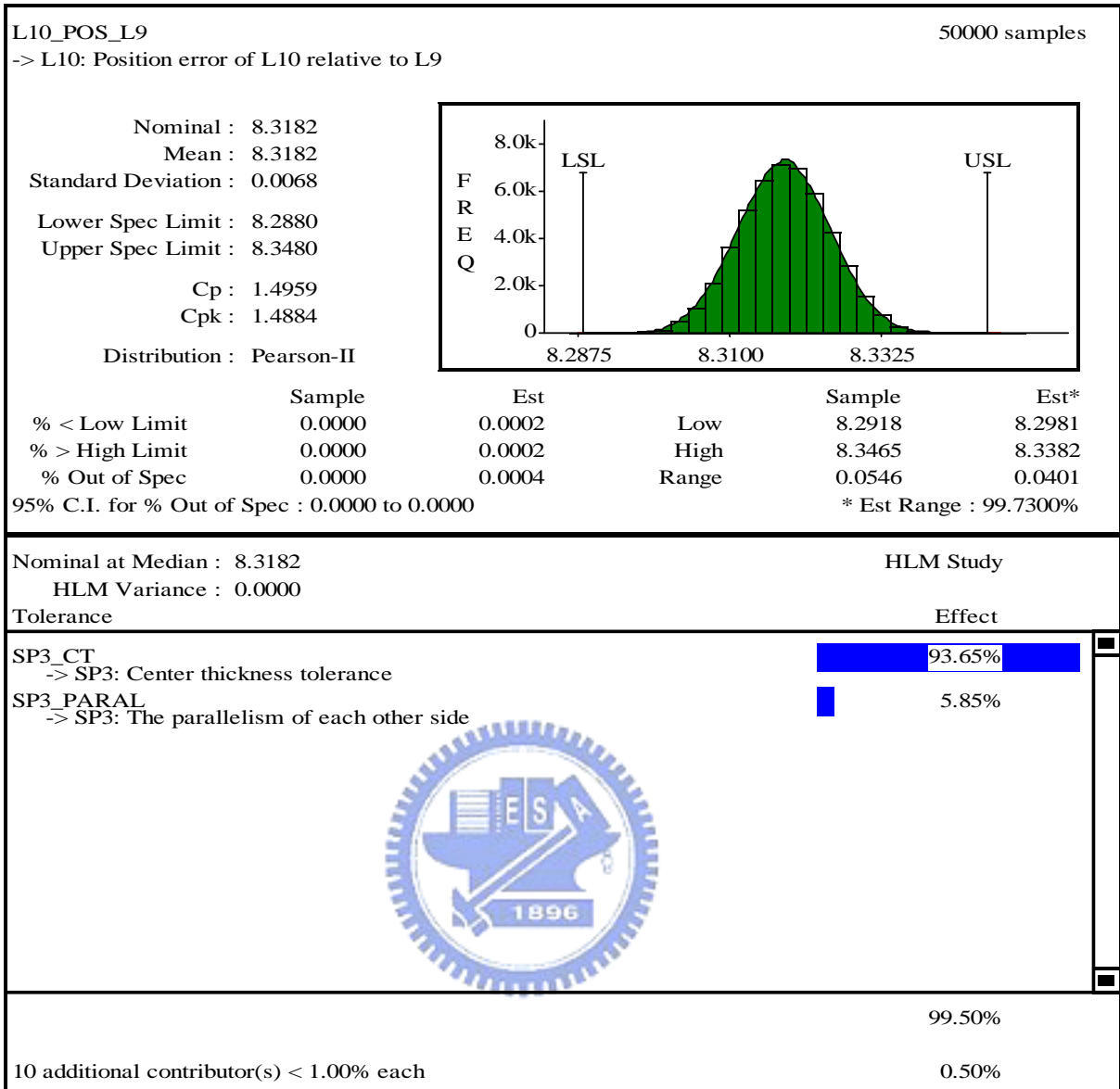


Figure 5-25 Despace of L6

5.5. Discussion

In order to read the above results in engineering aspect, all simulation results are listed in Table 5-4. The tilt and decenter of the mechanical axis in the simulation reports represents the element tilt and decenter of a lens within a cell. The position error of a lens represents the element despace relative to the preceding one. Although the optical axis tilt and decenter are not the tolerance analysis output of optical design software, these data can be easily calculated by the tolerance model developed in this study for discussion. In Table 5-4 the tilt angle has been converted from degree to minute. In addition, all data are expressed as the range of three standard deviations.

Both groups show that the element tilt gradually increases according to the order of assembly. Tolerance stack-up effect is the reason for the inclination. This is a major reason why “drop-in” design assembly cannot guarantee high precision lens alignment within a cell. For example, the major HLM contributors to the element tilt of L7 also play an important role on the element tilt of L6 and L5 lens. More factors which join the contributors for the element tilt of L6 and L5 result in the tolerance stack-up effect on the afterwards attached lens.

The mechanical axis decenter also slightly increases as the element tilt increases. The reason has been illustrated in Figure 4-12, the vertical unilateral gap between the cell and the lens is $(ID - OD)/2$, at the same time the arc length which can roll in that gap is $(ID - OD)/2\cos\theta$. Element tilt will slightly make the angle θ bigger; as a result, the decenter of mechanical axis will slightly increases as the element tilt increases.

The simulations results show that the initial opto-mechanical tolerance design make a good control over the element decenter and despace; however, the element tilt of L5, L6, L10, L11 lens cannot meet the requirements. The HLM analyses provide guidance for engineer to

modify the tolerance specifications to meet the optical requirements. However, the modification of the tolerances should be based on the process capability of fabrication shop. If the process capability cannot fulfill the demand of optical performance, the opto-mechanical engineer will face the dilemma of changing the opto-mechanical design or asking the optical engineer to modify the optical design.

As the surface tilt specification of sphere lens is quite small, the decenter of mechanical axis and optical axis are almost the same. An interesting phenomenon is that there seems no rule about the difference between the tilt of mechanical axis and optical axis. The explanation is illustrated in Figure 5-22 which is an extension of Figure 4-9. Point C1 is the center of curvature of surface 1 and is the stationary point of the optical element during assembly. It is reasonable to image that there is a mechanical axis variation zone centered in C1. Point M1 is the mechanical center of optical surface one. It is also reasonable to image that there is an optical axis variation zone centered in M1. According to the sphere lens tolerance model developed in Section 4.2.1, the size of the two variation zones are equal. Therefore, how C1 and M1 varied away from the mechanical datum axis will determine which axis will tilt more than the other. The major factor to bring about the deviation of point C1 is the runout of the cell shoulder. The principal contributor which leads to the deviation of point M1 is the gap between lens and cell.

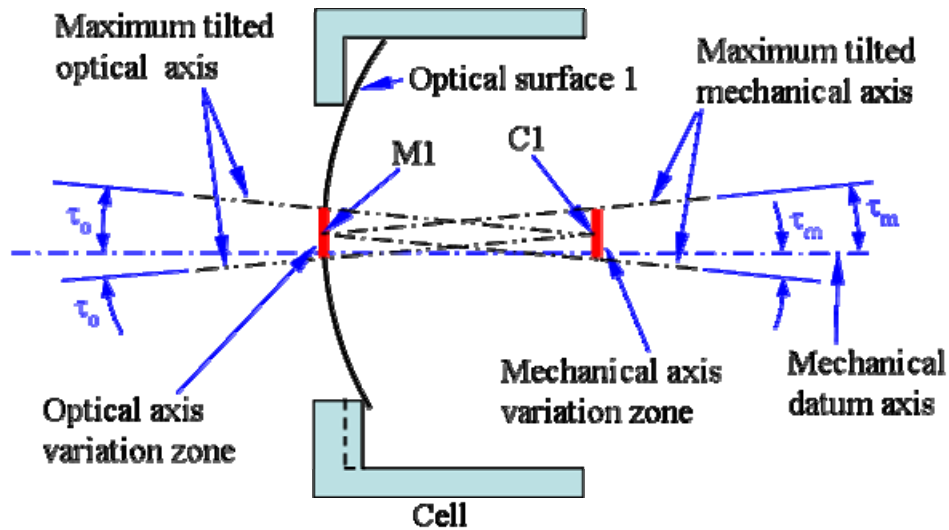


Figure 5-26 The variation of optical axis and mechanical axis

The simulation results show that the opto-mechanical tolerance model developed in this study can make a good performance prediction about the CTQs of an opto-mechanical system. For different lens group with “drop-in” assembly design, the model provide good consistency on the inclination of the stack-up effect of element tilt, decenter and desapce. The outputs of the model can be an input to optical design software to analysis the performance of the optical system. Therefore, a “Design for Manufacturing” optical system is achieved.

Table 5-4 The simulation results

Group	Group II			Group III			
Element name	L5	L6	L7	L8	L9	L10	L11
Assembly order	3	2	1	Independent	1	2	3
Element tilt (min.)	7.848	7.776	4.464	2.736	2.826	7.398	10.116
Optical axis tilt (min.)	8.010	7.182	4.176	2.196	4.068	7.218	9.972
Element decenter (mm)	0.020	0.018	0.018	Not CTQ	0.018	0.019	0.026
Optical axis decenter (mm)	0.020	0.019	0.018	Not CTQ	0.019	0.019	0.026
Element despace (mm)	First lens of the group	0.021	0.020	First lens of the group	0.021	0.020	Doublet

Chapter 6. Conclusions and future works

The element tilt, decenter and desapce of a lens within a cell are the critical to quality opto-mechanical parameters of a lens system. In this study, an opto-mechanical tolerance model for lens assembly has been developed and implemented by VSA-3D[®] software to simulate the distribution of these parameters by Monte Carol simulation method. The model integrates the tolerances of optical elements, the tolerances of mechanical component, and the variations of the assembly process. The model is represented as point geometry. Because the point geometry of the optical surfaces is derived by the mathematical equation of the surfaces and the dimensions of mechanical component that attached to it, a surface based opto-mechanical tolerance model is built. The outputs of the model are the statistical information about the element tilt, decenter and desapce of a lens or the resultant error of the optical axis of a lens within a cell. With this tolerance model the performance of an opto-mechanical system can be anticipated. The analysis results also can be an input to optical design software. As a result, a “Design for Manufacturing” optical system can be accomplished.

The opto-mechanical tolerance model outputs the desired measurements according to the characteristics of the input components and assembly process. Although it is easy for engineer to modify the inputs to meet the system requirements, an optimum tolerance design still cannot achieve. The future work will focus on the optimization of the tolerance design subjected to the system requirements, the process capability, and the production cost.

REFERENCES

- [1] Willy, R.R. and Parks, P.E., “Optical Fundamentals”, Optomechanical Engineering Handbook, Ed. Ahmad, A., Boca Raton: CRC Press LLC, 1999.
- [2] Vukobratovich, D., “Optomechanical Design Principles”, Optomechanical Engineering Handbook, Ed. Ahmad, A., Boca Raton: CRC Press LLC, 1999.
- [3] Hilbert, R.S., “Semi-automatic modulation transfer function (MTF) tolerancing”, Optical System Engineering, SPIE Vol. 193, pp. 34-43, San Diego, CA, USA, Aug. 1979.
- [4] Drake, P., “Auto-tolerancing on optical system”, Lens Design, Illumination, and Optomechanical Modeling, SPIE Vol. 3130, pp. 136-147, San Diego, CA, USA, July 1997.
- [5] Sasaki, T., Shinkai, M., Higashiyama, K., Tanaka, F. and Kishinami. T., “Development of Statistical Tolerancing System for Optical Product. – Virtual PT System and Mass Product Simulation”, International Optical Design Conference, SPIE Vol. 3482, pp. 528-537, Kona, HI, USA, June 1998.
- [6] Magarill, S., “Optomechanical sensitivity and tolerancing”, Optomechanical Engineering and Vibration Control, SPIE Vol. 3786, pp. 220-228, Denver, CO, USA, July 1999.
- [7] Lee K. J., Yoon, Y. and Maxwell, J., “Creative Optomechanical Tolerancing in Lens System”, International Optical Design Conference, SPIE Vol. 3482, pp. 187-220, Kona, HI, USA, June 1998.
- [8] Thompson, K. P., “Techniques for characterizing optical system fabrication”, Selected Papers on Optomechanical design, SPIE Vol. 770, Ed. O’Shea D. C., pp. 89-95, 1987.
- [9] De Witt IV, F., Nadorff, G., “Rigid Body Movements of Optical Elements due to Opto-Mechanical Factors”, Optical Modeling and Performance Predictions II, Proc. Of SPIE Vol. 5867, Ed. Kahan, 2005.
- [10] VSA-3D[®] software, Variation Systems Analysis Inc., St. Clair Shores, MI, USA, 2000.

- [11] Creveling, C. M., Tolerance design: a handbook for developing optimal specification, Addison Wesley Longman, Inc., 1997.
- [12] Benson, H., University Physics, Revised ed. John Wiley & Sons, Inc. pp 431-435, 1996.
- [13] ASME Y14.5M-1994, Dimensioning and Tolerancing, the American Society of Mechanical Engineers, 1995.
- [14] Van Wyk, D., "Predicting assembly quality (six sigma methodologies to optimize tolerances)", Dimensioning and Tolerancing Handbook, Ed. Drake, P. Jr., McGraw-Hill, 1999.
- [15] Chase, K. W., "Design Issues in Mechanical Tolerance Analysis", Manufacturing Review, ASME, vol. 1, pp. 50-59, Mar. 1988.
- [16] Drake, P., "Traditional Approaches to Analyzing Mechanical Tolerance Stacks", Dimensioning and Tolerancing Handbook, Ed. Drake, P. Jr., McGraw-Hill, 1999.
- [17] Greenwood, W. H. and Chase K. W., "A New Tolerance analysis Method for Designers and Manufacturers", Transactions of the ASME, Vol. 109, pp 112-116, May 1987.
- [18] Pradeep K. S., et al. "Tolerance Analysis of Mechanical Assemblies Using Monte Carlo Simulation", International Journal of Industrial Engineering, 10(2), pp 188-196, 2003.
- [19] Gerth R. J., Hancock W. M., "Computer aided tolerance analysis for improved process control", Computer & Industrial Engineering, Vol. 38, n1, pp 1-19, 2000.
- [20] Yoder, P. R., Jr., "Designing a durable system", Selected Papers on Optomechanical design, SPIE Vol. 770, Ed. O'Shea D. C., pp 17-23, 1987.
- [21] Yoder, P. R., Jr., Opto-mechanical systems design, 2nd ed., Marcel Dekker, Inc., New York, 1992.
- [22] Cade, J. W., "Mounting Optical Elements", Selected Papers on Optomechanical design, SPIE Vol. 770, Ed. O'Shea D. C., pp 146-148, 1987.
- [23] Hopkins, R. E., "Lens mounting and Centering", Applied Optics and Optical Engineering, Vol. VIII, Ed. Shannon, R. R. and Wyant, J. C., Academic Press, 1980.

- [24] Yoder, P. R., Jr., “Optical Mounts: Lenses, Windows, Small Mirrors, and Prisms”, Optomechanical Engineering Handbook, Ed. Ahmad, A., Boca Raton: CRC Press LLC, 1999.
- [25] ISO 10110, “Optics and optical instruments preparations of drawing for optical elements and system”, 1996.
- [26] Thorburn, E. K., “Concepts and misconceptions in the design and fabrication of optical assemblies”, Selected Papers on Optical Tolerancing, SPIE Vol. MS36, Ed. Wiese, G. E., pp 28-33. 1991.
- [27] Parks, R. E., “Optical component specifications”, Selected Papers on Optical Tolerancing, SPIE Vol. MS36, Ed. Wiese, G. E., pp 40-48, 1991.
- [28] Durie, D. S. L., “Stability of optical mount”, Selected Papers on Optomechanical design, SPIE Vol. 770, Ed. O’Shea D. C., pp 140-145, 1987.
- [29] Fisher E. F., Tadic-Galeb B., Optical System Design, McGraw-Hill, International Editions, 2001.
- [30] Whitney, D. E., Mechanical Assemblies, Oxford University Press, New York, 2004.
- [31] Code V Reference Manual, Optical Research Associates, Pasadena, CA, US, 2004.